2013

Development of a Starch-Based Mussel-Mimetic Adhesive Polymer

Jeffrey Kazimir de Kozlowski
Purdue University, jeff.dekoz@gmail.com

Graduate School ETD Form 9
(Revised 12/07)

PURDUE UNIVERSITY
GRADUATE SCHOOL
Thesis/Dissertation Acceptance

This is to certify that the thesis/dissertation prepared

By Jeffrey de Kozlowski

Entitled
Development of a Starch-Based Mussel-Mimetic Adhesive Polymer

For the degree of Master of Science

Is approved by the final examining committee:

Bernard Tao
Chair

Jonathan Wilker

Nathan Mosier

To the best of my knowledge and as understood by the student in the *Research Integrity and Copyright Disclaimer (Graduate School Form 20)*, this thesis/dissertation adheres to the provisions of Purdue University's "Policy on Integrity in Research" and the use of copyrighted material.

Approved by Major Professor(s): Bernard Tao

Approved by: Bernie Engel 10/11/2013
Head of the Graduate Program Date

DEVELOPMENT OF A STARCH-BASED MUSSEL-MIMETIC ADHESIVE POLYMER

A Thesis

Submitted to the Faculty

of

Purdue University

by

Jeffrey Kazimir de Kozlowski

In Partial Fulfillment of the

Requirements for the Degree

of

Master of Science

December 2013

Purdue University

West Lafayette, Indiana

To Amanda,

I know it was not easy for you to move with me to Indiana without the guarantee of a job. The past two years have brought us closer than I imagined and in the meantime you discovered your true professional aspirations. I am so happy that things worked out for the best and I thank you for putting up with the frustrations of my life as a graduate student. This thesis represents the time and commitment you deserve every day. I love you.

ACKNOWLEDGEMENTS

I would like to first thank my advisor Dr. Bernie Tao for his support throughout my graduate career. I have learned immensely from him educationally, professionally, and personally through conversations and advice. I am extremely grateful for his guidance throughout my project and towards my professional goals. I am glad to have worked with him.

Next, I would like to thank the Indiana and Iowa Corn Growers Associations for making this project possible. Thank you for your patience and support throughout this project.

I want to thank my committee member Dr. John Wilker for his insights into this project and for allowing me to use his organic chemistry lab. Additionally, I owe extreme gratitude to the Wilker lab group, especially Jess Roman, Cori Jenkins, Heather Meredith, and Michael North for their unwavering assistance in the lab and for helpful discussions.

I would also like to thank Lisa Mauer, Brad Reuhs, Anton Terekov, and the entire Whistler Center for their assistance with NMR and IR spectroscopy and for allowing me to use their labs. A special thanks to Anton Terekov for training me on NMR and other equipment.

I owe thanks to many members of the Hamaker lab including Madhuvanti Kale and Byung-Hoo Lee for their patience and knowledge in HPLC analysis of polysaccharides.

Thank you to Karl Wood for his timely assistance with mass spectrometry and general knowledge in analytical chemistry.

Thank you to my committee member Dr. Nate Mosier and to Dr. Michael Ladisch for their mentorship and support in my professional and academic goals.

To the faculty and staff of ABE and Food Science, thank you for everything you have done for me and other graduate students. Without your commitment, graduate school would be a nightmare.

Thanks to Dr. Bruce Applegate for my cat and his vaccinations, and interesting conversations.

Thank you to Dr. Yuan Yao and Dr. Susan Nielson for allowing me to attend the food science tour of China. It was a once-in-a-lifetime experience that I will never forget. I want to especially thank Dr. Yao for his guidance on the trip, for helpful discussions regarding starch and carbohydrate chemistry, and his friendship.

Finally, I want to thank my family and friends for their support. You are my motivation and backbone.

TABLE OF CONTENTS

Page

Page

Page

Page

Page

LIST OF TABLES

LIST OF FIGURES

Figure Page

Appendix Figure

Appendix Figure Page

LIST OF ABBREVIATIONS

1-Ethyl-3-(3-dimethylaminopropyl)carbodiimide EDC

3,4-dihydroxybenzoic acid DHBA

3,4-dimethoxybenzoic acid DMBA

Ascorbic Acid AA

Atmospheric Pressure Chemical Ionization APCI

Anhydroglucose unit AGU

Carbonyldiimidazole CDI

Carboxylic acid COOH

Carboxymethyl starch CMS

Concentration of "x" [x]

Degree of substitution DS

Dichloromethane DCM

Dimethylacetamide DMA

Dimethylformamide DMF

Dimethylsulfoxide DMSO

Electron impact/chemical ionization EI/CI

Electrospray Ionization ESI

Ethanol EtOH

Fourier transform infrared spectroscopy FTIR

Isopropanol IPA

Methanol MeOH

Molecular weight MW

N-hydroxysuccinimide NHS

Nuclear magnetic resonance spectroscopy NMR

Phenylboronic acid PBA

Proton NMR H-NMR

p-Toluenesulfonic acid chloride TosCl

Pyridine Py

Sodium monochloroacetate SMCA

Tetra-n-butylammonium fluoride TBAF

tert-Butyldimethylsilyl TBDMS

Ultraviolet-visible UV-vis

ABSTRACT

de Kozlowski, Jeffrey K. M.S., Purdue University, December 2013. Development of a Starch-Based Mussel-Mimetic Adhesive Polymer. Major Professor: Bernard Tao.

Mussel-mimetic adhesive polymers have gained lots of attention for their strong adhesive strength, moisture resistance, and unique ability to crosslink. These properties are mainly attributed to the high content of catecholic 3,4-dihydroxyphenylalanine (DOPA) in mussel adhesive proteins. While there has been success in creating mussel-mimetic synthetic polymers, less effort has been given to create a renewable, green, biocompatible counterpart. This thesis explores the possibilities of starch-based mussel-mimetic adhesives. Carboxymethyl starch of various molecular weights and degree of substitution was synthesized and subsequent conjugation of dopamine to these polymers by 1-Ethyl-3-(3-dimethylaminopropyl)carbodiimide was investigated. The polymers suffered from very low substitution ($DS_{catechol} < 0.02$) and easily precipitated from solution as an insoluble product. The cause of precipitation was investigated and was shown to be unrelated to autooxidation of conjugated dopamine by O_2 and pH. Instead, EDC seemed to be somehow responsible for the precipitation and most likely also for the very low $DS_{catechol}$ due to competing reactions and instability of EDC intermediates. Lap-shear strengths of the CMS-dopamine conjugates failed to exceed those of unmodified CMS.

In search of another path to starch-catechol conjugates with higher $DS_{catechol}$, 1,1'-carbonyldiimidazole was employed for direct conjugation of bis-O-protected 3,4-dihydroxybenzoic acid to unmodified starch. High DS was achieved with 3,4-dimethoxybenzoic acid, but demethylation techniques were incompatible with starch and its esters. Phenylboronic acid was then employed as an easily removable diol protecting group for DHBA, but the complex was apparently not stable enough in solution for selective activation of the carboxylic acid group of PBA-DHBA by either CDI or TosCl. Further screening of different protecting groups or a new coupling chemistry is needed to fully assess the possibilities of starch-catechol conjugates of high $DS_{catechol}$.

CHAPTER 1. INTRODUCTION

1.1 Objectives

The ultimate goal of this research was to create a novel starch-based adhesive inspired by marine mussel adhesive chemistry by covalent coupling of catecholic moieties to high amylose starch. The specific objectives of this project were to:

1. Modify the molecular weight of high amylose starch through controlled hydrolysis.
2. Synthesize carboxymethyl starch of various degrees of substitution.
3. Conjugate dopamine to carboxymethyl starch in aqueous reaction with EDC coupling agent and characterize the new polymer.
4. Evaluate the effectiveness of the catechol-substituted carboxymethyl starch as an adhesive.
5. Investigate alternative, non-aqueous methods for creating catechol-functionalized starch.

1.2 Organization

This thesis is divided into five chapters. The second chapter is a literature review to provide motivation for renewable adhesives, the basics of adhesion and mussel adhesion chemistry, and an overview of progress made in developing mussel-mimetic adhesives.

Chapter three discusses the materials and methods used in the research. The results of the research project are presented and discussed in chapter four. Finally, chapter five provides a summary of the findings of this research and considerations for future work.

CHAPTER 2. LITERATURE REVIEW

2.1 Adhesives

2.1.1 Introduction

On the most basic level, adhesives afford humanity the ability to join together dissimilar objects. With such a vast number of applications possible from such a simple concept, one can imagine the demand for adhesives and the market size they occupy. Adhesives have a significant value in construction, packaging, transportation, automotive, consumer, rigid bonding, and medical industries (Bosik, 2012).

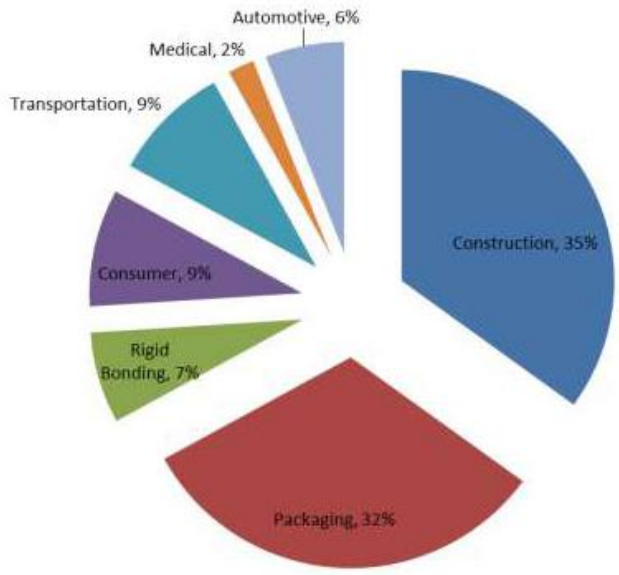

Figure 2.1 Share of Adhesives and Sealants Market Value by Industry Application (Bosik, 2012)

Globally, the adhesives and sealants market was worth about $22 billion in 2011. North America, Europe, and Asia represent the three largest adhesives and sealants markets; North America being the largest at $11.2 billion in 2011. About $7 billion of the North American market is represented by adhesives, specifically. Of this $7 billion, the market is mostly dominated by synthetic resin and rubber adhesives which account for about $6.5 billion, while natural based glues and adhesives account for the remainder. However, growth in almost all subcategories of the synthetic resin and rubber adhesives market has been relatively stagnant while certain subcategories of the natural based glues and adhesives market have seen significant growth; most notably protein adhesives, with a compound annual growth rate of nearly 8% from 2002 to 2011 (Bosik, 2012).

2.1.2 Motivation for Green Adhesives

The majority of current adhesives are based on petroleum-derived materials. While petro-based adhesives have advantages of superior bonding strength and some water resistance, they are non-renewable and may pose environmental and health issues (Li et al., 2012).

The main environmental/health concern with traditional adhesives is volatile organic compounds (VOCs). One common VOC is formaldehyde, a major contributor to indoor air pollution that may pose risk of cancer and respiratory complications like asthma (Deschamps, 2010; Li et al., 2012; Ruffing, Smith, & Brown, 2010). Urea formaldehyde and phenol formaldehyde are widely used as adhesives for construction of composite wood panels such as particle board or fiber board which are used for interior wood panels

of homes and for furniture. Additionally, adhesive formulations may contain other VOCs that pose environmental and health concerns such as trichloroethane and toluene which are used as solvents for adhesive application (Li et al., 2012). Environmental regulations are becoming more stringent with regards to VOC limits and green construction programs such as LEED offer credits for use of low-emitting products in new construction (Bosik, 2012). Therefore, high-performance natural based glues will become increasingly important.

Other ecological factors that should be considered include the degree of treatment necessary for waste from adhesives processing and the ability to reuse the materials onto which the adhesive is ultimately applied (Onusseit, VonByern, & Grunwald, 2010; Shuttleworth, Clark, Mantle, & Stansfield, 2010). Finally, it should not be overlooked that as petroleum stocks are gradually depleted, the cost of petro-chemicals will rise accordingly, further driving the need for renewable "green" adhesives.

2.1.3 Concepts

Although the concept of adhesion is very simple, the science and mechanistic understanding of adhesives can be very complicated. Some basic terminology, concepts, and theory related to adhesives are provided in the following section.

Adhesion is the force responsible for the joining of dissimilar surfaces. The objects being joined are referred to as the *adherends* and the substance responsible for adhesion is referred to as the *adhesive*. Adhesion cannot be discussed without cohesion, as it plays

an equally important role in adhesives. Cohesion can be thought of as internal adhesion, or the force that joins similar surfaces.

Higher energy exists at the surfaces of solid and liquid materials due to the inability of surface molecules to interact symmetrically with surrounding molecules as those in the material bulk do; resulting in an imbalance of intermolecular interactions for surface molecules. This energy associated with the potential for intermolecular interaction of surface molecules is known as the *surface energy* of a material.

When two dissimilar surfaces are in contact there exists an interfacial energy. After work is applied to separate these two surfaces, two new surfaces with distinct surface energies are the result, but the interfacial energy is no longer present. The sum of the surface energies of two materials minus the interfacial energy gives rise to the term *work of adhesion*.

While work of adhesion provides a fundamental measure of adhesive intermolecular forces, it is not a straight forward answer to the practical strength of adhesion between two surfaces because the mechanical response of the adhesive, substrate, and adhesive-substrate interface also factor into adhesive strength. In most cases this "practical adhesion" is measured by conducting one or several types of stress tests where the adhesive strength is equal to the amount of stress required for adhesive failure. Common stress tests include shear tests and tensile tests. Adhesive strength is often reported as the

result of a stress test. Expressions relating adhesive strength to work of adhesion can be used to gain a more fundamental picture of a given adhesive system (Packham, 2005). An important concept in the practical application of adhesives is the *weak boundary layer*. The weak boundary layer arises from any weakly covalent layer of matter associated with a surface that prevents the immediate contact of adhesive and adherend and ultimately leads to premature adhesive failure. For example, wet surfaces pose a problem for adhesives due to the presence of a weak layer of water molecules (Anderson et al., 2010). Additionally, dirt, grease, dust, or other impurities that can coat surfaces may act as a weak boundary layer (Waite, 2002). Therefore, surface preparation/treatment is often a necessary operation prior to adhesive application.

2.1.4 Mechanisms of Adhesion

The mechanisms responsible for adhesion can be broadly split into mechanical and chemical adhesive forces.

2.1.4.1 Mechanical Adhesion

Mechanical adhesion refers to interlocking between adherend surfaces on the microscopic level. Although mechanical forces have been shown to be significant in a few specific applications, it is generally disregarded as an important mechanism of adhesion (Pocius, 2002).

2.1.4.2 Chemical Adhesion

Chemical adhesion refers to a host of different forces, chemical in nature, responsible for adhesion. These forces include ionic bonds from electrostatic interactions, physical

bonds from van der Waals interactions, and chemical bonds from electron pair sharing (Pocius, 2002).

Electrostatic forces are those that arise between two charged atoms or molecules. Atoms or molecules with like charges repel each other while those with dissimilar charges attract. Electrostatic forces are considered the second strongest interaction between atoms or molecules (Pocius, 2002).

Van der Waals interactions are based mainly on differences in electron densities on or between molecules. These interactions include dipole-dipole (including hydrogen bonding) and dipole-induced dipole interactions, and dispersion forces (Pocius, 2002). Electron pair sharing interactions encompass both covalent and donor-acceptor interactions. Covalent bonds are the result of electron pair sharing between atoms in a molecule. Covalent bonds are considered the strongest interaction between atoms or molecules. Acid-base interactions are a special case of donor-acceptor interactions where interaction occurs between an electron-deficient Lewis acid and the lone electron pair of a Lewis base. Acid-base interactions have been extensively studied and deemed to play an important role in adhesion (Pizzi & Mittal, 2003; Pocius, 2002).

2.1.5 Adhesion in Nature – Mussel Adhesion

In nature, a wide variety of organisms naturally produce unique adhesives to aid their survival. One such adhesive that has been extensively studied is that of the marine mussel from the genus *Mytilus* (Bruce P. Lee, 2006; Waite, Andersen, Jewhurst, & Sun,

2005). Marine mussels depend on adhesion in order to permanently cling to substrates such as rock in order to endure the harsh environment of the shores where they reside. Such an adhesive must be able to function on rough, untreated surfaces submerged in turbulent marine waters (Sagert, Sun, & Waite, 2006). Significant research and interest in developing materials based on the marine mussel adhesive spur from its ability to quickly set, effectively displace water from the attachment surface, withstand a range of temperatures and salinity, and adhere to practically any type of surface (Crisp, Walker, Young, & Yule, 1985; Deming, 1999; Lin et al., 2007; Waite, 2002). The utility of mussel adhesives have yet to be rivaled by any synthetic adhesives (Sever, Weisser, Monahan, Srinivasan, & Wilker, 2004).

In order to scout out surfaces for adhesion, mussels have an organ called a foot. At the base of the foot is a stem-like structure known as the byssus where a collection of collagenous threads meet. The individual threads are known as byssal threads and are responsible for the adhesion of the mussel to surfaces. Byssal threads extend radially from the underside of the organism to the surface of attachment. The area of a byssal thread furthest from the mussel is known as the distal end which ends with the plaque, where adhesion between thread and surface occurs (Waite et al., 2005).

The thread and plaque are made up of a variety of proteins. The threads themselves are primarily composed of collagen-like proteins, preCol-P and preCol-D. PreCol-P predominates at the proximal end (closest to the byssus) and preCol-D at the distal end of the byssal thread (Deming, 1999). The difference in amount of preCol-P and preCol-D is

thought to be responsible for a mechanical gradient that exists along the thread. The proximal end is elastic in nature whereas the distal end is more rigid, with an intermediate stiffness between the two regions (Deming, 1999; Sagert et al., 2006). The stiffness gradient along the thread is thought to help dampen contact deformation between the soft mussel body and rigid support surface (Sagert et al., 2006). The distal end of the byssal thread spreads into the plaque like a series of roots. Within the plaque are a number of proteins, namely mussel foot proteins (mfp) 2-5 that form a solid foam-like adhesive. Mfp-3 and -5 are responsible for surface interactions while mfp-2 and -4 are responsible for forming the rigid, cohesive core of the plaque (Stewart, Ransom, & Hlady, 2011; Waite et al., 2005; Wiegemann, 2005). Finally, surrounding the entire thread and plaque, excluding the attachment site, is a protective cuticle comprised mainly of mfp-1 (Sagert et al., 2006).

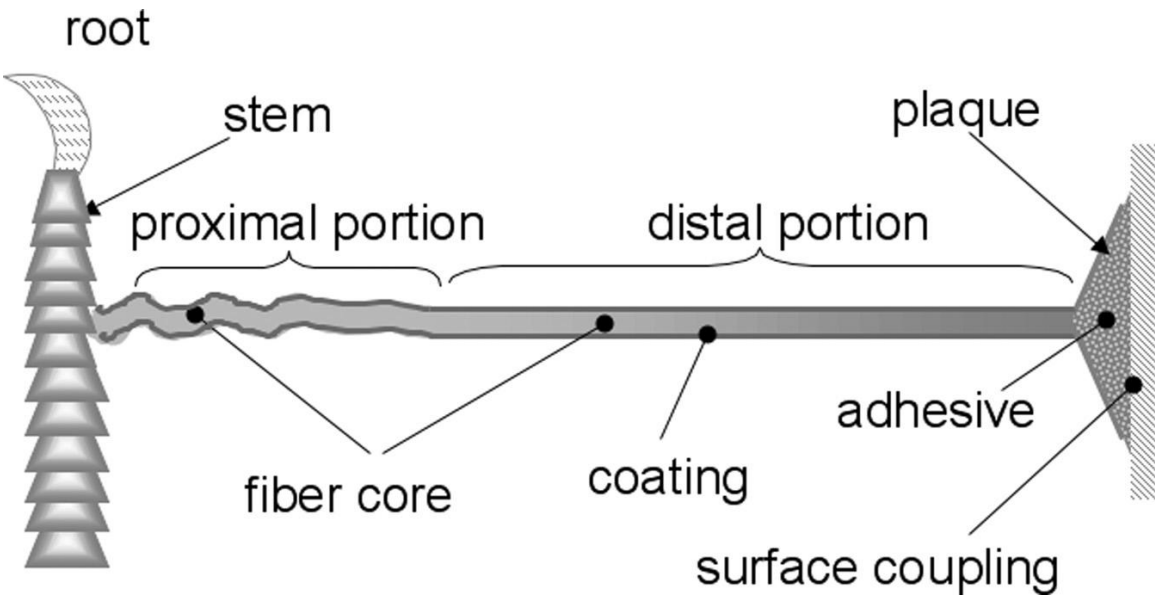

Figure 2.2 Basic diagram of a mussel byssal thread extending from the stem (within mussel) to attachment surface (Waite et al., 2005).

In all of the mussel foot proteins, there exist post- or co- translationally modified amino acids. These modified amino acids include 3,4-dihydroxyphenylalanine (DOPA), *o*-phosphoserine, 4-hydroxyproline, 3,4-dihydroxyproline, and 4-hydroxyarginine (Wiegemann, 2005). DOPA and phosphoserine are implied in the actual adhesive properties of the plaque based on their abilities to interact strongly with metals and metal oxides (Haemers, Koper, & Frens, 2003). DOPA has received the most attention because it is universally present in mussel foot proteins as well as the adhesion proteins of some other organisms (Stewart et al., 2011). Furthermore, DOPA content is especially high in the interfacial plaque proteins mfp-3 and -5, where it is present up to about 20 mol% and 30 mol%, respectively (Sagert et al., 2006). DOPA is also found up to about 15 mol% in mfp-1 where it is thought to facilitate cohesion and hardening of the protective cuticle (H. Lee, Scherer, & Messersmith, 2006; Rischka et al., 2010)

2.2 DOPA Chemistry

DOPA is a post-translationally modified amino acid that arises from hydroxylation of tyrosine. DOPA is generally understood to be the primary facilitator of both adhesion and cohesion of mussel foot proteins. However, the mechanisms for adhesion and cohesion are still not fully established. Moreover, DOPA's adhesive mechanisms are generally less understood than its cohesive mechanisms (Bruce Lee, Dalsin, & Messersmith, 2006). DOPA is also attributed to the water-resistant adhesion of mussel proteins (M. Yu, Hwang, & Deming, 1999) and the ability of mussel plaques to adhere to a wide variety organic and inorganic surfaces.

2.2.1. Redox and Metals

The underlying principle behind the overall adhesive and cohesive properties of mussel adhesives is the oxidation/reduction of DOPA and the maintenance of a balance between oxidized and reduced forms. DOPA readily undergoes oxidation to its highly reactive DOPA-quinone and –semiquinone forms, especially in basic conditions (Haemers et al., 2003). *In vivo*, it is thought that the mussel employs the enzyme catechol oxidase to catalyze DOPA oxidation. *In vitro*, the enzyme tyrosinase has been used to facilitate oxidation of DOPA in addition to chemical oxidants (Haemers et al., 2003; Yamada et al., 2000)

Experiments have shown that both increasing pH and increasing presence of oxidizing agents leads to decrease in mussel adhesive performance on metal oxide surfaces while increasing adhesive strength on organic surfaces, specifically amine-functionalized surfaces (H. Lee et al., 2006; J. Yu, Wei, Danner, Israelachvili, & Waite, 2011). Therefore, on metal oxide surfaces, it is supposed that in its reduced form DOPA aids in adhesive interactions while the oxidized form is primarily involved in cohesive interactions (Wilker, 2011). The relationship between oxidized DOPA and its adhesion to organic surfaces is less clear.

As with any adhesive, a balance of cohesion and adhesion is necessary for optimal adhesive performance. Thus, balance between oxidized and reduced forms of DOPA must be maintained in order for proper adhesion to exist. In nature, it has been suggested that this balance is maintained by secretion of thiol-rich mfp-6 along with the DOPA-rich

mfps. Through oxidation of the thiol groups, DOPA-quinone can be reduced to restore an optimal balance of adhesive and cohesive forms of DOPA (J. Yu, Wei, Danner, Ashley, et al., 2011).

Mussels are able to accumulate metals in their byssal threads. The plaque, specifically, contains metal ions including copper, iron, zinc, and manganese concentrated up to 100,000 times greater than in ocean water. These metal ions play many important roles in DOPA chemistry. First, transition metals provide a route of cross-linking between DOPA-containing proteins (Monahan & Wilker, 2004). More specifically, it is proposed that iron atoms are primarily responsible for protein cross-linking by creating a tris-DOPA complex (Sever et al., 2004; Zeng, Hwang, Israelachvili, & Waite, 2010). Another important role of transition metal ions is they facilitate oxidation of DOPA by aligning the aromatic side chain of DOPA molecules thus lowering the energy of oxidation. Finally, transition metal ions provide a center for interactions between DOPA-proteins and surfaces, thereby facilitating adhesion (Brooksby, Schiel, & Abell, 2008).

2.2.2 DOPA in Adhesion

DOPA in its reduced form is primarily responsible for adhesive interactions with surfaces (Wilker, 2011). Polar interactions between the hydroxyl groups present on the side chain of DOPA and the adhesion surface are presumably the reason for these interactions (Frank & Belfort, 2001). DOPA's hydroxyl groups can participate in hydrogen binding, as either donor or acceptor, with electrophilic groups along polar, hydrophilic surfaces. Additionally, it has been shown that DOPA's hydroxyl groups are able to strongly

complex with metals and minerals on inorganic surfaces (Wiegemann, 2005). Furthermore, the hydrogen bonding activity of DOPA's catecholic side chain may allow DOPA to compete with water for interactions on polar surfaces (Bruce Lee et al., 2006).

It is proposed that π-π orbital interactions between the aromatic ring of DOPA and other aromatic groups may account for the ability of mussels to adhere to organic surfaces (Frank & Belfort, 2001; Wiegemann, 2005). It has also been suggested that covalent bonds formed by reaction of oxidized DOPA with organic functional groups could also be responsible for adhesion of mussel plaques to organic surfaces. An example of this is DOPA-quinone forming a covalent bond with surface amine groups via Michael addition-type reactions (Bruce Lee et al., 2006; H. Lee et al., 2006; J. Yu, Wei, Danner, Israelachvili, et al., 2011). The catechol side group of DOPA is also attributed to the mucoadhesive properties of mussel adhesive proteins (Schnurrer & Lehr, 1996).

2.2.3 DOPA in Cohesion

The oxidized form of DOPA (DOPA-quinone) is primarily responsible for cross-linking interactions that give rise to the cohesive properties of mussel adhesives. Yu et al. proposed many possible mechanisms for DOPA-mediated cross-linking including aryl coupling, metal chelation, imine formation, and Michael addition (M. Yu et al., 1999). In aryl coupling, DOPA-quinone is partially reduced by unoxidized DOPA resulting in two reactive radicals that form a diDOPA complex. Similar to the way that metal ions such as copper facilitate adhesion by cross-linking DOPA and surface functional groups, they can also cause cross-linking between DOPA residues not involved in surface interactions,

resulting in cohesion (M. Yu et al., 1999). Finally, the most popular explanation for DOPA cross-linking is Michael addition reactions. In Michael additions, the double bonds of the aromatic ring are susceptible to nucleophilic attack (Sagert et al., 2006). The free amine groups on the side chains of lysine and histidine as well as free thiol groups from cysteine residues in proteins are all nucleophilic candidates for Michael addition to DOPA-quinone (Sagert et al., 2006). Thiol groups are preferentially added to DOPA-quinones over the amine groups of lysine and histidine (Sagert et al., 2006).

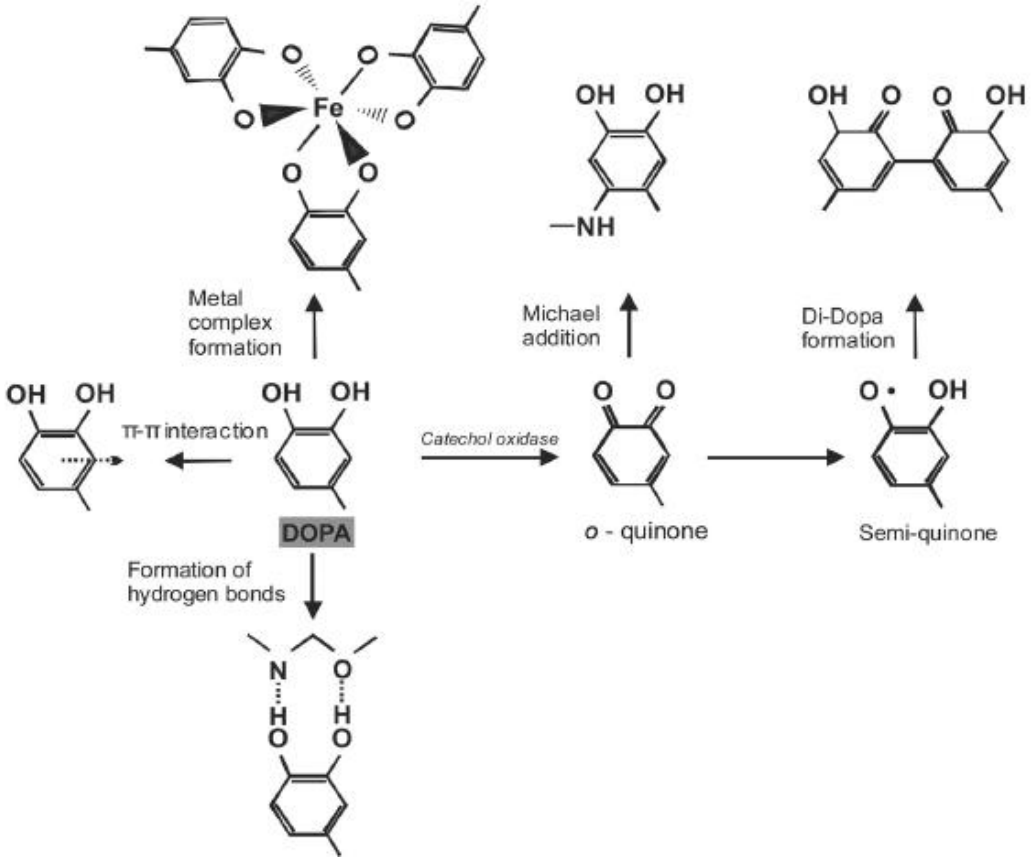

Figure 2.3 Adhesive and cohesive interactions of DOPA (Wiegemann, 2005)

2.3 Mussel-Mimetic Adhesive Polymers

There are essentially two approaches for creating mussel-mimetic adhesive polymers. The first approach is to directly incorporate DOPA or another catechol-containing molecule onto the backbone of a polymer. This can be accomplished by reacting a functional group of the catechol monomer with a functional group on the polymer. The second approach incorporates DOPA or one of its analogs onto a monomer which is subsequently polymerized, usually with another monomer, in order to achieve polymers of various catechol contents.

Attaching DOPA to another molecule without affecting the functionality of DOPA requires that its catechol group is excluded from any reactions. DOPA exists in mfps as a member of a chain of amino acids linked by peptide (amide) bonds which are formed between the amine group or N-terminus of one amino acid and the carboxyl group or C-terminus of another. Amide bonds can just as well be made between the amine or carboxyl groups of DOPA and reactive groups of a monomer or polymer to form DOPA-functionalized polymers.

Because the adhesion/cohesion roles of DOPA are attributed to the catechol group, other catechol-containing molecules can, and have been successfully used to create mussel-mimetic adhesives. For simplicity, in many cases it is actually preferable to use a catecholic molecule having just one reactive group on its side-chain as opposed to two reactive groups like DOPA. Some of these DOPA analogs include 3,4-dihydroxyphenethylamine (dopamine) , 3,4-dihydroxybenzoic acid, caffeic acid, and 3,4-

dihydroxybenzaldehyde. Many researchers have successfully functionalized different polymers with catecholic groups using a variety of approaches. The following section summarizes the work that has been done so far based on the conjugation chemistry used.

2.3.1. Catechol-Functionalized Polymers

2.3.1.1 Benzotriazoles

Benzotriazoles have been widely used as organic coupling reagents. In the case of peptides, benzotriazoles function by activating the carboxyl group, making it prone to nucleophilic attack by an amine group (Scott, 2009). Because each amino acid in the reaction has one carboxylic acid and one amine group, the amine group of the activated amino acid requires blocking to ensure the desired reaction occurs.

Utilizing this chemistry, several researchers from the Messersmith Research Group developed DOPA-functionalized adhesive hydrogels. In each case *tert*-butyloxycarbonyl (Boc)-protected DOPA was reacted with triethylamine (Et_3N), 1-hydroxybenzotriazole (HOBt), and *O*-(benzotriazol-1-yl)-*N*,*N*,*N*',*N*'-tetramethyluronium hexafluorophosphate (HBTU) in a solvent system of dichloromethane (DCM) and dimethylformamine (DMF) to covalently link the carboxyl group of DOPA to the amine groups of various polymers. Above 80% coupling efficiency was achieved when linking DOPA to linear and four-armed poly(ethylene glycol) (PEG_4) (BP Lee, Dalsin, & Messersmith, 2002). A following study synthesized DOPA-PEG_4 using the same materials and reported DOPA content of 6% by weight (Burke, Ritter-Jones, Lee, & Messersmith, 2007). DOPA was

also grafted onto a triblock copolymer consisting of PEG sandwiched between methacrylated poly(lactic acid) and glycine, referred to as G-PPM, in which case 2% DOPA content by weight was achieved (BP Lee et al., 2006). Guvendiren et al. developed modified methacrylic triblock copolymers consisting of poly(methacrylic acid) (PMAA) sandwiched between poly(methyl methacrylate) (PMMA) end blocks with DOPA contents of 0, 20, and 40 mol % . In this case, the N-terminus of DOPA methyl ester was incorporated into the PMAA portion of the triblockcopolymer (Guvendiren, Messersmith, & Shull, 2008).

In a similar manner, Messersmith et al. functionalized four-arm PEG amine with 3,4-dihydroxyhydrocinnamic acid (DHCA). The group utilized their mussel-inspired adhesive to aid in extrahepatic islet transplantation in mice. The adhesive remained intact with adipose tissue for up to one year and resulted in minimal inflammatory response; a testament to the capability of catechol-functionalized polymer adhesives (Brubaker, Kissler, Wang, Kaufman, & Messersmith, 2010).

2.3.1.2 Carbodiimide

A popular chemistry for the conjugation of dopamine with carboxyl-containing polymers is 1-ethyl-3-(3-dimethylaminopropyl)carbodiimide hydrochloride (EDC) cross-linking. EDC is a water-soluble zero-length crosslinker that can function between pH 3.5 – 8 at room temperature (Hattori, Yang, & Takahashi, 1995; Nakajima & Ikada, 1995); making it convenient to use in many biochemical reactions. Peptide bond formation by EDC

begins with reaction of a free carboxyl group with EDC to form the active intermediate o-Acylisourea. Next, o-acylisourea undergoes nucelophilic attack by a primary amine which leads to formation of the peptide bond and isourea byproduct (Hermanson, 2008).

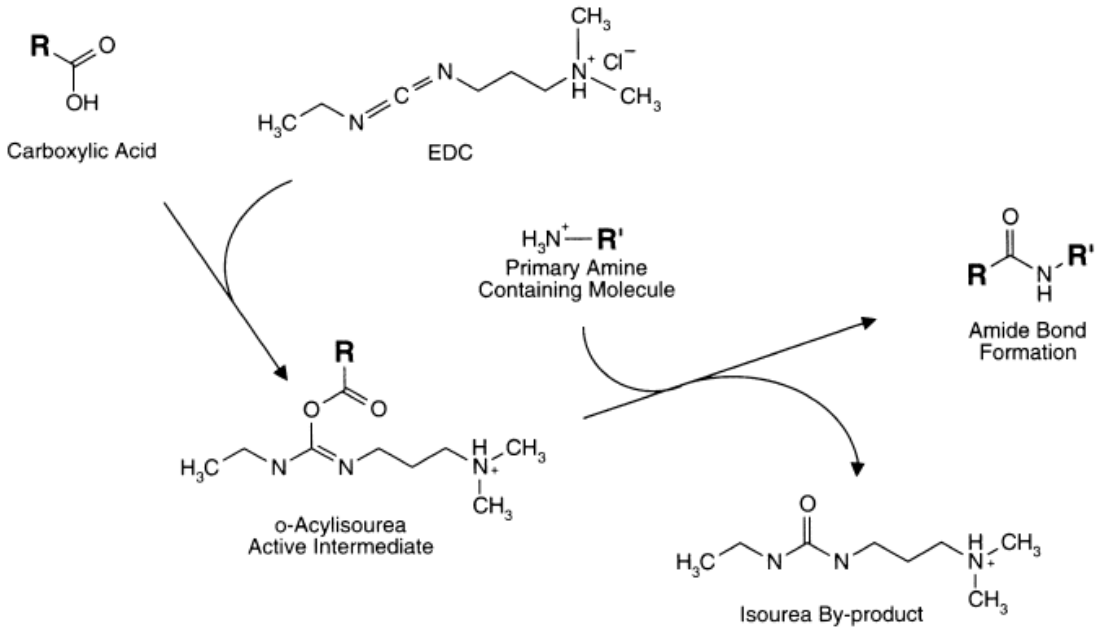

Figure 2.4 Mechanism for amine-to-carboxyl conjugation by EDC (Hermanson, 2008)

Higher yields of amide bond formation using EDC can be achieved by adding N-hydroxysulfosuccinimide (sulfo-NHS) or N-hydroxysuccinimide (NHS). NHS creates a more soluble, stable, and reactive intermediate than o-acylisourea and prevents unwanted hydrolysis or formation of N-acylurea, thus increasing the yield of conjugation. Furthermore, EDC/Sulfo-NHS systems allow for two-step reactions in which the compound with the desired crosslinking carboxyl group is first activated by incubation with EDC/Sulfo-NHS, followed by isolation of the activated compound and incubation with the compound containing the desired crosslinking amine group. This way, the

reaction is more controlled and undesired self-polymerization can be avoided (Hermanson, 2008).

Wu et al. covalently bound dopamine to poly(acrylic acid) (PAA) using EDC chemistry. The group determined the catechol content of their conjugate to be about 12%. The dopamine-PAA ultimately served as a cohesive agent to form stable, multilayer, thiol-modified films composed of poly(allylamine hydrochloride) (Wu et al., 2011).

Most recently, Karabulut et al. employed EDC to covalently modify carboxymethyl cellulose nanofibrils (CNFC) with dopamine in order to create strong layer-by-layer films with improved adhesion. The group was able to functionalize about 76% of the carboxyl groups with dopamine. Interestingly, the group found that the addition of NHS to the EDC cross-linking reaction did not enhance the extent of conjugation. Modification of CNFC with dopamine was found to lower the colloidal stability of the polymer dispersions, most likely due to the loss of carboxyl groups and consequent loss of overall charge in the system (Karabulut, Pettersson, Ankerfors, & Wagberg, 2012).

Liu and Li grafted dopamine onto soy protein isolate (SPI) using EDC chemistry in effort to enhance the SPI for wood bonding. By controlling the concentrations of EDC and dopamine, the two researchers obtained SPI-dopamine conjugates with varying dopamine content. Plywood samples bonded with the conjugates exhibited significantly greater shear strengths and water resistance compared to regular SPI and actually exhibited performance comparable to traditional urea- or phenyl-formaldehyde resins. The group

found that higher dopamine content led to greater shear strength and moisture resistance in prepared wood samples. Additionally, the group showed that the hydroxyl groups of unoxidized dopamine are necessary for good adhesive strength and moisture resistance (Liu & Li, 2002).

2.3.1.3 Schiff Base

DOPA's amine group has also been utilized in conjugation via Schiff base reactions. When a primary amine reacts with aldehyde, ketone, or glyoxal groups they may form a Schiff base/imine intermediate which can then be further converted to a secondary amine bond (Hermanson, 2008).

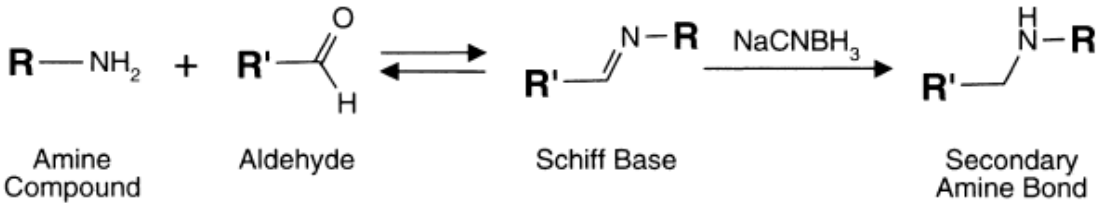

Figure 2.5 Simplified Mechanism of Amide Bond Formation via Schiff Base

Hoffman et al. designed bioadhesive bone glues comprised of starch or dextran, chitosan, and DOPA. First, starch or dextran was oxidized to provide reactive aldehyde groups. For systems including DOPA, the starch/dextran was oxidized in its presence in order to promote Schiff base reactions between the alehyde groups of the oxidized starch/dextran and the amine group of DOPA. Finally, the starch/dextran-DOPA complex was oxidized in the presence of low molecular weight chitosan. Cross-linking was achieved in two

ways: aldehyde groups of oxidized starch/dextran interacted with amino groups of chitosan, and/or the oxidized DOPA (DOPA-quinone) reacted with the amino groups of chitosan. Unfortunately, no data was offered concerning the DOPA content of the final adhesive (Hoffmann et al., 2009). Similarly, an adhesive polymer with up to 12% DOPA content by weight was developed by modifying oxidized dextran with DOPA, followed by conjugation with star PEG to form a hydrogel (Shazly et al., 2010).

Most recently, Schiff base reaction was used by Ni et al. to form a catechol-chitosan conjugate from 3,4-dihydroxy benzaldehyde and chitosan. In this case, the aldehyde group of the 3,4-dihydroxy benzaldehyde was utilized for Schiff base reaction with the amine groups on chitosan. The researchers reported a degree of substitution of 52% with respect to conjugated catechol groups. The catechol-chitosan conjugate demonstrated adhesion to iron nanoparticles over which a layer of the conjugate could be formed. Free catechol groups on the outside of the catechol-chitosan-iron nanoparticles were then used to immobilize enzyme. These nanoparticles dispersed well in aqueous solution and could be easily recovered by magnets (Ni et al., 2012).

2.3.2 Polymerization of Catechol-Functionalized Monomers

2.3.2.1 Condensation

Mehdizadeh et al. synthesized a mussel-inspired adhesive in a one-step polycondensation reaction with monomers of citric acid, PEG, and dopamine or L-DOPA. The reaction

was carried out under vacuum at 140-160°C for the duration of time required for a particular degree of polymerization. Catechol content of the polymers could be varied by adding different amounts of dopamine or L-DOPA to the reaction mixture. The polymers formed from the reaction were then crosslinked to form adhesive hydrogels by oxidizing the catechol moieties with sodium periodate. The citric acid units served two important roles: to promote biodegradable ester bonds and to act as a conjugation site for the amine group of dopamine or L-DOPA (Mehdizadeh, Weng, Gyawali, Tang, & Yang, 2012). These adhesives exhibited wet tissue strength up to 8 times greater than traditional fibrin glue.

Kaneko et al. developed an adhesive copolymer based on polycoumarates, DHCA and 4-hydroxycinnamic acid (HCA). DHCA and HCA monomers were polymerized at 200°C in the presence of sodium acid phosphate catalyst and absence of oxygen. The poly(DHCA-co-4HCA) adhesive demonstrated impressive adhesive strength compared to conventional super glue on inorganic and organic surfaces. However, no information was provided concerning the compatibility of the adhesive with wet surfaces (Kaneko et al., 2011).

2.3.2.2 Ring-Opening Addition of N-Carboxyanhydrides

Deming et al. synthesized synthetic polypeptides containing lysine and DOPA by creating N-carboxyanhydrides of lysine and DOPA by phosgenation, followed by ring-opening addition which was initiated by sodium *tert*-butoxide. For these reactions, the

hydroxyl groups of DOPA and the amine side-group of lysine were protected by carbobenzoxyl groups which were removed after polymerization. Synthetic poly(lysine-DOPA) polypeptides with up to 20% DOPA content were synthesized and showed adhesive strengths ten times greater than poly(L-lysine). Adhesive strength of the poly(lysine-DOPA) polypeptides could be further enhanced by crosslinking via oxidation of DOPA. Lap-shear adhesion tests of the polymer demonstrated relatively weak adhesive capability between plastics (>0.5 MPa), but much greater adhesion between glass and metal (up to~2.5 MPa and ~5 MPa, respectively) (M. Yu & Deming, 1998).

2.3.2.3 Reactive Anhydride or Acid Chloride

Lee et al. combined the adhesive strategies of both geckos and mussels to create a reversible, wet-dry adhesive. Poly dimethyl siloxane was microfabricated into an array of pillars which were then coated with a mussel-mimetic adhesive. The mussel-mimetic adhesive was formed by first synthesizing dopamine methacrylate via nucleophilic attack of the amine group of dopamine on methacrylic anhydride. The reaction was able to take place in a high pH aqueous environment without oxidation of dopamine because a high concentration of sodium borate was provided to protect the catechol group. Dopamine methacrylate was then copolymerized with methoxyethyl acrylate to yield poly(dopamine methacrylamide-co-methoxyethyl acrylate). The mussel-mimetic adhesive was designed based on the criteria that catechol content of the synthetic adhesive must be high (~27 mol %), and the polymer should have low solubility in water (H. Lee, Lee, & Messersmith, 2007).

Lee et al also demonstrated conjugation of DOPA with methacroyl chloride by nucleophilic attack of the amine group of DOPA with the acid chloride group of methacroyl chloride in an alkaline aqueous environment containing borax to protect DOPA from oxidation. To synthesize the polymer, the hydroxyl groups of DOPA's catechol side chain were first blocked by t-butyldimethylsilyl chloride. The DOPA-methacrylate monomers were then photopolymerized with PEG-diacrylate to form an adhesive hydrogel. DOPA content was found to be about 15 µgram per gram of gel (BP Lee, Huang, Nunalee, Shull, & Messersmith, 2004).

2.3.2.4 Vinyl Polymerization

Westwood et al. synthesized mussel-mimetic styrene based polymers by copolymerizing styrene and 3,4-dimethoxystyrene using *n*-Butyllithium to initiate polymerization of the vinyl groups. Synthesis and recovery of the copolymer was followed by demethylation of the methoxy groups by BBr_3 to furnish the active catechol. By varying the feed ratio of 3,4-dimethoxystyrene:styrene, polymers of varying catechol content could be obtained. Lap-shear adhesive tests were carried out with poly[(3,4-dihydroxystyrene)-*co*-styrene] of MW = 16,000 and 3,4-dihydroxystyrene:styrene = 3.4:96.6 which showed significantly stronger adhesion than pure styrene polymers of comparable MW. Adhesion of the copolymer was also tested after crosslinking by treatment with various oxidizing agents. Adhesive strength was shown to increase upon crosslinking, with a maximum adhesive strength of 1.2 MPa attained (Westwood, Horton, & Wilker, 2007).

2.3.3 Characterizing DOPA-polymer Conjugates

2.3.3.1 DOPA Content

A relatively simple and common method for DOPA-content determination of water-soluble DOPA compounds is a colorimetric test based on the work of Waite and Benedict (Waite & Benedict, 1984). When catecholic compounds are oxidized, they produce a red-orange color which is quantified by UV-vis absorbance at 500 nm (BP Lee et al., 2006). Typically, a nitrite reagent and NaOH are used to induce oxidation (Guvendiren et al., 2008; Huang, Lee, Ingram, & Messersmith, 2002; BP Lee et al., 2002; BP Lee et al., 2004). This method is especially useful in situations where other aromatic groups may be present as it is specific to catechols.

As with most aromatic compounds, catechol has a characteristic UV-vis absorbance at 280 nm. While this method is not fit for quantifying DOPA in compounds containing other aromatic amino acids and DNA (due to absorbance overlap), it has been used for DOPA quantification in DOPA- and dopamine-functionalized polymers where the catechol moiety is the sole contributor to absorbance at 280 nm (BP Lee et al., 2006; Wu et al., 2011). However, care must be taken to prevent any oxidation of the sample for this method to yield accurate results.

DOPA content can also been determined with proton nuclear magnetic resonance spectroscopy (^{1}H NMR). The three protons in the aromatic ring of DOPA have a distinct

chemical shift around 6.4-6.9 in deuterium oxide (BP Lee et al., 2006; Shazly et al., 2010; Wu et al., 2011). From a standard curve, the integral value of the peaks may then be used to determine the concentration of catechol in solution and ultimately the catechol content of the conjugate (% wt.). Additionally, if the monomer units of the polymer have a unique proton signal, then a direct value for the degree of catechol substitution may be obtained by calculating the ratio of the integral values of catechol to monomer (% mol).

2.3.3.2 Verification of Conjugation

In many instances, it may be useful to verify that conjugation between catechol and polymer is achieved through the desired chemical bond. Spectroscopic analysis of catechol-modified compounds provides a relatively easy way to assess successful conjugation thanks to the ability to detect specific bond types. Conjugation can also be confirmed by comparing the abundance of free attachment sites before and after conjugation reaction.

FTIR spectroscopy was used to verify the amide bond formed by cross-linking dopamine to poly(acrylic acid) by EDC, evident by the presence of an amide II band (Wu et al., 2011). Conjugation of dopamine to carboxymethyl cellulose nanofibrils by Karabulut et al. was evident by loss of intensity of the peak for asymmetric stretching vibrations of deprotonated carboxyl groups and the appearance of Amide I bands (Karabulut et al., 2012).

Proton NMR can also be used to detect specific bonds. Shazly et al. used ^{1}H NMR to verify whether Schiff base reaction occurred between oxidized dextran and DOPA by detecting the resulting imine proton (Shazly et al., 2010).

2.3.4 Performance of Mussel-Inspired Adhesives

In most cases, incorporation of DOPA or catechol-containing moieties into polymer or copolymer systems was associated with increased moisture resistance and higher adhesive strengths (Guvendiren et al., 2008; Karabulut et al., 2012; BP Lee et al., 2006; H. Lee et al., 2007; Liu & Li, 2002; Mehdizadeh et al., 2012). In only one instance did incorporation of DOPA have a negative effect on the adhesive (Hoffmann et al., 2009). However, it should be noted that in the later study the adhesive was applied to bovine femora, whereas titanium, wood, or polymer surfaces were used in the other studies. Therefore, the benefits of mussel-inspired adhesives may be dependent on the application and surface type.

In general, higher catechol content in mussel-mimetic polymers is associated with greater adhesive capabilities (BP Lee et al., 2006; Liu & Li, 2002). As previously noted, mussel foot proteins can contain up to 30 mol % DOPA. Most of the adhesives mentioned in this review fail to achieve such an extent of catechol functionalization so it is not clear whether the adhesive benefits of catechol moieties continue with increasing catechol content indefinitely. There may be some optimal degree of catechol functionalization for mussel-mimetic adhesives. Furthermore, the optimal catechol content may depend on the nature of the particular adhesive system.

As with most adhesives, molecular weight can greatly affect the adhesive abilities of DOPA-functionalized polymers. For a synthetic poly(lysine-DOPA) peptide, the adhesive strength demonstrated by the polymer with MW = 255,000 was over twice that of MW = 98,000 (M. Yu & Deming, 1998). Therefore, molecular weight should be fine-tuned for maximum adhesion of mussel-mimetic polymers.

The adhesive performance of mussel-inspired adhesives has been shown to be dependent on pH and oxidation state of the incorporated catechol group. Increasing pH was associated with weaker adhesive strengths to titanium; presumably due to oxidation of DOPA's catechol group (Guvendiren et al., 2008). Similarly, oxidized DOPA-adhesives were shown to exhibit lower work of adhesion when compared to their unoxidized counterparts (BP Lee et al., 2006). This work indicates that the reduced form of the catechol group is necessary for strong adhesion of mussel-mimetic polymers to titanium surfaces. However, crosslinking of mussel-mimetic polymers by oxidation of the incorporated catechol groups has been shown to significantly enhance the adhesive strength and moisture resistance of mussel-mimetic adhesives (Westwood et al., 2007; M. Yu & Deming, 1998). A balance of reduced and crosslinked forms of catechol in mussel-mimetic adhesives is therefore necessary to ensure there is an adequate amount of both adhesive interactions, between the hydroxyl groups of catechol and the adherend, and cohesive interactions, through intermolecular crosslinking, for maximum moisture-resistance and adhesive strength.

2.3.5 DOPA for Adhesive Polymer Crosslinking

In addition to its adhesive functionality, DOPA is also attractive for facilitating cohesive forces within adhesive polymer networks through oxidation of its catechol side group. Oxidized DOPA can undergo various reactions, therefore a number of cross-linking pathways exist depending on the chemical make-up of the adhesive polymer.

2.3.5.1 Chemical Oxidants

Periodate has widely been used to induce crosslinking of mussel-inspired adhesives through oxidation of their catechol groups.

Lee et al. developed adhesive polymers based on DOHA, PEG, and polycaprolactone (PCL). Periodate was used to induce cross-linking of the adhesive polymers. The group found that there was an optimal degree of crosslinking for maximum adhesive strength and work of adhesion (Murphy, Vollenweider, Xu, & Lee, 2010).

Messersmith et al. prepared periodate-loaded liposomes as a means to crosslink DOPA-modified PEG polymers. The prepared liposomes had a bilayer melting transition of 37° C (physiological conditions). The researchers were able to thermally trigger the release of periodate in a mixture of liposomes and DOPA-modified PEG to create an adhesive hydrogel. The cross-linked DOPA-PEG hydrogel exhibited significantly greater shear strength than a commercially available fibrin adhesive when applied to porcine skin.

This technology could be applied in the biomedical field as a unique method for inducing cross-linking of catechol-functionalized tissue adhesives (Burke et al., 2007).
Other oxidizing agents such as H_2O_2, NaOH, can also be used to trigger catechol crosslinking (Guvendiren et al., 2008).

2.3.5.2 Metals

In the work by Karabulut et al., the researchers used iron ions to induce catechol coordination complexes and thus increase the internal film strength of their dopamine-carboxymethyl cellulose nanofirbil conjugates. The presence of Fe^{3+} increased the wet adhesion force of the conjugate to inorganic surfaces up to three times when compared to water or NaCl solution. Additionally, the group observed stable wet adhesion of a single layer CNFC-dopamine film to a polystyrene petri dish after solvent-casting in $FeCl_3$, whereas a pure CNFC film failed to adhere (Karabulut et al., 2012).

Westwood et al. found that dichromate anion was an extremely effective crosslinking agent for poly[(dihydroxystyrene)-*co*-styrene] polymers. In lap-shear tests of their polymer, those crosslinked by dichromate ions resulted in the highest adhesive forces. Crosslinking of the catechol-containing polystyrene adhesive was also demonstrated using permanganate ion; however, it was much less effective than dichromate or periodate (Westwood et al., 2007).

2.3.5.3 Enzymes

Yamada et al. developed adhesive systems based on chitosan, dopamine, and tyrosinase. The group showed that a dilute solution of chitosan, in the presence of dopamine and tyrosinase, could cross-link to form a viscous, water-resistant, adhesive gel. The cross-linking was attributed to the oxidation of dopamine by tyrosinase to dopamine-quinone which then presumably underwent Schiff base or Michael-type reactions with the amine groups of chitosan. Adhesive strength increased by increasing chitosan concentration, molecular weight of chitosan and concentration of amino groups. On glass slides, shear strengths of up to 400 kPa were achieved; greater than that of chitosan cross-linked with glutaraldehyde, a typical chemical cross-linking agent (Yamada et al., 2008; Yamada et al., 2000).

Another enzymatic method for the cross-linking of catechol-containing polymers that has been used is horseradish peroxidase (HRP) in conjunction with hydrogen peroxide (H_2O_2) (BP Lee et al., 2002). HRP is an oxidoreductase which functions by catalyzing the transfer of electrons from, in this case, a catechol group to an oxidizing agent such as H_2O_2. This method has been used to form hydrogels from tyramine-functionalized polysaccharides as well (Ogushi, Sakai, & Kawakami, 2007).

2.4 Opportunity for Catechol-Functionalized Biopolymers

While there has been moderate success in developing, and in some cases applying, DOPA-based adhesives using synthetic polymers, there has been relatively little focus on catechol-functionalized biopolymers.

The most available renewable biopolymers are polysaccharides, proteins, and natural rubber. Of polysaccharides, those most commonly used for adhesives are starch, cellulose, dextran, and chitosan. In fact, the majority of natural adhesives used today are those based on starch and dextran, used in the packaging and paper industries. Important adhesive proteins include those of both animal origin, such as casein and gelatin, and plant origin, such as soy protein. The traditional use of animal glues in book making continues to this day (Onusseit, VonByern, & I, 2010). Soy protein-based adhesives are becoming increasingly popular, especially thanks to renewed demand for its application in the composite wood industry (Deschamps, 2010). The demand for biocompatible, non-toxic, moisture resistant adhesives in the medical field has driven the discovery of a variety of protein and/or polysaccharide-based adhesives as well. Natural rubber (polyisoprene) is predominantly used in the production of band-aids and adhesive tape (Onusseit, VonByern, & Grunwald, 2010).

Polysaccharides in particular are an interesting source for adhesives for many reasons. First, they are the most abundant biopolymer in nature and are therefore readily available and relatively cheap as a raw material. Polysaccharides also come in a variety of molecular sizes and can be easily and cheaply modified in a number of different ways to impart desirable characteristics. Furthermore, polysaccharides are generally biocompatible and biodegradable. These characteristics may be especially desirable for adhesives in medical applications or construction as they present a less significant threat to human health and the environment compared to their petroleum-based counterparts. However, one major drawback of polysaccharide adhesives is their tendency to hydrate

and lose adhesion in humid conditions. Functionalization of polysaccharides with catechol groups may ameliorate this problem.

While catechol-functionalized chitin, dextran, and carboxymethyl cellulose have been investigated, starch has so far failed to gain attention as a target for catechol-functionalization.

2.5 Starch and Starch Adhesives

2.5.1 Introduction

Starch serves as an energy storage molecule for plants and is consequently one of the most abundant natural polymers on earth. Starch lends itself as an attractive biomaterial for many reasons. First, starch is readily obtainable and renewable from a variety of agricultural products including maize, potatoes, and rice, to name a few. Second, starch is non-toxic and biodegradable. Finally, chemical and physical modification of starch is relatively easy and can generally be carried out in gentle aqueous or dry conditions (Humphreys & Solarek, 2001). The unique properties of starch have led to its application in a variety of industries including: food, paper, adhesives, fuel, pharmaceuticals, and personal care products.

2.5.2 History of Starch Adhesives

The adhesive abilities of starch have been exploited for some time. The earliest uses of starch as an adhesive began with the Egyptians who used wheat starch as both a sizing

agent to coat the surface of papyrus and as a joint adhesive to combine individual papyrus strips (BeMiller & Whistler, 2009). There was a Roman treatise that detailed the production of starch and starch has also been detected in the paper of Chinese documents that date back as far as 1700 years ago. The ability and versatility of starch and modified starch adhesives have been realized since then and now include: corrugated cardboard, gypsum wall board, paper bags, carton and case sealing, bottle labeling, cigarettes, paper and board tube winding, laminated paper board, envelopes, wallpaper, textile sizing, pharmaceuticals, personal care products, building materials, and paints, inks, and toners (BeMiller & Whistler, 2009; "Measuring the dynamic viscosity of starch adhesives in the paper and packaging industry," 2011).

2.5.3 Structure

Starch is extracted from its agricultural sources as a powder of water-insoluble starch granules. The properties, shape, and composition of the starch granules may vary greatly depending on the botanical source. Starch granules are composed mainly of two macromolecules; amylose and amylopectin. Amylose is a primarily linear polymer of glucose units linked by α-(1,4) glycosidic bonds. Amylose chains are very long and may have a molecular weight typically ranging from 100,000-1,000,000 Daltons. Amylopectin is also an α-(1,4)-glucan polymer, but it contains many α-(1,6) branch points. The branches may also have additional branches to give a “branch-on-branch” structure. The range of molecular weight of amylopectin is about ten times greater than that of amylose, but because of branching, amylopectin is more spatially consolidated (Gozzo, Glittenberg, & Hofer, 2009). Amylopectin is the main constituent of native

starch granules, but genetic modification of crops has resulted in the ability to attain starch of various proportions of amylose and amylopectin (BeMiller & Whistler, 2009).

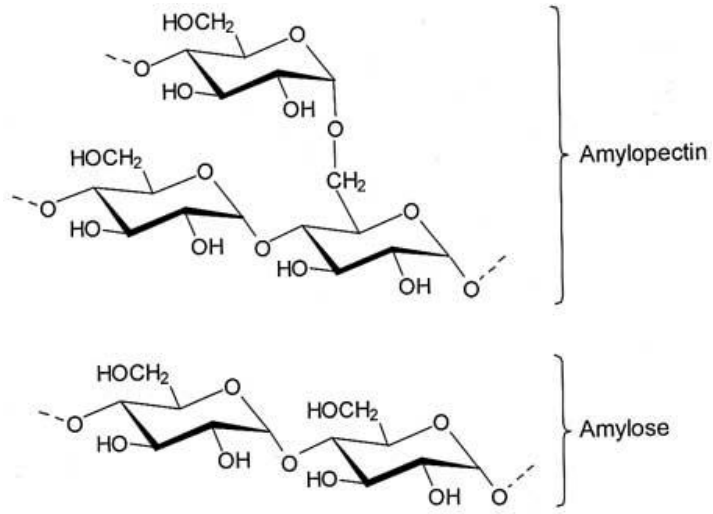

Figure 2.6 Basic structures of amylose and amylopectin (Nuffield Foundation)

Figure 2.7 "Branch-on-branch" structure of amylopectin (Thompson, 2000)

Hydroxyl groups along the backbone of starch molecules facilitate hydrogen bonding and other Van der Waals forces which cause inter- and intramolecular interactions among starch molecules. These interactions of amylose and amylopectin are responsible for the insolubility of native starch granules, gelatinization, and retrogradation. The network of hydrogen bonding in starch granules prohibits penetration of water and thereby prevents

hydration of starch molecules. Cooking the starch overcomes the hydrogen bonds and leads to gelatinization, where the starch becomes hydrated and a new weaker network of hydrogen bonds is formed. Retrogradation occurs when hydrated starch reverts to crystalline structure. Retrogradation can be facilitated either by tight association of the linear amylose chains or by formation of double helices between adjacent amylopectin branches (Gozzo et al., 2009). Clearly, starch hydroxyl groups also provide reactive sites for interactions with other molecules as well.

2.5.4 Modified Starch

It is often desirable to modify starch in order to take advantage of its beneficial properties (ie. non-toxic) or to reduce its negative properties (ie. water insoluble), depending on the application. Starch modification can drastically alter properties including: solubility, rheology, hydrophobicity/hydrophilicity, ionic charge, and retrogradation (Gozzo et al., 2009).

The abundance of hydroxyl groups available along the backbone of starch molecules makes modification relatively easy. Starch modifications usually entail substitution of some desired functional group onto the available hydroxyl groups of the glucose monomers via esterification, oxidation, or etherification reactions (BeMiller & Whistler, 2009). The properties imparted by modifications of starch may depend greatly on the average number of substituted sites per glucose molecule, known as the degree of substitution (DS). For each glucose molecule in starch, three hydroxyl groups are available for reaction while the other two are involved in glycosidic linkages. Thus the

maximum possible DS is three. Additionally, the distribution of substituent groups affects modified starch properties (Richardson & Gorton, 2003).

2.5.5 Carboxymethyl Starch

One type of modified starch that has been used for adhesive purposes is carboxymethyl starch (CMS). CMS was first synthesized in 1924 and has since been applied in a wide range of industries including food, pharmaceuticals, petroleum, paper, textile, and adhesives (El-Sheikh, 2010; Zhang & Wu, 1992).

Synthesis of CMS traditionally involves reacting native starch with monochloroacetate in aqueous alkaline solution (T Heinze & Koschella, 2005) to perform an S_N2 reaction on the hydroxyl groups of starch. The reaction occurs in two steps as follows:

1. Starch-OH + NaOH ↔ Starch-O-Na + H_2O
2. Starch-O^- + $ClCH_2COONa$ → Starch-O-CH_2COONa + NaCl

Along with the possible side reaction:

3. NaOH + $ClCH_2COONa$ ↔ OH-CH_2COONa + NaCl

Many processing methods have been developed for optimization and control of the carboxymethylation of starch (T Heinze & Koschella, 2005). Commercially produced CMS based on one-step aqueous methods generally have a DS below 0.3, but much higher DS, around 1, is possible and has been achieved through heterogenous reaction of starch in non-aqueous media such as alcohols (T Heinze, Liebert, Heinze, & Schwikal, 2004; Kwon et al., 1997; Volkert, Loth, Lazik, & Engelhardt, 2004). Also, CMS with

very high DS (above 2) has been achieved by multiple-step heterogenous reactions in non-aqueous media (T Heinze et al., 2004; Tijsen, Kolk, Stamhuis, & Beenackers, 2001). The DS of carboxymethyl starch is mostly responsible for the extent of its properties. Some of the most useful properties of carboxymethyl starch is that it is cold-water soluble and forms viscous solutions (T Heinze & Koschella, 2005).

2.5.6 CMS Bioconjugates

The available carboxylic acid groups of CMS and its ability to completely solubilize in cold water and physiological conditions make it a useful platform for conjugation with other biomolecules like proteins and amino acids. More specifically, creation of amide bonds between the carboxyl groups of starch and primary amines of peptides or other molecules is possible.

As previously mentioned, EDC is one of the most commonly used cross-linking reagents. EDC has been used to successfully create amide bonds between proteins, peptides or amino acids and a number of other materials including: other proteins (Hoare & Koshland, 1967), PAAc, PEG-dioglycolic acid, fumaric and maleic acids (Nakajima & Ikada, 1995), heparin (X. Yu et al., 2005), uronic acid-/amine-containing polysaccharides (Danishefsky & Siskovic, 1971; X. Yu et al., 2005), and carboxymethylated polysaccharides (Hoare & Koshland, 1967; Kobayashi, Yanagihara, & Ichishima, 1989). However, there have been relatively few studies using EDC to alter the functionality of CMS, especially outside the realm of food applications.

Whey protein was conjugated to carboxymethylated potato starch (degree of modification = .034) in an aqueous EDC solution, resulting in 6% protein content for the conjugate. This resulted in decreased swelling and solubility of starch granules (Hattori et al., 1995). Also, zein has been conjugated to carboxymethyl (degree of modification = .06) corn starch films in ethanol and acetone via EDC by Takahashi et al in order to increase the hydrophobicity of CMS films (Takahashi, Ogata, Yang, & Hattori, 2002). The film conjugate had a protein content of 0.4-0.6%. Clearly, there is an opportunity for catechol conjugation to CMS.

2.6 Future Studies in Mussel-Inspired Biopolymer Adhesives

The efforts made so far to create mussel-mimetic biopolymer adhesives have produced some promising results and should encourage future research endeavors to enhance and better understand these adhesives. This area of research is still relatively young so there are multiple approaches for further study.

Screening catechol-functionalized polysaccharides and proteins for their adhesive abilities is one approach for further study. In addition to carboxymethyl starch, there are a host of other economical modified and unmodified polysaccharides, such as those of bacterial origin like xanthan gum and curdlan, which have yet to be functionalized with catecholic groups. Likewise, the only protein source that has been catechol-functionalized is soy protein isolate. Industrial sources of protein like whey and zein protein could also be functionalized.

Another direction for future study is optimization of the adhesive capabilities of catechol-functionalized biopolymers. The chemistries available for conjugation of catechol groups to polymeric backbones have been established, but few studies go further to examine the effects of the characteristics of the adhesive polymers on adhesion. Characteristics of interest could include the molecular weight distribution of the polymer, degree of catechol substitution, presence of other functional groups, and extent of cross-linking. In-depth studies taking into consideration all of these parameters would give better insight into the behavior of catechol-functionalized biopolymer adhesives and perhaps suggest, roughly, common guidelines for optimal adhesion.

Finally, the type of polymer and its characteristics for optimal adhesion may vary depending on surface type. Analysis of the factors previously mentioned on different types of surfaces may also yield important findings to enhance the understanding of catechol-functionalized biopolymer adhesives.

Combining the catechol-based adhesive strategies of nature with the abundance, diversity, and natural adhesive abilities of biopolymers could lead to a new class of environmentally friendly adhesives that surpass their predecessors in performance.

CHAPTER 3. MATERIALS AND METHODS

3.1 Materials

Chemicals

Commonly used chemicals were reagent grade or better. Hi-maize® 260 starch was obtained from Granary Bulk Foods, Appleton, WI. This particular starch was chosen because it is an easily attainable, unmodified, high-amylose starch. The reason behind using high-amylose starch was that linear molecules are better able to associate with one another, thus making better adhesives than branched molecules.

Equipment

Adam Moisture Analyzer, Adam Equipment, Danbury, CT. Chemglass CG-1929-X11, Chemglass, Vineland, NJ. Chemglass CG-1950, Chemglass, Vineland, NJ. Chemglass Tempstir, Chemglass, Vineland, NJ. Hitachi U-2910 Spectrophotometer, Hitachi High Technologies America, Inc., Pleasanton, California. Shimadzu LC-10AT VP HPLC, Shimadzu Corperation, Kyoto, Japan. Dawn Heleos-II, Wyatt Technology, Santa Barbara, California. Optilab rEX, Wyatt Technology, Santa Barbara, California. 300 Mhz Varian NMR, Agilent Technologies, Santa Clara, California. Thermo Nicolet Nexus 670 FTIR, Thermo Scientific, Waltham, MA. Waring 700G laboratory blender,

Waring Laboratory & Science, Torrington, CT. VWR 1410D, VWR Scientific Products, Radnor, Pennsylvania.

Donations

Fungal α-amylase from *Aspergillus orzyae* was kindly supplied by Deerland enzymes, Kennesaw, GA.

Buffers

Acetate Buffer with CaCl (100 mM, pH=5)

- Add 5.8 mL glacial acetic acid to 500 mL of distilled water
- Adjust pH to 5 with 1 M NaOH
- Add 0.74 g CaCl dihydrate and dissolve
- Bring total volume to 1 liter with distilled water.
- Store in fridge

HEPES Buffer (100 mM, pH=7.4)

- Add 5.9575 g dry HEPES to 200 mL distilled water
- Adjust pH to 7.4 with small additions of 15% NaOH
- Adjust total volume to 250 mL with distilled water

MES Buffer (100 mM, pH=4.5)

- Add 19.5240 g MES hydrate to 900 mL distilled water
- Adjust pH to 4.5 with small additions of 15% NaOH
- Adjust total volume to 1 L with distilled water

Phosphate Buffer (1 M, pH 7)

- Add 5.8362 g monosodium phosphate, monohydrate and 15.4660 g disodium phosphate, heptahydrate to 80 mL of distilled water
- Adjust pH as needed with small additions of 15% NaOH or 6 M HCl
- Adjust total volume to 100 mL with distilled water
- Dilute buffer as needed

Phosphate Buffer with Saturated Borate (500 mM phosphate buffer, pH = 8.8)

- Dilute 1 M phosphate buffer (pH 7) 1:1 with distilled water
- Heat solution to just under boiling and begin adding sodium borate while stirring
- Continue adding sodium borate in decreasing amounts until it is obviously no longer dissolving
- Remove solution from heat and let slowly cool to room temperature, excess sodium borate will fall out of solution

3.2 Preparation of Hydrolyzed Non-Granular Starch

3.2.1 Enzymatic Hydrolysis Time Study

In order to have some control over the extent of starch hydrolysis, a time study was conducted as follows. In a 50 mL Erlenmeyer flask, 1.2 grams of Hi-Maize® 260 corn starch was dissolved in 30 mL 90% DMSO/10% water by heating the solution to 98°C and maintaining this temperature while stirring with magnetic stir bar for about 2 hours, or until the solution became transparent and bits of starch were no longer visible. While

dissolving the starch, the flask was covered with tin foil to prevent loss of liquid to evaporation.

Once the starch was dissolved, the solution was transferred to a 125 mL Erlenmeyer flask and placed in an incubator at 50°C where it was allowed to slowly cool over the course of about an hour to the temperature of the incubator. Meanwhile, 45 mL of acetate buffer was placed in the incubator and also allowed to reach 50°C. Once both the dissolved starch solution and the acetate buffer reached 50°C, the dissolved starch solution was placed in an incubated flask shaker at 50°C and 200 rpm. While the dissolved starch solution was being stirred, the acetate buffer was slowly added to it using a glass funnel. After the acetate buffer was added to the starch solution, the mixture was left for about 30 minutes to ensure thorough mixing.

A 1 mg/mL α-amylase solution was prepared in acetate buffer and a 24 µL aliquot was taken from this and added to the dissolved starch/acetate buffer mixture to begin the hydrolysis reaction with an enzyme loading of 0.01 mg enzyme/g starch. Samples of 3 mL were taken at various time intervals, inactivated by addition of 50 µL 6 M HCl, and added to a 15 mL centrifuge tube with 12 mL of 100% ethanol to precipitate the starch. The starch was recovered by centrifugation and washed with 15 mL 80% ethanol until the pH of the supernatant was neutral. A final wash with acetone was performed, the supernatant discarded, and the starch placed in an incubator at 60°C to dry.

The dry samples were then prepared for molecular weight distribution analysis by HPLC-SEC-RI-MALS by placing 2 mg of sample per 1 mL distilled water in a screw-top glass vial. The vial was then placed in the pressure cooker for 1 hour to dissolve as much sample as possible.

3.2.2 Gram-Scale Preparation of Non-Granular Hydrolyzed Starch

3.2.2.1 Starch Dissolution

In a glass batch reactor with temperature controlled water jacket and overhead stirrer, 10 g of Hi-maize® 260 starch was dispersed in 200 mL of 90% DMSO/10% distilled water. This mixture was stirred at 300 rpm and kept at about 98°C for at least 2 hours or until the solution became transparent and visible bits of starch were no longer apparent. The dissolved starch solution was then allowed to cool to 50°C.

3.2.2.2 Enzymatic Hydrolysis of Dissolved Starch

To the dissolved starch solution, 300 mL of acetate buffer at 50°C was slowly added with stirring to produce a mixture of 40% dissolved starch solution and 60% acetate buffer. The mixture was allowed to stir at 300 rpm for an hour in order to ensure it was completely mixed and the temperature was uniform throughout the mixture. The pH of this mixture was 6.0.

An enzyme loading of 0.02 mg enzyme/g starch was achieved by adding 200 µL of 1 mg/mL fungal α-amylase prepared in acetate buffer to the acetate buffer/DMSO mixture.

The mixture was kept at 50°C and stirred at 300 rpm for the duration of the hydrolysis reaction.

3.2.2.3 Starch Recovery

Starch was recovered from the hydrolysis mixture by ethanol precipitation. The 500 mL of hydrolysis mixture was poured into 2 L of 100% ethanol in a 4 L separatory flask for a final concentration of 80% ethanol. This solution was stirred for about 10 minutes before being allowed to completely settle. Once settled, the top layer of starch-free liquid was removed and discarded. The remaining layer of precipitated starch was then transferred to centrifuge bottles and centrifuged at 6,000g for 5 minutes at room temperature and the supernatant was discarded.

To wash the recovered starch, the solids were placed in a Warring blender with 300 mL of 80% ethanol and breifly homogenized. The mixture was poured into a beaker with stir bar and allowed to stir for 15 minutes. Then the mixture was split equally into two centrifuge bottles and centrifuged at 6,000g for 5 minutes at room temperature. The supernatant was discarded and the washing procedure was repeated for a total of three washes with 80% ethanol. Following the washes in 80% ethanol, the starch was washed once with 100% methanol and then finally with acetone to help dehydrate the starch so that it could be quickly dried.

After the starch was washed with acetone and recovered by centrifugation, it was deposited onto a watch-glass and placed in an oven at 60°C overnight. The starch was then removed from the incubator, blended into powder using a Warring blender, and stored in a desiccator. After 24 hours in the desiccator, the starch was blend again to ensure it was entirely ground to a fine powder.

3.2.3 Molecular Weight Distribution of Hydrolyzed Starch

Analysis of the molecular weight distribution of hydrolyzed starch was carried out on a Sephacryl S-500 column using HPLC-SEC with tandem refractive index and multi-angle laser light scattering detectors at a flow rate of 1.3 mL/min. Samples were prepared by adding the appropriate mass of dried non-granular starch to the corresponding volume of distilled water to achieve a concentration of 2 mg/mL. This mixture was placed into a pressure cooker and cooked for one hour to dissolve the starch as much as possible. 1 mL of the solution was taken and filtered through a 0.5 µm nylon filter before injection.

Data was analyzed using ASTRA software. Light scattering analysis was conducted based on the Debye model with a Fit Degree of 2 and a dn/dc value of 0.146. Additionally, the mass data was fit to a polynomial model for lowest statistical error.

3.3 Carboxymethyl Starch

3.3.1 Synthesis

3.3.1.1 One-Step Non-Granular CMS

3.3.1.1.1 Batch

Carboxymethylation of non-granular starch was based on the methods of Heinze et al. (T Heinze et al., 2004). In a 300 mL glass batch reactor with temperature-controlled water jacket and overhead stirrer, 5 g of dry starch (~11% moisture) was dispersed in 150 mL isopropanol. Then 13 mL of 15% NaOH was added and the mixture was allowed to mix at 300 rpm at room temperature for an hour. Next, the temperature of the reactor was increased to 50°C and 6.11 g of sodium monochloroacetate were added. The reaction was then allowed to proceed for an allotted amount of time.

After the allotted amount of time, the reaction mixture was collected and the solids were separated from the reaction liquid using a fritted glass Buchner funnel (porosity F). The solids were then dissolved in water and pH was adjusted to neutral by addition of 8.5 M acetic acid. Unreacted bits of starch were then removed by centrifugation. The CMS solution was then precipitated in four volumes of ethanol and centrifuged for recovery. The recovered CMS was then washed twice more by dissolving the material in water followed by precipitation in ethanol or until the supernatant tested negative by the silver

nitrate test for chloride ions. It should be noted that sometimes recovery of the precipitated material was difficult, and in these instances, the pH of the precipitated starch mixtures was dropped slightly with drop-wise addition of 0.5 M HCl to aid precipitation.

After the last wash, the CMS pellet was briefly blended in methanol via Warring blender and allowed to sit for 15 minutes before being recovered by centrifugation. Finally, a Warring blender was used to briefly blend the CMS in acetone. The mixture was transferred to a beaker with stir bar and allowed to stir for half an hour before it was centrifuged to recover the CMS. The CMS was then collected on a watch-glass, and placed in an incubator at 60°C overnight. The dry CMS was then ground using a Warring blender and placed in a desiccator. After desiccation, the CMS was ground again to ensure it was a fine powder.

3.3.1.1.2 Fed-Batch

3.3.1.1.2.1 Additional SMCA

Fed-batch synthesis of non-granular CMS was initially carried out in the same manner as the batch method, however after 4 hours an amount of SMCA equivalent to that added for the first four hours was added and the reaction was allowed to proceed overnight (about 16 hours).

3.3.1.1.2.2 Additional SMCA and NaOH

This reaction was carried out identically to 3.3.1.1.2.1; However; when it came time to add additional SMCA, NaOH pellets were also added. The mass of NaOH pellets added was equivalent to mass of NaOH added by the initial volume of 15% NaOH in order to avoid changing the reaction volume and water content.

3.3.1.2 Multi-Step Granular CMS

Preparation of granular carboxymethyl starch was based on the multi-step methods of Tijsen et al. (Tijsen et al., 2001). Granular Hi-Maize 260® was first washed three times by suspending 15 grams of starch in 250 mL of distilled water, stirring for 15 minutes, and removing the liquid via fritted glass Buchner funnel (porosity F). Finally the starch was dispersed in acetone for 15 minutes and filtered in a similar fashion. The dehydrated starch was then put on a watch-glass and placed in an oven at 60°C for one hour before being stored in a vacuum desiccator overnight. The carboxymethylation of the washed granular starch was then carried out with the following parameters:

Table 3.1 Parameters for Multi-Step Carboxymethylation of Granular Starch

	First Step	**Second Step**	**Third Step**
W_{AGU}	0.04	0.04	0.04
W_{H2O}	0.10	0.05	0.05
NaOH:AGU	1	1.6	1.3
SMCA:AGU	1	1.6	1.3
Reaction Time (hr)	2.5	7	26.5

where,

W_{AGU} = mass fraction of starch (kg/kg)

W_{H2O} = mass fraction of water in reaction medium (including starch moisture)

First, the appropriate volumes of isopropanol and distilled water were combined and mixed in a glass batch reactor with temperature controlled water jacket and overhead stirrer. The starch was then added and stirred for 15 minutes at 350 rpm. The appropriate mass of NaOH pellets were then added and allowed to dissolve for at least 12 hours at 40°C in order to completely activate the starch. Next, the prescribed amount of sodium monochloroacetate was added to start the reaction and the reaction temperature was kept at 40°C. After the defined reaction time elapsed, the slurry was removed from the reactor and filtered through a fritted glass Buchner funnel (porosity F) to remove the reaction liquid. The granular CMS was then suspended in 95% isopropanol and the pH was adjusted to neutral with 8.5 M acetic acid. The suspension was then filtered and the granular CMS was washed by suspending it in 95% isopropanol for 15 minutes and filtering off the liquid. The wash was continued in this way until the filtrate tested negative for silver nitrate test for chloride ion. Finally, the granular CMS was suspended in acetone, filtered, transferred to a watch-glass, and put in an oven at 60°C for one hour before being stored in a vacuum desiccator overnight.

Subsequent carboxymethylation steps were carried out following the same procedure, with a reaction temperature of 40°C in each step. This procedure was also applied to hydrolyzed non-granular starch.

3.3.2 Degree of Substitution

Determination of the degree of substitution of carboxymethyl starch was based on the titration methods of Eyler et al. for determination of degree of substitution of carboxymethyl cellulose (Eyler, Klug, & Diephuis, 1947) and Stojanovic et al. (Stojanovic, Jeremic, Jovanovic, & Lechner, 2005). 2 g of dry CMS was converted to its acid form after being dispersed in a mixture of 60 mL acetone and 6 mL of 6M HCl for half an hour. This mixture was then filtered through a fritted glass Buchner funnel (porosity F) and the liquid was removed via vacuum filtration. The CMS was then washed with 90% acetone until the filtrate was neutral and tested negative for silver nitrate test for chloride ion, indicating removal of excess HCl.

The CMS was then suspended in acetone for 15 minutes to dehydrate the material before being filtered through a fritted glass Buchner funnel (porosity F). The solids were then deposited onto a watch glass and allowed to dry at 60°C in an oven for one hour before being stored in a vacuum desiccator overnight. The moisture content of the CMS was determined using a moisture analyzer. For this procedure, the moisture content was about 11% after overnight desiccation, as verified by multiple moisture analyses by an Adam Moisture Analyzer.

0.5 grams of acidified CMS was dissolved in 20 mL of 0.2 M NaOH. 50 mL of water were then added and the solution was transferred to a 100 mL volumetric flask where water was added up to the 100 mL line. This solution was inverted three times to completely mix. A blank was also prepared in the same manner excluding CMS.

25 mL of the solution was transferred to an Erlenmeyer flask and diluted with 75 mL water. A drop of phenolphthalein was added for indicator. The solution was then titrated with 0.05 M HCl until the solution lost all pink color. DS was calculated as follows:

$$DS = \frac{162 * n_{COOH}}{m_{ds} - 58 * n_{COOH}}$$

where,

n_{COOH} = moles of carboxylic acid = $(V_b - V) * C_{HCl} * 4$

V_b = volume of HCl used to titrate blank (mL)

V = volume of HCl used to titrate sample (mL)

C_{HCl} = Concentration of HCl (mol/dm^3) = 50 mol/dm^3 for 0.05 M HCl = 0.00005 mol/mL

4 = ratio of total solution volume to volume taken for titration (100mL / 25mL)

m_{ds} = mass of dry sample (g) = $m_s - m_s$ * % moisture

It should be noted that V_b and V were calculated as the average of three titrations.

3.4 Starch-Catechol Conjugates

3.4.1 CMS-Dopamine Synthesis by EDC

3.4.1.1 One-step Reaction

High MW CMS (DS=1.12) was first dissolved in 0.1 M MES buffer (pH=4.5) at a concentration of 10 mg/mL. The pH was then adjusted to just under 5.0 by dropwise addition of 6 M HCl. Next, dry dopamine-HCl was added to the solution. Once the

dopamine was completely dissolved, dry EDC was slowly added to solution in order to start the conjugation reaction. The reaction was stopped after the allotted time by precipitation of the conjugate in four volumes of alcohol. The product was separated by centrifugation and washed with 80% ethanol until the supernatant no longer visibly changed color with addition of $NaIO_4$. A final wash with acetone was then performed and the conjugate was dried at 50°C in an oven.

3.4.1.2 <u>One-Step Anaerobic Reaction</u>

60 mL of 0.1 M MES buffer in a 125 mL Erlenmeyer vacuum flask was sparged with N_2 for 15 minutes, stoppered and put under vacuum for 30 minutes to degass. 600 mg of low MW CMS (DS=0.5) was then added while continually sparging the reaction medium with N_2. The pH of the mixture was then adjusted to 4.5 before adding dopamine to achieve 5:1 [dopamine]:[COOH]. The pH was then adjusted to 4.0 by slow dropwise addition of 6 M HCl and the mixture was sparged with N_2 for an additional 15 minutes before putting the reaction vessel under vacuum for 30 minutes to degass. At this point, the mixture tested negative for dissolved O_2 by resazurin indicator. Finally, EDC was added under N_2 to achieve 2:1 [EDC]:[COOH]. The reaction mixture was then capped under N_2 and the reaction was allowed to proceed until precipitation occured.

3.4.1.3 One-Step Reaction with Ascorbic Acid

3.4.1.3.1 Reaction 1

200 mg of high MW CMS (DS=1.12) was dissolved in 20 mL 0.1 M MES buffer. Once dissolved, ascorbic acid was added to obtain 2:1 ascorbic acid:COOH. Dopamine was then added to obtain 1:1 dopamine:COOH. The pH of the mixture was adjusted to 4.6 by dropwise addition of 6 M HCl. Finally, EDC was added to obtain 1:1 EDC:COOH. The reaction was allowed to proceed for 4 hours. The polymer was precipitated with 4 volumes of EtOH and recovered by centrifugation. The supernatant was discarded, and the solids were dissolved in water. The polymer was again precipitated with excess ethanol and dropwise addition of 6 M HCl to aid precipitation, followed by centrifugation. The last few steps were repeated once more, followed by two washes with 80% EtOH/H_2O and a final wash with acetone before being dried at 50°C.

3.4.1.3.2 Reaction 2

200 mg of low MW CMS (DS=0.5) was dissolved in 20 mL of 0.1 M MES buffer. Once CMS was dissolved, ascorbic acid was added to obtain 10:1 ascorbic acid:COOH. The pH was then adjusted to 4.2 before adding an amount of dopamine to achieve 10:1 dopamine:COOH. After adding dopamine, the pH was 3.9. Finally, EDC was added to achieve 2:1 EDC:COOH. The reaction was allowed to proceed for 4 hours. The polymer was precipitated with 4 volumes of EtOH and recovered by centrifugation. The supernatant was discarded, and the solids were dissolved in water. The polymer was

again precipitated with excess ethanol and dropwise addition of 6 M HCl to aid precipitation, followed by centrifugation. The last few steps were repeated once more, followed by two washes with 80% EtOH/H_2O and a final wash with acetone before being dried at 50°C.

3.4.1.4 Two-Step Reaction

3.4.1.4.1 Reaction 1: Method based on Wang et al.

High MW CMS (DS = 1) was dissolved in 0.1 phosphate buffer (pH=7) to obtain a 10 mg/mL solution. After CMS was dissolved, the pH was adjusted to 5.7 by dropwise addition of 6 M HCl. NHS (2:1 NHS:COOH) was then added and allowed to completely dissolve, followed by addition of EDC (2:1 EDC:COOH). This solution was allowed to stir at room temperature for 45 minutes to activate the acid groups of CMS while being sparged with N_2. After 45 minutes the pH was adjusted to 5.8 by dropwise addition of 15% NaOH. Finally dopamine HCl (4:1 dopamine:COOH) was added under N_2 and the pH of the solution was adjusted to 5.5 if needed. This mixture was sparged for 5 more minutes with N_2 before the mixture was capped and the headspace flushed with N_2. The reaction was then allowed to proceed at room temperature for at least 12 hours. The reaction mixture was then precipitated in excess acetone and centrifuged to recover the solids. The solids were then dissolved in a small volume of water before being precipitated again with acetone followed by centrifugation. These steps were repeated once more for a total of three precipitations. Dilute HCl was added to aid in recover of precipitated material

when needed. After the last precipitation, the product was dissolved in water and lyophilized.

3.4.1.4.2 Reaction 2: Removal of Excess EDC

CMS was first dissolved in 0.1 M MES buffer (pH=4.5). Once the CMS was thoroughly dissolved, dry NHS was added and allowed to completely dissolve. Dry EDC was then added to begin the activation reaction. The reaction proceeded for 45 minutes before purifying the activated CMS by centrifugal ultrafiltration. The activated CMS was washed by addition of distilled water, followed by ultrafiltration until the pH of the filtrate was neutral, indicating complete removal of buffer salt and ideally the free EDC and NHS as well.

Once thoroughly washed, a final wash with 0.1 M HEPES buffer (pH=7.4) or 0.1 M MES buffer (pH=4.5) was performed. The concentrated activated CMS was then reconstituted in 0.1 M HEPES buffer (pH=7.4) or 0.1 M MES buffer (pH=4.5) to the desired reaction volume and dopamine was added slowly. The reaction was allowed to proceed for 24 hours before the conjugate was precipitated in four volumes of 100% ethanol. The precipitated conjugate was separated by centrifugation and washed with 80% ethanol until the supernatant no longer changed color with addition of $NaIO_4$. A final wash with acetone was then performed and the conjugate was dried overnight at 60°C.

3.4.1.4.3 Reaction 3: Two-Step Reaction with Protection of Dopamine by Borate

A 4% solution of carboxymethyl starch in 0.5 M phosphate buffer was prepared and the pH was adjusted to 5.5. NHS was added to this solution to give 10:1 NHS:COOH. The pH of the solution after addition of NHS dropped to 4.5. An equimolar amount of EDC was then added and the pH rose above 6 before falling. Bubbles and heat were observed during the activation of concentrated CMS. The reaction was allowed to proceed for 45 minutes. The pH of the solution was kept around 5.5 by dropwise addition of 15% NaOH.

During the activation of CMS, a solution of dopamine was prepared in phosphate buffer with saturated sodium borate in a three-neck flask. The volume of the solution was three times that of the CMS-activation mixture so that the final polymer volume would be 10 mg/mL and the amount of dopamine added was enough to give 10:1 dopamine:COOH. To prepare the solution, the pH of the buffer was first adjusted from 8.8 to 9.2 by addition of 15% NaOH. The buffer was then sparged vigorously with N_2 for 15 minutes, followed by vacuum to remove O_2. Dopamine HCl was then added to the buffer under N_2.

The activated CMS solution was then added to the dopamine solution and the pH was gradually adjusted to 7.2 by dropwise addition of 15% NaOH. The reaction was allowed to proceed for 20 hours. 100 mL of reaction mixture was then dialyzed (6-8k MWCO) against 4 L distilled water for four days, with two complete exchanges per day, or until the dialysis water no longer showed any absorbance by UV-vis. The pH of the dialysis water was maintained at about 3.5 throughout dialysis to remove the borate complex and prevent auto-oxidation of dopamine.

3.4.2 Starch-Dopamine Synthesis by CDI

3.4.2.1 In DMSO

400 mg of hydrolyzed starch was added to 20 mL of DMSO and allowed to completely dissolve. CDI was then added at a 2:1 molar ratio to starch hydroxyl groups and allowed to react for 1.5 hours before precipitating the polymer into 4 volumes of acetone and proceeding with three washes of the polymer by dissolution in a small volume of DMSO followed by precipitation with acetone. The polymer was then dissolved in 20 mL fresh DMSO. Next dopamine was added at a 2:1 molar excess to original starch hydroxyl content. This mixture was then allowed to react for 48 hours.

The product was then precipitated in 4 volumes of ethanol, washed three times by dissolution in a small volume of DMSO followed by precipitation by excess ethanol, and dried at 50°C.

3.4.2.2 In DMF

600 mg hydrolyzed starch was added to 20 mL DMF and stirred overnight. CDI was then added at a 2:1 molar ratio to starch hydroxyl groups and allowed to react for 1.5 hours before precipitating the activated polymer into 4 volumes of acetone and washing the polymer three times by dissolution in a small volume of DMSO followed by precipitation with acetone. The polymer was then dissolved in 20 mL fresh DMF. Once

dissolved, dopamine was added at a 2:1 molar excess to original starch hydroxyl content. This mixture was then allowed to react for 18 hours.

The product was then precipitated in 4 volumes of ethanol, washed three times by dissolution in a small volume of DMSO followed by precipitation by excess ethanol, and dried at 50°C.

3.4.3 Starch-Benzoic Acid Conjugates

3.4.3.1 Starch-DMBA

3.4.3.1.1 Synthesis

To a flame-dried round-bottom flask, 3,4-dimethoxybenzoic acid (DMBA) and N,N'-carbonyldiimidazole were added in equimolar amounts to DMSO that was dried over molecular sieves. After initial vigorous bubbling due to CO_2 production, the flask was stoppered and the headspace was flushed with nitrogen before being placed in an incubated flask shaker at 60°C for at least 16 hours. Meanwhile, nongranular starch was added to dry DMSO in a separate round-bottom flask, stoppered, and placed in the shaker along with the DMBA/CDI solution.

After DMBA was activated by CDI, the activated DMBA solution was added to the starch solution, stoppered, and the headspace flushed with nitrogen and placed back in the flask shaker for another 24 hours at 70°C.

To recover the product, the solution was added to 4 volumes of isopropanol to precipitate the polymer which was then recovered by centrifugation. The product was then dissolved in a small volume of DMF followed by precipitation in excess isopropanol and recovery by centrifugation again. To aid recovery, a 0.5 M HCl was added drop-wise until floccs were evident before centrifugation. Precipitation was carried out once more before the recovered polymeric material was washed twice with methanol and finally with acetone, recovering the material by centrifugation between each wash. The acetone-washed product was then dried in an oven at 50° C under vacuum. The color of the dried product varied from light tan to brown depending on the DS.

3.4.3.1.2 Demethylation of Starch-DMBA

3.4.3.1.2.1 BBr_3 Demethylation

An oven-dried three neck round-bottom flask with magnetic stir bar was fitted with a rubber septum in one of the side necks, an addition funnel (capped with rubber septum) with pressure-equalized arm in the middle neck, and a rubber tube adapter in the other neck. The apparatus was then connected to a Schlenk line via the tube adapter and evacuated at least three times by flame drying under vacuum and back-filling with argon. Once the flask was evacuated and flame-dried, dried starch-DMBA conjugate was added, followed by addition of a given volume of DMF dried over molecular sieves. The polymer was allowed to completely dissolve before the flask was placed on ice and allowed to reach 0°C. Once the mixture was cooled, 1 M BBr_3 in hexanes was added to

the addition funnel and added dropwise to the solution. The reaction was then allowed to warm to room temperature over the course of at least 16 hours.

The reaction mixture was then added to a volume of 0.5M HCl equal to the reaction volume. To this mixture, excess cold methanol was added to precipitate the polymer. Once the precipitated material settled, the supernatant was decanted and the remaining methanol was pumped down using a Rotovap so that a small volume of polymer dissolved in DMF remained. Excess methanol was then added to precipitate the polymer again and the procedure just described was repeated twice more followed by a final precipitation by acetone before drying under vacuum.

3.4.3.1.2.2 Demethylation by Sodium Ethanethiolate

A 50 mL three-neck round bottom flask fitted with a rubber tube adapter and a rubber septum in the side necks and a reflux condenser (capped with septum) in the middle neck was flame dried five times and evacuated with argon. 0.3 grams of high MW starch-DMBA (DS = 1) and 30 mL of dry DMF were added under argon. The starch-DMBA was allowed to dissolve at room temperature. Once dissolved, dry sodium ethanethiolate was added to achieve 6:1 ethanethiolate:DMBA group. The reaction mixture was then heated to 100°C and left under reflux for 20 hours. The mixture was allowed to reach room temperature before addition of 1 mL 0.5 M HCl. Next the entire mixture was poured into excess MeOH. The precipitated material was sparse and cloudy.

The precipitated material was set in a freezer and allowed to settle before the top layer was poured off and the remaining liquid was pumped down by Rotovap. Once most liquid was removed, the solids dissolved back into the small volume of DMF remaining. An additional 2 mL of 0.5M HCl was added to this solution which caused the solution to "break", resulting in a dark red colored solution with pink precipitate. The precipitated material was dissolved in a small volume of fresh DMF and precipitated with MeOH. A small volume of additional 0.5 M HCl was added to aid in precipitation. The precipitated material was allowed to settle before discarding the liquid layer and pumping down the remaining liquid so that what remined was the product dissolved in a small volume of DMF. From this solution, the product was precipitated with methanol again, washed with methanol, and then dried under vacuum. The dried product was brown and only about 25 mg were recovered.

3.4.3.2 Starch-DHBA

3.4.3.2.1 Protection of DHBA with PBA

Equimolar amounts of dry DHBA and PBA were co-ground using pestle and mortar. The mixture was then placed in a round-bottom flask and put in an oven at 120°C for one hour. After an hour the mixture was put under vacuum at 80°C for at least 2 hours and then cooled to room temperature in a vacuum desiccator.

3.4.3.2.2 Synthesis of Starch-DHBA-PBA by CDI

Conjugation of DHBA-PBA to starch using CDI was carried out using the same method as starch-DMBA conjugation.

3.4.3.2.3 Synthesis of Starch-DHBA-PBA by TosCl

Based on the methods of Heinze et al. (Thomas Heinze, Liebert, & Koschella, 2006), A 2.5% (w/v) solution of starch in DMAc or DMF with 7.5% LiCl (w/v) was prepared by heating a mixture of starch and solvent to 130°C while stirring in a round-bottom flask for one hour before letting the mixture cool to 100°C. At this point anhydrous LiCl was added and the mixture was stirred until the solution was clear. The mixture was then allowed to cool to room temperature under N_2. Once the solution reached room temperature, a volume of pyridine was added to achieve 2:1 Py:TosCl. Once the pyridine was added, TosCl was added to achieve 2:1 TosCl:AGU. Once the TosCl dissolved, DHBA-PBA was added and allowed to dissolve (1:1 DHBA-PBA:TosCl). The headspace of the flask was then flushed with N_2 and the mixture was placed in a flask shaker at 80°C and allowed to react for 24 hours.

3.4.4 Characterization of Catechol-Functionalized Starch Polymers

3.4.4.1 Catechol Content

3.4.4.1.1 Colorimetric Assay

To quantify the catechol content of CMS-dopamine conjugates, a colorimetric assay developed by Arnow (Arnow, 1937) was used. A 0.5 M HCl solution was made by diluting 4.17 mL of concentrated HCl (12 M) to 100 mL with distilled water. A 1 M NaOH solution was made by dissolving 4.0010 g of NaOH pellets in 100 mL of distilled water. Nitrite reagent was made by dissolving 10.0037 g sodium nitrite and 10.0260 g sodium molybdate in 100 mL of distilled water. To construct a standard curve, three separate solutions of 1 mM dopamine were prepared by dissolving approximately 0.0190 g dopamine HCl in 100 mL of distilled water before being used in a series of dilutions. The standard curve was constructed as follows:

Table 3.2 Dilution Series for Arnow Assay Calibration Curve

1 mM dopa (µL)	0	10	20	30	40	50	60	70	80	90	100
Water (µL)	100	90	80	70	60	50	40	30	20	10	0
0.5 M HCl (µL)	300	300	300	300	300	300	300	300	300	300	300
Nitrite rgt. (µL)	300	300	300	300	300	300	300	300	300	300	300
1 M NaOH (µL)	400	400	400	400	400	400	400	400	400	400	400

To perform the assay, 1 mM dopamine and water were combined in a 1.5 mL centriguge tube and mixed by vortex for five seconds. Next, 300 µL of 0.5 M HCl was added and the solution was mixed again by vortex for 5 seconds. Then 300 µL of nitrite reagent was added and the solution was mixed again in the same manner, producing a yellow color. Finally, 400 µL of 1 M NaOH was added and the solution was mixed again as before, producing a red color in presence of dopamine. 1 mL of the oxidized dopamine solution was then pipetted into a quarts cuvette and its absorbance at 499 nm was recorded.

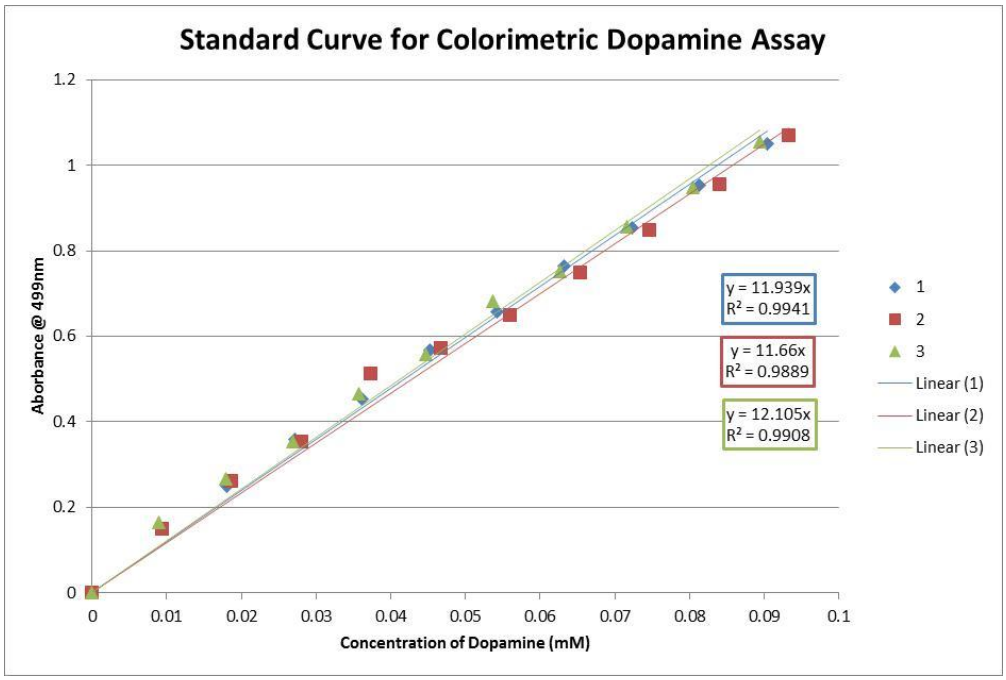

Figure 3.1 Standard Curve for Colorimetric Dopamine Assay

The slope of the standard curve was determined to be 11.90 ± 0.22.

Catechol content of CMS-dopamine conjugates were assessed by dissolving enough washed, dry conjugate in distilled water to make a 1 mg/mL solution. A 100 µL aliquot of the solution was then used for the assay unless dilution was necessary.

To estimate the degree of substitution of dopamine, the following calculation was used:

$$\frac{\frac{A500}{11.90} * \frac{1100\ \mu L}{\mu L\ \text{CMS-dopa solution}}}{[\text{CMS-dopamine solution}] * \left(\frac{1\ \text{mmol}}{162 + DS_{CMS} * 44}\right) * 1000}$$

Where "1100/µL CMS-dopamine solution" is a dilution factor, [CMS-dopamine solution] is the concentration (mg/mL) of CMS-dopamine prepared for the assay before dilution, DS_{CMS} is the DS of the CMS used in the conjugation reaction,162 is the MW of AGU, 44

is the MW of COOH – H from the substituted OH, and 1000 is to convert to mM CMS monomer.

3.4.4.1.2 H-NMR

10 mg of starch-benzoic acid conjugate was dissolved in 1 mL of DMSO-d6. The solution was centrifuged to remove any residual material. The solution was then transferred to an NMR tube (Wilmad, 535-PP-8) for analysis on a 300 MHz Varian NMR.

Starch: δ(ppm) = 3.4-4.0 (H-2,3,4,5,6), 4.55 (OH-6), 5.1 (H-1), 5.4 (OH-2), 5.5 (OH-3) (Chi et al., 2008; Peng & Perlin, 1987; Wesslen & Wesslen, 2002).

DMBA: δ(ppm) = 3.8 (CH3), 7.0-7.6 (H aromatic)

DHBA: δ(ppm) = 6.6-7.6 (H aromatic)

PBA: δ(ppm) = 7.2-8.2 (H aromatic)

Starch-DMBA: 3.4-4.0 (H-2,3,4,5,6 from starch & CH3 from DMBA), 4.6-5.0 (OH-6 and unknown), 5.2 (H-1), 5.7 (OH-3), 6.9-7.7 (H aromatic).

Residual solvents: δ(ppm) = 2.09 (acetone), 2.50 (DMSO),2.73, 2.89, 7.95 (DMF), 3.16, 4.01 (MeOH), 3.33 (H_2O)

The DS of starch-DMBA was determined by taking the ratio of the integral of the aromatic H signal to the integral of the H-1 signal.

$$DS_{\text{starch-DMBA}} = \frac{[\int \delta(6.9\text{-}7.7)]/3}{\int \delta(5.2)}$$

The DS of starch-DHBA-PBA was found by taking the ratio of the integral of the aromatic H signal corresponding to DHBA at 7.0 to the integral of the H-1 signal.

$$DS_{\text{starch-DHBA-PBA}} = \frac{\int \delta(7.0)}{\int \delta(5.2)}$$

3.4.4.2 Verification of Conjugation Bond-Type by FTIR

FTIR experiments were conducted on a Nicolet Nexus 670 FTIR spectrometer equipped with Thermo Smart Diffuse Reflectance FT-IR accessory. Samples were prepared by grinding 25-50 mg of sample with 500 mg KBr using a Wig-L-Bug grinding mill. The powder was collected and allowed to dry in a vacuum desiccator overnight before being analyzed. Spectra were obtained with 128 scans and a resolution of 4 and processed using OMNIC software.

3.4.4.3 Characterization of Dihydroxybenzoic acid-Phenylboronic acid Esters

3.4.4.3.1 Gravimetric Analysis

The mass of the PBA, DHBA mixture was recorded after grinding, before being put in the oven. Once the mixture was reacted and dried, the mass was again recorded. For a complete reaction, the final theoretical mass was calculated based on the initial mass, the loss of water, and the new molecular weight of DHBA-PBA (MW = 240). The yield was calculated as the ratio of the theoretical molecular weight of DHBA-PBA (assuming 100% conversion) to the actual final mass.

$$\text{Yield} = \frac{\text{mass}_{\text{theoretical, 100\%}}}{\text{mass}_{\text{final, observed}}} * 100\%$$

3.4.4.3.2 Mass Spectrometry

To verify that only phenylboronic acid esters of DHBA were being formed, dry samples were analyzed by EI/CI mass spectrometry.

For ESI and APCI MS analysis of DHBA-PBA and its product with CDI, 20 mg of CDI and/or 30 mg of DHBA-PBA were dissolved in about 0.5 mL of DMSO or THF in a gaskted, screw-cap, 1 mL centrifuge tube. Samples were directly injected. Samples were analyzed within 24 hours of preparation.

3.4.5 Lap-Shear Adhesive Test

Lap-Shear testing was performed with an Instron materials testing machine. Polished aluminum strips of dimensions 10 cm × 1.25 cm were used as the adherends for the tests. 300 mg/mL solutions of CMS or CMS-dopamine in distilled water were prepared, using a sonicator to aid dissolution. 22.5 µL aliquots of the solution were applied to each adherend over an area roughly 1.25 cm × 1.25 cm. A 15 µL aliquot of distilled water was then applied to one adherend. The areas of the adherends over which the adhesive was applied were then overlapped and allowed to cure for 1 hour at room temperature before being placed in an oven at 55°C for 24 hours, and finally cooled for 1 hour at room temperature. For each test, three samples were evaluated and the adhesive force averaged.

CHAPTER 4. RESULTS AND DISCUSSION

4.1 Enzymatic Hydrolysis of Hi-Maize® 260

Enzymatic hydrolysis by α-amylase was investigated for reducing the molecular weight of starch because it is quick, easy to control, environmentally friendly, and could be carried out while starch was dispersed in DMSO. Successful enzymatic hydrolysis of starch in DMSO was affected by factors including: DMSO/buffer ratio, type of buffer, presence of CaCl, and pH.

Initially, hydrolysis was attempted by adding α-amylase (1 mg/g starch) in 20 mL of 1 M phosphate buffer (pH=7) to 200 mL of a 5% solution of starch in 90/10 DMSO/H2O at 50°C. Hydrolysis was not obvious by HPLC-SEC-RI-MALLS and it appeared that the buffer salts may have fallen out of solution. The pH of the reaction mixture was 8.25 which was in the upper range for stability of the enzyme.

To lower the pH and hopefully keep the buffer salts in solution, the parameters were kept the same as above, but a 50/50 mixture of 1 M phosphate buffer containing enzyme and 5% starch solution in 90% DMSO was prepared to commence hydrolysis. The pH of this mixture was 8, but again it appeared that there was significant precipitation of buffer salts.

In attempt to keep the buffer salts in solution and also keep the pH lower, the same reaction described above was carried out, except the buffer capacity was reduced to 0.1 M and the pH was manually adjusted by HCl to 7.35. While it appeared that the components of the reaction mixture stayed in solution better than previously, there was still no significant starch hydrolysis.

After searching the literature for a procedure detailing enzymatic starch hydrolysis in DMSO, a procedure was adopted from Megazyme's "Total Starch Assay". The procedure called for a 60/40 ratio of 0.1 M acetate buffer (pH=5) containing CaCl to DMSO/starch solution. Applying this to a 5% starch solution in 90% DMSO/H_2O yielded an overall pH of 6 and the components of the reaction mixture seemed to stay in solution, although some cloudiness was obvious. Initial reactions using these parameters were run overnight using enzyme loadings of 1 mg α-amylase/g starch, 0.1 α-amylase/g starch, and 0.01 α-amylase/g starch. The next morning, four volumes of ethanol were added to the reaction mixtures to precipitate the starch. It was immediately obvious that there was significant starch hydrolysis because no material could be precipitated from the reaction containing 1 mg α-amylase/g starch, indicating that all of the high molecular weight starch had been hydrolyzed into smaller units which could not be separated via precipitation by 80% ethanol. Thus, this procedure was adopted for further use and the lowest enzyme loading was chosen because hydrolysis of starch progressed slowly enough to be controlled and studied.

4.1.1 Enzymatic Hydrolysis Time Study

The results from the small-scale enzymatic hydrolysis study can be seen in Figure 4.1.

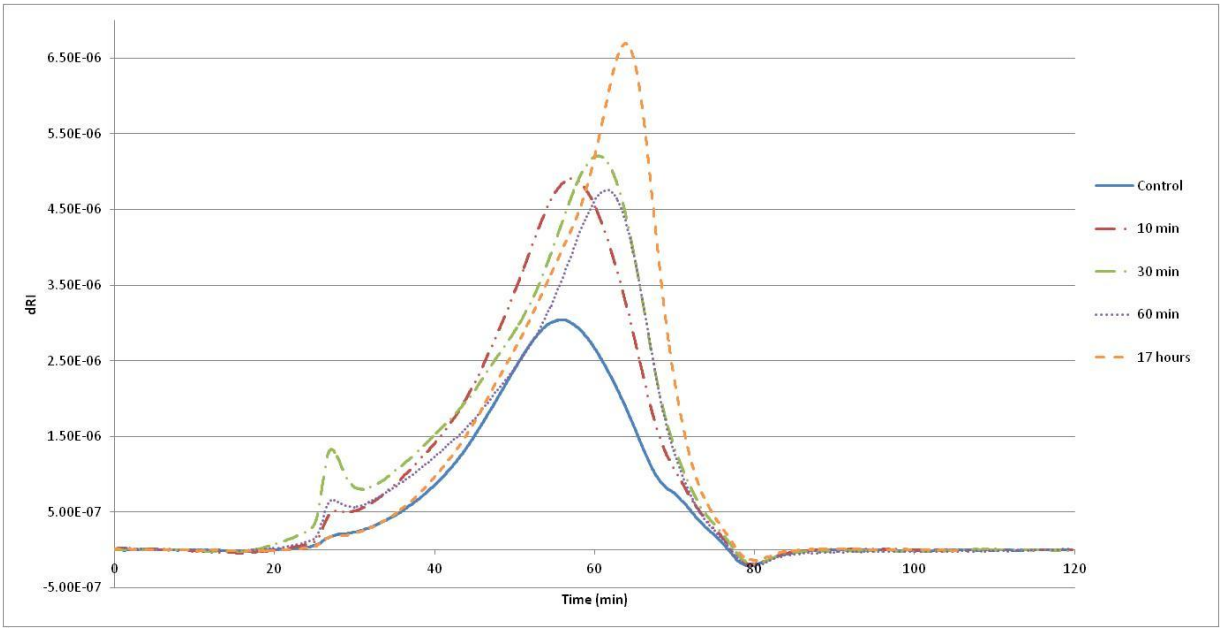

Figure 4.1 Elution Profile of Hydrolyzed Starch from Hydrolysis Time Study

From the chromatogram, it can be seen that the elution time for starch increases as a function of hydrolysis time. This verifies that the starch is in fact being hydrolyzed because longer elution times coincide with smaller molecules based on the concept of size exclusion chromatography. The lack of peaks beyond 90 minutes indicates that the product was free of the hydrolysis products maltotriose, maltose, and glucose after precipitation and washing.

The first small peak to be eluted represents amylopectin eluted in the void volume. It should be noted that the amylopectin peak diminishes as a function of hydrolysis time.

While α-amylase cannot debranch the amylopectin molecules, it can hydrolyze the side chains to the point that the amylopectin more closely resembles amylose.

The corresponding molecular weight and statistical error can be seen in Table 4.1. The recorded molecular weight after a reaction time of 30 minutes is inconsistent with the rest of the data as it indicates that the average molecular weight actually increased. However, the chromatogram clearly indicates that the peak for the 30 minute sample elutes later than the 10 minute peak as expected. It is unclear why such a high molecular weight was calculated for the 30 minute sample, but issues with starch-starch interactions and starch-column interactions causing reproducibility issues have been reported (Chen & Bergman, 2007).

Table 4.1 Molecular Weight of Major Elution Peaks

Sample	Mw	Stat Error
0 min	1182000	0.9
10 min	426200	1
30 min	644800	1
60 min	290600	2
17 hr	63010	9

4.1.2 Gram-Scale Preparation of Hydrolyzed Non-Granular Starch

The molecular weight distribution of starch as a function of hydrolysis time was again analyzed once the procedure was scaled up. The results can be seen in Figure 4.2.

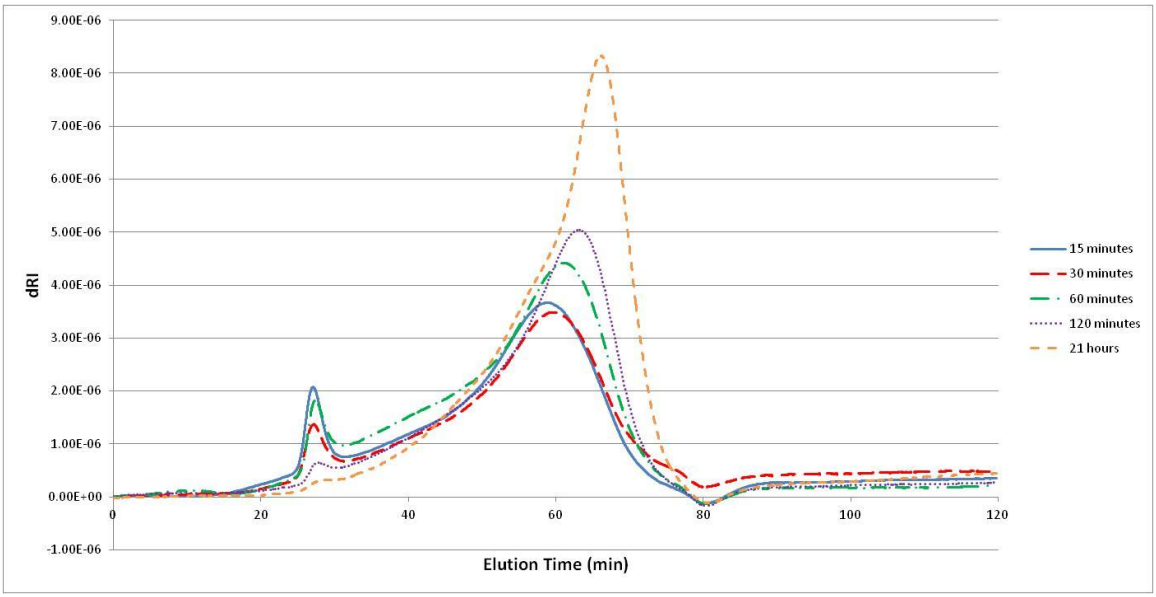

Figure 4.2 Elution Profile for Hydrolyzed Starch from Gram-Scale Preparation

Table 4.2 Molecular Weights of Major Elution Peaks

Sample	Mw	Stat Error
15 min	763700	1
30 min	536700	3
60 min	284600	2
21 hr	57700	10

Again, it can be seen that the molecular weight decreases as a function of time. The rate of hydrolysis also seems to be very similar to that of the small scale hydrolysis study. Based on the hydrolysis experiments, about 50-60 kDa is the lowest molecular weight attainable after 24 hour hydrolysis under the reaction conditions specified and the washing procedure. The precipitation method used may have selected for starch molecules about 50k Da and higher.

For simplicity, only unhydrolyzed and 24 hour-hydrolyzed starch was used as starting material for further modification and functionalization. Unhydrolyzed starch and 24-hour hydrolyzed starch will be referred to as high MW and low MW starch, respectively from here on.

4.2 Carboxymethylation of Hi-Maize® 260

4.2.1 One-Step Non-Granular CMS

The first attempts at making carboxymethyl starch were done based on the process of Heinze et al., but non-granular starch was used. The reaction parameters included reaction temperature of 55°C and 5 hour reaction time. The earliest attempts were done in Erlenmeyer flasks which were placed in an incubated shaker. These trials resulted in agglomerated, sticky, yellow masses that were difficult to handle. Additionally, there were chunks of unreacted starch which were evident when attempting to dissolve the product in water. By lowering the reaction temperature to a maximum of 50°C, shortening the reaction time to 4 hours, finely grinding and drying the non-granular starch, and moving the reaction into a glass reactor with overhead stirrer and temperature control, it became possible to synthesize carboxymethyl starch from non-granular starch without complete gelatinization of the product or significant color development. There was also significantly less unreacted material; however, some still remained.

Table 4.3 Summary of One-Step, Non-Granular, Batch CMS Reactions

	MW	% starch (kg/kg)	% water (kg/kg)	NaOH:AGU	SMCA:AGU	Time (hr)	Temp (°C)	DS
1	Low	3.4	5	1.7	1.7	4	50	0.49
2	Low	3.4	10	1.7	1.7	4	50	0.71
3	High	3.4	10	1.7	1.7	4	50	1.11

Oddly, the high MW non-granular starch resulted in a higher DS than the low MW non-granular starch. This may have been a function of the high MW non-granular starch having higher amylopectin content and/or a difference in the nature of the solid structure of low MW vs high MW non-granular starch.

4.2.2 Fed-Batch Non-Granular CMS

A fed-batch strategy was adopted in attempt to synthesize CMS of very high DS.

4.2.2.1 Additional SMCA

The reaction resulted in an unimpressive DS of 1.3 considering the total amount of SMCA added. While recovering the CMS from this reaction, it was found that the pH of the reaction mixture was nearly neutral, due to the second addition of SMCA. Because the carboxymethylation reaction depends on alkaline conditions to activate the starch hydroxyl groups for nucleophilic substitution, it was thought that perhaps the neutralization of the reaction mixture by addition of only SMCA may have been the reason for the relatively low DS. Therefore, the reaction was carried out with addition of both SMCA and NaOH.

4.2.2.2 Additional SMCA and NaOH

The DS of the CMS synthesized by this method was not drastically different than the previous method. The addition of more NaOH may have favored the side reaction towards sodium glycolate and actually resulted in a lower DS.

Table 4.4 Summary of Fed-Batch Non-Granular CMS Reactions

	MW	% starch (kg/kg)	% water (kg/kg)	NaOH:AGU	SMCA:AGU	Time 1 (hr)	Time 2 (hr)	Temp (°C)	DS
1	High	3.4	10	1.7	1.7	4	16	50	1.30
2	High	3.4	10	1.7	1.7	4	16	50	1.16

Based on the conditions used, a fed-batch strategy with non-granular starch does not seem to be an effective way to greatly increase DS of non-granular CMS.

4.2.3 Single and Multi-step Granular CMS

Performing carboxymethylation of starch in granular form presents many benefits over non-granular starch. Starch granules basically provide a neat package of starch in a particle of defined size. While intuitively it would seem like the starch granule would provide a significant mass transfer barrier between the starch molecules and the reactants, the liquid phase is apparently able to adequately penetrate the starch granules. The water fraction of the reaction medium is not only useful for dissolution of the sodium hydroxide and sodium chloroacetate, but also helps to swell the starch granules, allowing greater access of reactants to the starch molecules.

One of the main benefits of granular starch in carboxymethylation reactions is that the starch reacts uniformly. Very little, if any, unreacted chunks of starch remained after

reaction of granular starch, whereas a small fraction of the added starch remained unreacted in the case of non-granular starch. Granular carboxymethyl starch is also much easier to process. Granular CMS can be easily filtered and washed whereas non-granular CMS agglomerates and clogs filters, requiring multiple precipitations, or preparatory chromatography to thoroughly wash. Additionally, due to the uniform granule size, and undisrupted molecular structure of granular CMS, a ready-to-use powder can be obtained simply by drying in an oven after washing. Non-granular CMS, on the other hand, forms various sized chunks of agglomerated material when recovered from precipitation, making thorough grinding necessary or ultimately requiring lyophilization which requires water and time.

While granular CMS has many clear benefits over non-granular CMS, the molecular weight of the starting material cannot be varied. It is fortunate then, that processing conditions for non-granular starch were worked out because it was necessary to carboxymethylate enzyme-hydrolyzed starch.

Synthesis of CMS with DS greater than 2 has been achieved using multiple-step reaction strategies (T Heinze et al., 2004; Tijsen et al., 2001). In order to successfully perform multi-step carboxymethylation of starch, a delicate balance of parameters must be maintained in order to avoid gelation of the starch granules while still achieving high reaction efficiency. The most important parameters to control are temperature, water content, and reaction time. If any of these parameters are too high, gelation of CMS can occur.

4.2.3.1 Method 1

In the first trial, the material was successfully reacted twice, but completely gelatinized when a third attempt was made. The product from the second step was somewhat swollen and would easily gelatinize in an environment with moderate water content. The DS of the product from the second step of the first trial was determined to have a DS of about 1.70. For the second trial, some material was set aside after the first step to check DS and the rest was reacted further. The DS of the product from the first step was determined to be about 1.00. On the second and third step of the second attempt, the water content was halved compared to the other steps, but the product of the second step was semi-agglomerated and full gelation still occurred on the third step.

Table 4.5 Summary of Multi-Step Granular CMS Reactions using Method 1

	Step	% starch (kg/kg)	% water (kg/kg)	NaOH:AGU	SMCA:AGU	Time (hr)	Temp (°C)	DS
1	1	3.4	10	1.7	1.7	5	40	-
	2	3.4	10	1.7	1.7	5	40	1.70
	3	3.4	10	1.7	1.7	5	40	-
2	1	3.4	10	1.7	1.7	5	40	1.03
	2	3.4	5	1.7	1.7	5	40	-
	3	3.4	5	1.7	1.7	5	40	-

4.2.3.2 Method 2

The second approach was done using the exact same parameters and following, as closely as possible, the procedure of Tijsen et al. While the product from these reactions never broke out of granular form, the DS after three steps was only 0.87. The most likely reason for this is the difference in starch type. Higher water content is actually required to obtain carboxymethyl corn starch with a DS comparable to that of potato starch (Tijsen et al., 2001). Additionally, Hi-Maize 260® is a high-amylose variety of corn starch.

Highly branched amylopectin molecules swell easily in water, whereas linear amylose molecules maintain rigid structure. Therefore, swelling of Hi-Maize 260® granules may require more water than for normal corn or potato starch to obtain DS values comparable to that obtained by Tijsen et al. One potential drawback to this reaction strategy is that depolymerization may result from long contact times between NaOH and starch at elevated temperature before addition of SMCA.

No further attempts to synthesize CMS with DS higher than 2 were made due to time constraints and because it was outside the scope of the project. Optimization of multi-step reaction parameters, specifically for high amylose corn starch, would be necessary to attain carboxymethyl high-amylose starch with DS greater than 2. Adjusting the water content of the reactions seems to be a good starting point.

4.3 Starch-Catechol Conjugates

4.3.1 Synthesis of CMS-dopamine by EDC

Early attempts to create a dopa-functionalized conjugate were made by trying to conjugate DOPA to carboxymethyl cellulose using EDC as crosslinker. Carboxymethyl cellulose was used as a place-holder while CMS synthesis methods were developed and applied. While the initial conjugation attempts were not very successful, it quickly became obvious that dopamine was a much better candidate for conjugation to carboxylic acid groups than DOPA for a couple of reasons. First, the solubility of dopamine is much higher than that of DOPA in water. The solubility of DOPA in water is limited to less

than 10 mg/mL which places a limit on the concentration of carboxylic acid groups in the reaction if there is to be an excess of DOPA. The higher water solubility of dopamine allows greater concentrations of carboxylic acid groups to be used while still providing dopamine in excess. Second, dopamine does not have a carboxylic acid group. Without the carboxylic acid group, dopamine does not run the risk of self-polymerization by EDC. Additionally, the lack of a carboxylic acid group on dopamine means there is no chance for repulsion from the carboxylic acid groups of CMS, or steric hindrance of the amine group.

Early reactions of CMS with dopamine suffered from an inadequate washing method and therefore afford mostly only qualitative observation. Some quantitative observation of these reactions is included in Appendix A for comparison amongst other samples with similar concentrations of dopamine and purified in the same way.

4.3.1.1 One-step Reaction

Many procedures for EDC crosslinking advise using an excess (up to 10X) of both EDC and the second molecule to be conjugated for effective conjugation. Therefore, initial attempts to create CMS-dopamine were carried out using an excess of EDC and dopamine. Upon addition of EDC to the solution of dopamine and CMS, the pH slowly began to rise and the reaction mixture gradually became cloudy over the course of about 15 minutes, due to precipitated material. The change in pH is consistent with observations in reactions between EDC and other carboxylic acids and indicates the

formation of O-acylisourea (Mojarradi, 2011). The reason for material precipitating out of solution was thought to be caused either by solubility change imparted on CMS by dopamine conjugation, or crosslinking of CMS as a result of di-DOPA links formed by oxidation of conjugated dopamine molecules, leading to extremely large polymers.

The product was extremely insoluble; it could not be dissolved in water, polar organic solvents, or nonpolar organic solvents, even when heat was applied. The only methods effective at dissolving the material were raising the pH significantly above neutral, or by autoclaving the material in water; both of which resulted in a brown solution due to oxidation of dopamine. Various measures were taken to gain more insight into what might have been causing precipitation and how to avoid it.

4.3.1.1.1 Lower EDC and dopamine

By lowering EDC:COOH and dopamine:COOH to 0.5, precipitation could be avoided. However, an equimolar ratio of EDC and dopamine to carboxyl groups still caused precipitation. Using lower EDC:COOH and dopamine:COOH presumably led to less conjugated dopamine, thus lowering the chance of oxidized dopamine groups interacting to form di-DOPA crosslinks between adjacent polymers.

4.3.1.1.2 Anhydride Formation by EDC

To rule out the possibility that EDC was directly cross-linking CMS through formation of anhydrides between neighboring COOH groups, the reaction was carried out without

dopamine using high MW CMS (DS = 1.7) and EDC:COOH = 1, a condition that resulted in precipitated material when carried out with dopamine. No precipitated material resulted, ruling out the possibility that EDC was directly responsible for precipitation.

4.3.1.1.3 Lower pH

Initial attempts to create CMS-dopamine conjugates allowed the pH to drift over 5 once EDC was added, making auto-oxidation of dopamine more likely. To address the possibility of high pH causing dopamine oxidation and subsequent precipitation, the pH of the reaction was adjusted so that it would not exceed 4.5 after addition of EDC. It was found that precipitation still resulted, regardless of the lower pH.

4.3.1.1.4 Lower Molecular Weight

By using CMS of lower molecular weight, cross-linked material should be more likely to stay in solution because the individual molecules are much smaller to begin with. In addition to a lower molecular weight, the CMS used for these experiments had a DS of 0.5; roughly half the DS of the high MW CMS initially used.

Table 4.6 Summary of Reactions with Low MW CMS

	MW	DS	mg/mL	EDC:COOH	dopamine:COOH	pH	Precipitation
1	Low	0.5	10	2	4	< 4.5	Y
2	Low	0.5	10	1	2	< 4.5	N
3	Low	0.5	5	2	4	< 4.5	Y
4	Low	0.5	10	2	2	< 4.5	Y
6	Low	0.5	10	1	20	< 4.5	N

Based on the results in Table 4.6, a greater EDC:COOH could be used with the lower molecular weight CMS with no precipitation. However, excess EDC:COOH still caused precipitation. It is not completely clear whether the ability to use a higher relative concentration of EDC can be attributed to the lower molecular weight, or the lower DS of the CMS used.

Another important point is that precipitation of CMS-dopamine conjugate during reaction seems to be dependent on the concentration of EDC, but not of dopamine. The same dopamine concentration could be used with different outcomes, depending on the concentration of EDC used. As seen in Table 4.6, when using 2:1 dopamine:COOH and 1:1 EDC:COOH precipitation did not occur, yet precipitation was obvious when EDC:COOH was increased to 2:1 under the same conditions. Even when using 20:1 dopamine:COOH, precipitation did not occur with 1:1 EDC:COOH. These results indicated two possibilities: precipitation of the polymer depended on a critical amount of conjugated and oxidized dopamine, which was limited by the concentration of EDC, or that EDC was in some other way responsible for the observed precipitation.

4.3.1.1.5 Removal of O_2

Another factor possibly causing auto-oxidation of conjugated dopamine was the presence of O_2 in the reaction mixture. The reaction was therefore carried out with care to exclude O_2 to check whether reducing the presence of O_2 in the reaction mixture would prevent polymer precipitation. Despite low pH and absence of O_2, precipitation still occurred.

Therefore, O_2 was not responsible for precipitation of the polymer. The fact that precipitation of the polymer proceeded despite conditions preventing auto-oxidation of dopamine (low pH and absence of O_2) in the presence of excess EDC led to question whether there was some interaction between EDC and conjugated dopamine that could be causing precipitation of the polymer.

4.3.1.1.6 Addition of Ascorbic Acid

To take even further measures to prevent possible oxidation of conjugated dopamine, addition of ascorbic acid to the reaction was investigated. While there are many chemical anti-oxidants, ascorbic acid was chosen because it is water-soluble, cheap, readily available, does not interact with catechol, and lacks nucleophilic thiol or amine groups that could interfere with conjugation of dopamine by EDC.

Reaction 3.4.1.3.1, utilizing 2:1 AA:dopamine prevented precipitation of the polymer, but the product had a yellow hue, indicating conjugation of ascorbic acid. Therefore, it was not clear whether the antioxidant capabilities of ascorbic acid were responsible for preventing precipitation, or competing conjugation between dopamine and ascorbic acid to CMS resulted in an overall lower amount of conjugated dopamine; essentially preventing precipitation in the same manner as lowering the amount of EDC and dopamine in the reaction.

A small amount of the recovered, purified material was dissolved in water, diluted, and analyzed by UV-vis spectroscopy for evidence of ascorbic acid conjugation. The results can be seen in Figure 4.3.

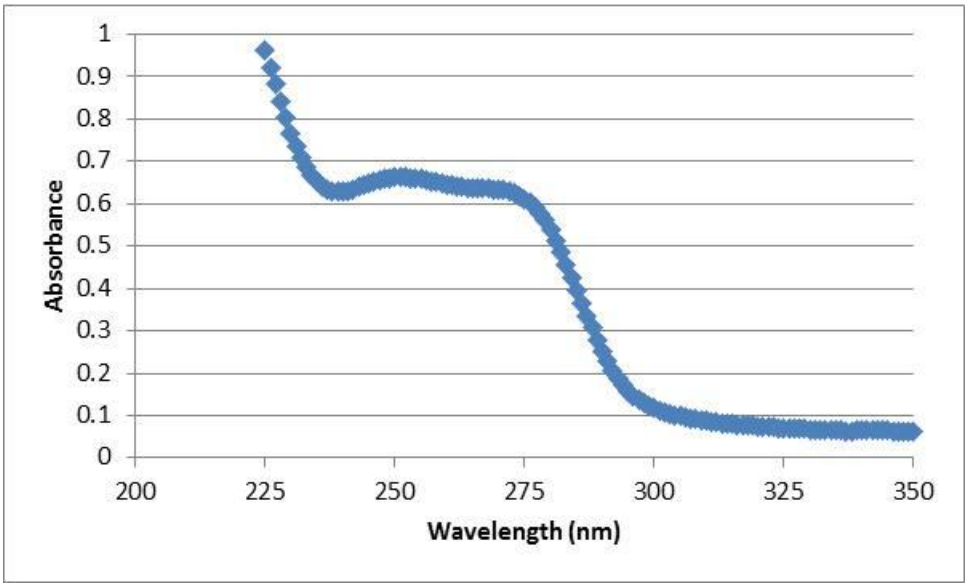

Figure 4.3 UV-Vis Spectrum of CMS-dopamine-AA

According to literature, UV absorbance by ascorbic acid can range from about 240 nm to 270 nm due to contribution from both its neutral and ionic forms (Markarian & Sargsyan, 2011). Figure 4.3 shows a broad peak between 240 nm and 290 nm, indicating conjugation of ascorbic acid in addition to dopamine. Moreover, while ascorbic acid lacks amine or thiol groups, it is still able to behave as a strong nucleophile because of its ability to exist as an enolate ion (Kesinger & Stevens, 2009). Therefore, it makes sense that ascorbic acid was actually able to participate in conjugation.

In order to reduce the conjugation of ascorbic acid to CMS and retain its benefits as an antioxidant, it would be desirable to use the lowest concentration of AA possible while still preventing precipitation. Reaction 3.4.1.3.1 was carried out with various AA:dopamine and evaluated with respect to precipitation. The results can be seen in Table 4.7.

Table 4.7 Identification of Lowest AA:dopamine for Prevention of Precipitation

ascorbic acid:dopamine	**Precipitation?**
0.1	Y
0.25	Y
0.5	Y
1	N
2	N

According to the results, at least 1:1 ascorbic acid:dopamine was required to prevent precipitation of the CMS conjugate.

Using this information, an attempt was made to synthesize a CMS-dopamine conjugate with high dopamine substitution according to reaction 3.4.1.3.2**.** In addition to using the lowest ascorbic acid concentration necessary for preventing precipitation, the pH of the reaction was kept at or just below the pKa of ascorbic acid, 4.2, in order to keep ascorbic acid in its fully protonated, neutral state, thereby decreasing its capabilities as a nucleophile to conjugate to CMS. The substitution of dopamine on the final product was determined to be about 0.04; very low. Additionally, UV-vis revealed a broad peak

corresponding to ascorbic acid. Therefore, it was determined that while ascorbic acid is effective at preventing precipitation during the reaction of dopamine and EDC with CMS, it competed with dopamine for conjugation and ultimately led to a very low degree of catechol substitution. It remains unclear whether the route by which ascorbic acid prevented precipitation was by preventing oxidation of conjugated dopamine or by competing with dopamine for conjugation to CMS.

4.3.1.2 Two-Step Reaction

It was clear that using EDC to couple dopamine to CMS was potentially bound by the inability to use excess EDC without causing precipitation. The use of NHS in EDC conjugation reactions is commonly used to create a more stable intermediate and increase the reaction efficiency.

Without excess EDC:COOH, Wang et al. successfully conjugated dopamine to alginic acid, another carboxylic acid-containing polysaccharide, with graft ratios of about 30-40% using EDC/NHS chemistry (Wang et al., 2012). Attempts to synthesize CMS-dopamine conjugates with higher dopamine content were made based on the success of Wang et al.

Initial reactions were conducted using NHS to assess its effect on precipitation of polymer from the reaction mixture.

Table 4.8 Results of NHS Addition to EDC Reaction with Respect to Precipitation

	MW	DS	mg/mL CMS	EDC:COOH	NHS:COOH	dopa:COOH	pH	Precipitation
1	Low	0.5	10	2	2	10	< 4.5	N
2	High	0.84	10	1	1	2	< 4.5	N
3	High	0.84	10	2	2	4	< 4.5	N
4	High	0.84	10	2	-	4	< 4.5	Y
5	High	1.7	10	2	2	4	< 4.5	Y

From Table 4.8, it can be seen that under reaction conditions that previously resulted in precipitation, the addition of NHS prevented precipitation. However, excess EDC/NHS:COOH, in the case of high MW CMS with very high DS still resulted in precipitation.

4.3.1.2.1 Replication of Method by Wang et al.

An attempt was made to replicate the work of Wang et al. The reaction resulted in a $DS_{catechol}$ of 0.018. Unfortunately, the catechol content of the CMS-dopamine conjugate was much lower compared to the alginate-dopamine conjugate of Wang et al. Details of the reaction by Wang et al. are slim so it is difficult to compare the methods to those used for this project in order to form some idea about the discrepancy in $DS_{catechol}$. The source of COOH groups and buffer strength are the only obvious differences.

4.3.1.2.2 Removal of Excess Reactants

Based on the finding that excess NHS and EDC could still cause precipitation, reactions were carried out by first washing the activated CMS free of reactants before reaction with dopamine.

The original plan to remove excess EDC and NHS from activated CMS was to precipitate the activated intermediate with acetone for subsequent reaction. However, the precipitated intermediate formed a gel and would not dissolve for conjugation with dopamine. Therefore, filtration was used to isolate activated CMS and avoid bringing the polymer out of solution. Precipitation was effectively avoided using this method even though the dopamine was clearly oxidized at high pH, suggesting precipitation was not caused by oxidized dopamine.

Quantitative results for these reactions were inaccurate due to improper purification. Results are included in Table A.3 for comparison to reactions carried out with similar purification steps.

4.3.1.2.3 High pH Conjugation with Dopamine Protection by Borate

When amide bond formation by EDC/NHS is carried out in a two-step method, it is advisable for each step is carried out at a different pH. For activation of COOH by EDC and NHS, the optimal pH is around 4.5-6 while the displacement of the NHS ester by an amine occurs most efficiently at pH 7-8 ("NHS and Sulfo-NHS,"). Low pH was maintained throughout the previous reactions in this thesis due to the tendency of dopamine to auto-oxidize in neutral to alkaline conditions. Therefore, high pH could have been preventing high efficiency amide bond formation between CMS and dopamine.

Reactions of dopamine in high pH can be successfully performed when a high concentration of sodium borate is present. Sodium borate can form a stable complex with the hydroxyl groups of dopamine at elevated pH, essentially protecting it from oxidation (BP Lee et al., 2004). Conjugation of dopamine to CMS was carried out in two steps, a low pH activation step followed by high pH conjugation. Additionally, very high concentrations of EDC, NHS, and dopamine were used. No oxidation or precipitation resulted, but the $DS_{catechol}$ of the CMS-dopamine conjugate was only 0.015; no higher than what could be achieved with EDC and NHS at equal molar concentrations to COOH at low pH

4.3.1.3 Summary of EDC Reactions

Table 4.9 Results for Conjugation of Dopamine to CMS by EDC in Aqueous Solution

		MW	DS_{CMS}	mg/mL CMS	EDC:COOH	NHS:COOH	dopamine:COOH	pH 1	pH 2	$DS_{catechol}$
One-Step	1*	High	0.84	10	2	-	4	< 4.5	-	0.021
	2	Low	0.50	10	1	-	10	5	-	0.006
Two-Step	1	Low	0.50	10	2	2	10	< 4.5	< 4.5	0.021
	2	Low	0.50	10	2	2	10	5	5	0.016
	3[a]	High	1.00	10	2	2	4	5.5	5.5	0.018
	4[b]	Low	0.50	10	10	10	10	5.5	7.2	0.015

*EDC added 15 minutes before dopamine

[a]Method based on Wang et al.

[b]Buffer with Sodium Borate

From Table 4.9 it can be seen that despite various reaction strategies to increase the catechol content of dopamine-CMS and regardless of the MW or DS of CMS, the

$DS_{catechol}$ never exceeded 0.02 for any conjugates. Also, excess EDC was successfully used when added to CMS 15 minutes before addition of dopamine.

4.3.1.4 FTIR Characterization of CMS-Dopamine

For comparison, FTIR spectra of low MW starch and its carboxymethylated counterpart are included in Figure 4.4 and 4.5, respectively. The CMS-dopamine conjugates in Figures 4.6-4.8 were synthesized from the CMS of Figure 4.5.

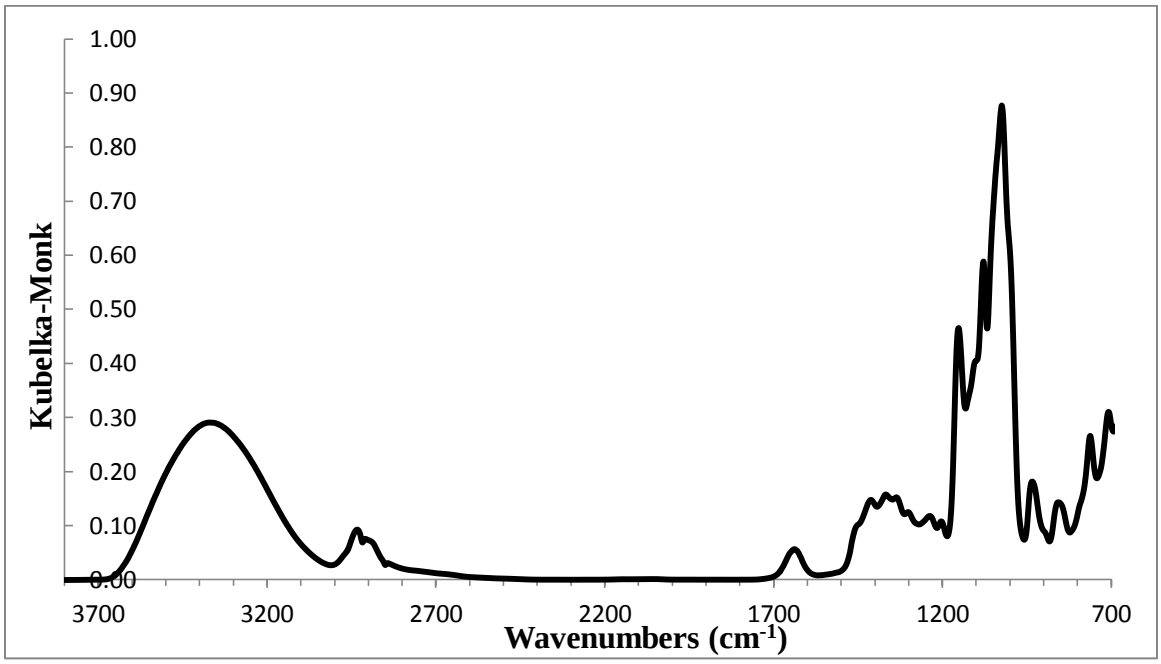

Figure 4.4 FTIR Spectrum of Low MW Starch

The spectrum in Figure 4.4 is typical for starch. The broad peak between 3000 cm^{-1} and 3700 cm^{-1} represents OH stretching from hydrogen bonding between starch molecules. The band at 2932 cm^{-1} represents CH_2 symmetrical stretching. The peak at 1637 cm^{-1} represents bending vibrations of starch-bound water molecules. The bands between 1000 cm^{-1} and 1150 cm^{-1} are assigned to C-Ostretching vibrations from C-O-C and C-O-H

within the glucose units of starch. Finally, the bands at 762 cm^{-1} and 856 cm^{-1} are assigned to stretching vibrations along the starch backbone (Lawal, Lechner, & Kulicke, 2008; Yaacob, Amin, Hashim, & Abu Bakar, 2011).

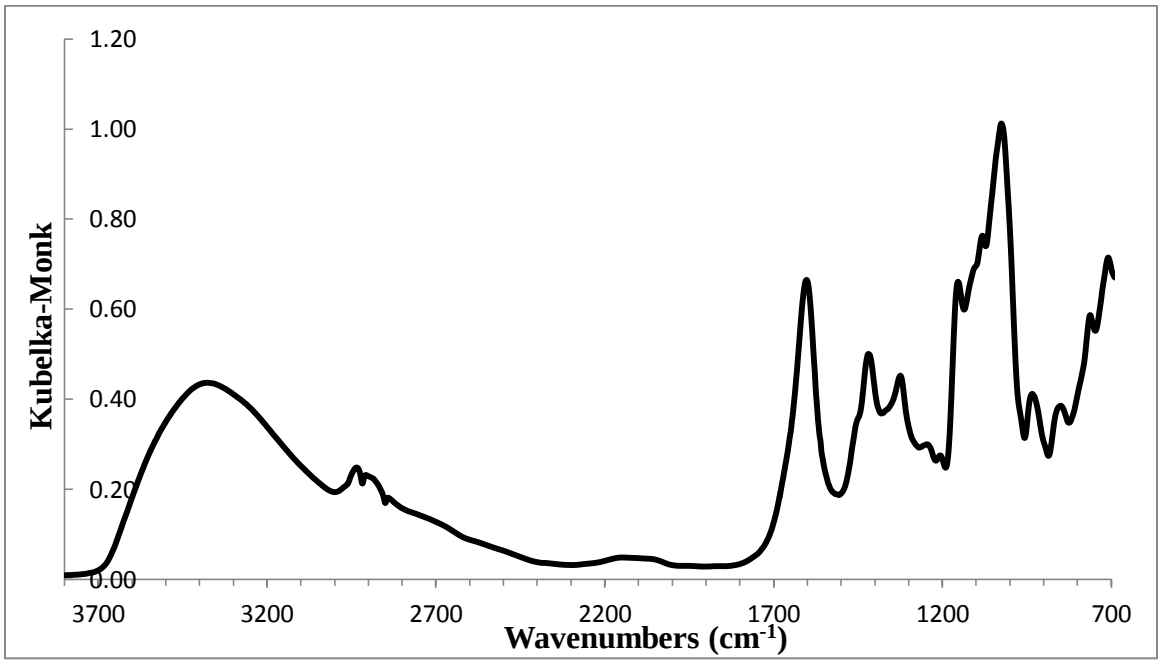

Figure 4.5 FTIR Spectrum of Low MW CMS (DS = 0.50)

New peaks can be seen near 1600 cm^{-1}, 1420 cm^{-1}, and 1330 cm^{-1} and are characteristic of the carboxymethyl moiety of CMS (Lawal et al., 2008). The band at 1600 cm^{-1} is indicative of the carbonyl stretch of the $-COO^-Na^+$ group while the other two bands are related to symmetrical and asymmetrical stretching of $–COO^-$ (Yaacob et al., 2011).

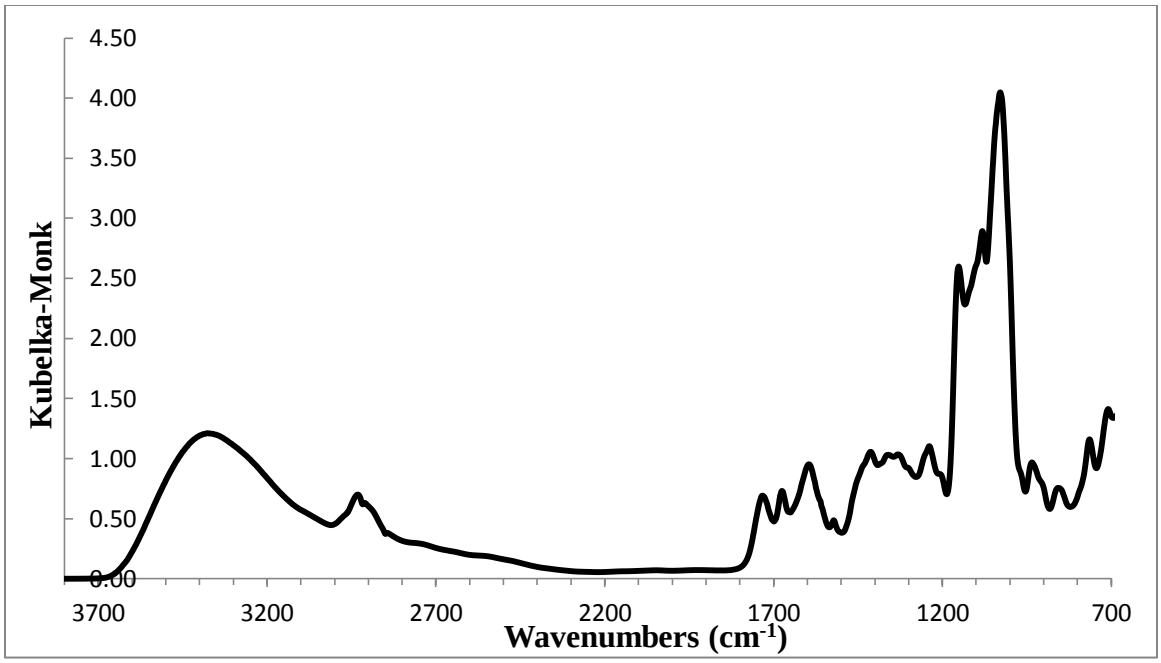

Figure 4.6 Representative FTIR Spectrum of CMS-Dopamine by One-Step Reaction with EDC

After conjugation with dopamine, a new peak appears at 1732 cm^{-1} which represents conversion of $-COO^{-}Na^{+}$ to –COOH (Bendahou, Dufresne, Magnin, Mortha, & Kaddami, 2014), in addition to disappearance of the bands at 1330 cm^{-1} and 1420 cm^{-1} due to acidic conditions of the reaction and dialysis. Bands at 1674 cm^{-1} and 1521 cm^{-1} can be assigned to Amide I and II bands, respectively, from the formation of amide bonds between dopamine and CMS. Additionally, it can be seen that the band originally at 1600 cm^{-1} has slightly downshifted, indicating conjugation on the $–COO^{-}$ group.

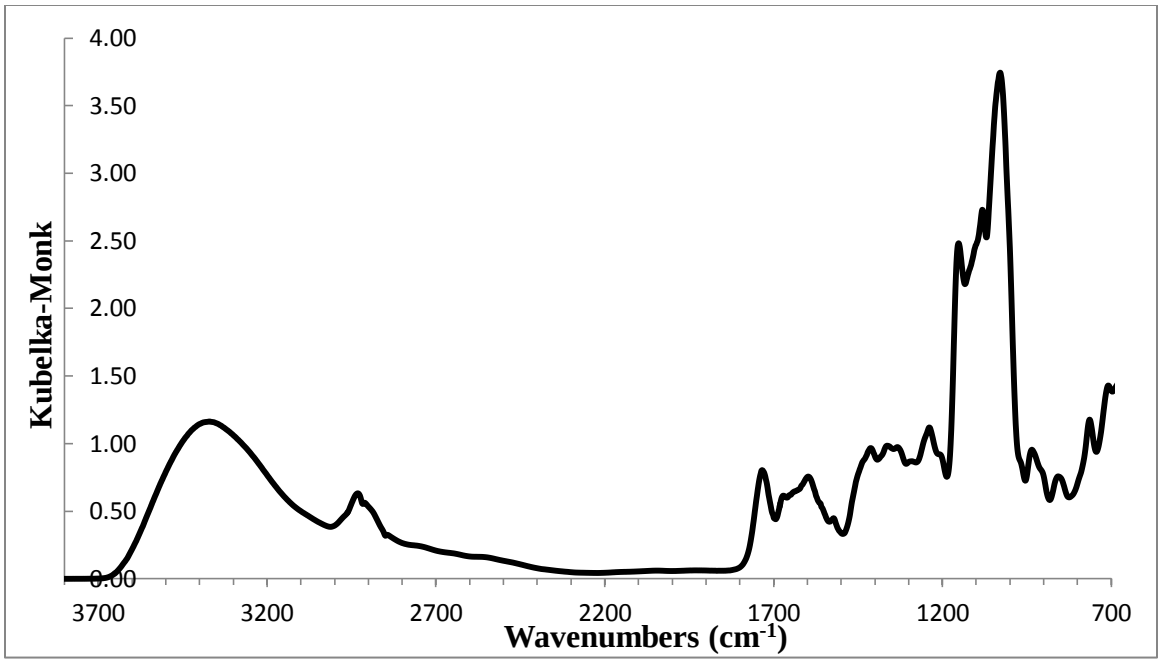

Figure 4.7 Representative FTIR Spectrum of CMS-Dopamine by EDC/NHS Low pH

Similar to Figure 4.6, new bands are apparent at 1733 cm^{-1}, 1670 cm^{-1} as a shoulder peak, and 1522 cm^{-1}, as well as a downshifted peak at 1596 cm^{-1}.

4.3.1.5 Adhesive Strength of CMS-Dopamine

Adhesive capabilities of CMS-dopamine conjugates were tested to see whether even low catechol content would increase adhesive performance.

Table 4.10 Results of Lap-Shear Tests

	MW	DS_{CMS}	$DS_{catechol}$	Lap Shear Strength (MPa)
1	High	0.84	0	0.98 ± 0.17
2	High	0.84	0.021	0.97 ± 0.18
3	Low	0.5	0	1.83 ± 0.12
4	Low	0.5	0.021	0.96 ± 0.46

The results from the lap-shear tests show that the adhesive strength of the CMS-dopamine conjugates failed to achieve higher adhesive performance than catechol-free CMS. In one case, the adhesive strength was actually lower which could have occurred due to oxidation of dopamine. Additionally, it can be seen that the low MW, low DS CMS exhibits significantly higher adhesive strength than the CMS with higher MW and higher DS. However, it is unclear whether MW, DS, or both variables are responsible for this result. Moreover, the higher adhesive strength of low MW CMS could have been a factor of its lower amylopectin content.

4.3.2 Starch-Catechol Conjugates

The synthesis of CMS-dopamine conjugates by EDC in aqueous solution suffered from low catechol substitution. One complicating factor may have been water as the solvent. Water competes with dopamine for activated carboxyl groups by hydrolyzing the active intermediates back to carboxylic acid groups. Generally, coupling reactions in organic solvents yield products with higher substitution. In order to overcome the drawbacks of the aqueous conjugation of dopamine to EDC, a new reaction strategy was devised utilizing organic solvents and a more efficient coupling agent.

N,N'-carbonyldiimidazole (CDI) is a well-established coupling agent that functions by activating carboxylic acid or hydroxyl groups, making them prone to nucleophilic attack, even by other hydroxyl groups (Thomas Heinze et al., 2006; Hermanson, 2008). The coupling mechanism of CDI functions differently depending on whether a carboxylic acid or hydroxyl group is first activated. CDI has been successfully used to facilitate the conjugation of various carboxylic acid-containing molecules to starch and cellulose with high substitution (Thomas Heinze et al., 2006). Figure 4.8 shows the mechanisms by which CDI crosslinking can occur with respect to polysaccharides and carboxylic acid-containing molecules. CDI is attractive as a coupling agent for polysaccharides because of its reactivity towards hydroxyl groups; therefore not requiring prior modification, its benign and easy to remove reaction by-products, low cost, high efficiency, and compatibility with DMSO as solvent.

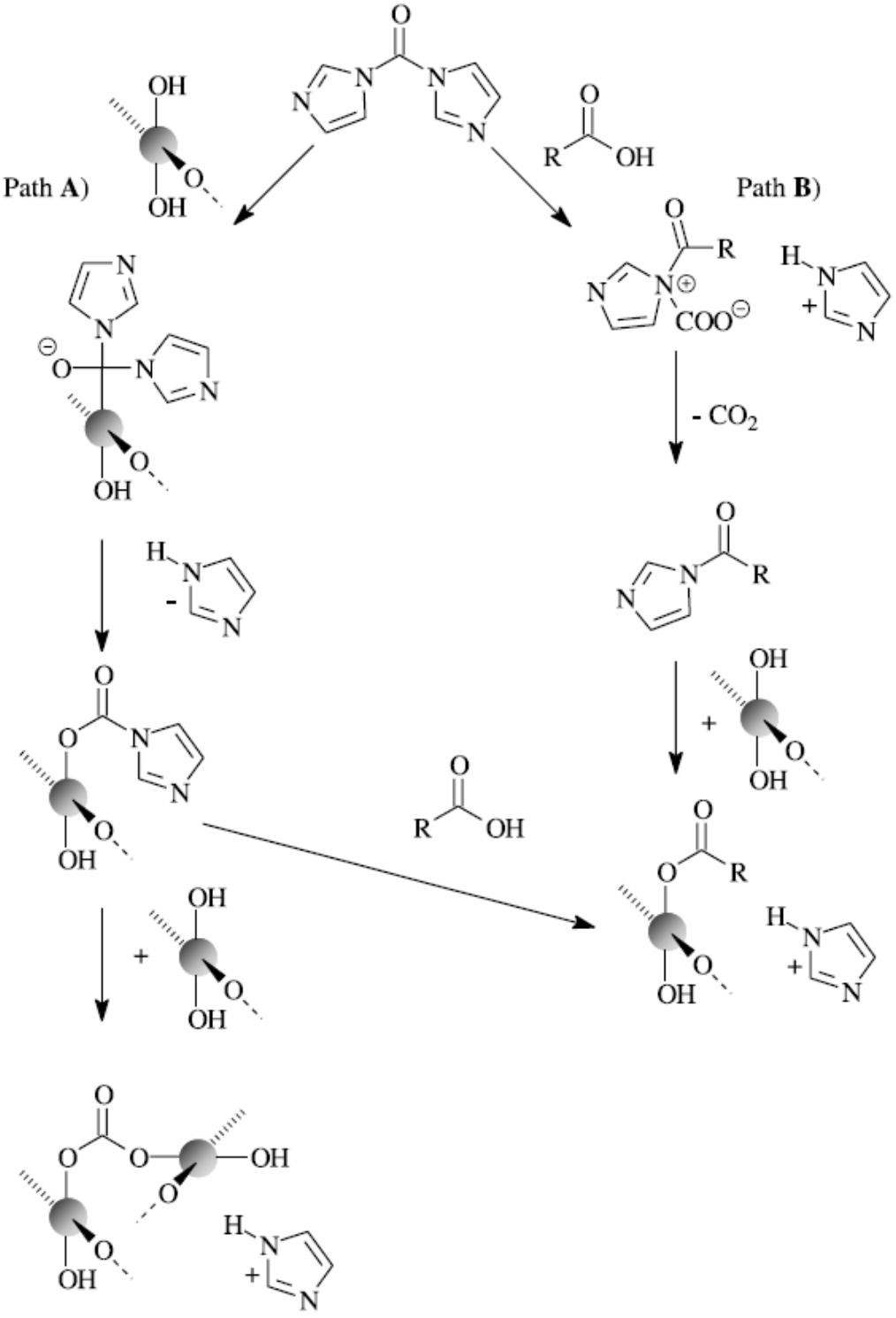

Figure 4.8 Reaction pathways of CDI leading to carbonate (path A) or ester linkages of polysaccharides (Thomas Heinze et al., 2006)

Initially, CDI was used as the coupling agent in a two-step reaction between hydrolyzed starch and dopamine in DMSO or DMF. The goal was to directly attach dopamine to the hydroxyl groups on the backbone of starch via carbamate bond as depicted in Figure 4.9.

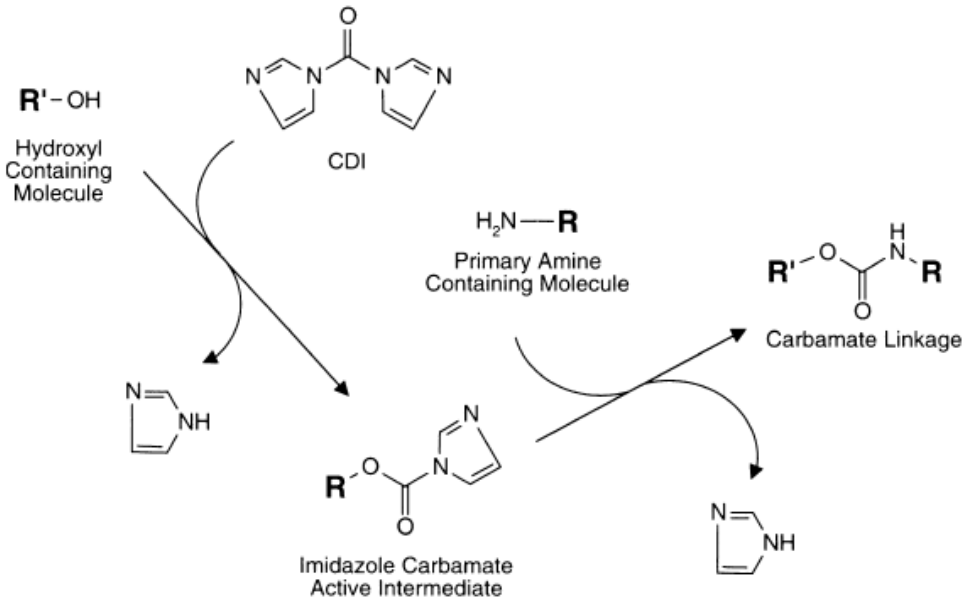

Figure 4.9 Direct conjugation of amine-containing molecule to hydroxylic molecule via CDI.

The product from these reactions was resistant to dissolution in DMSO which indicated cross-linking had occurred between starch molecules. Cross-linking may have resulted from the formation of carbonate ester links between hydroxyl molecules of starch or by the amine and hydroxyl groups of dopamine both coupling to the activated hydroxyl groups of starch, essentially making a dopamine bridge between starch molecules.

One interesting observation was that starch became soluble in DMF upon addition of CDI over the course of an hour, indicating its activation by CDI. However, there were solubility issues after the activated starch was isolated, washed, and added to fresh DMF

for conjugation. Again, this was most likely due to cross-linking. While CDI was apparently very reactive towards starch, a different approach was needed to avoid unwanted reactions.

4.3.2.1 Starch-DMBA

The issues with the initial attempts to make starch-dopamine made two things clear: First, that activating starch with CDI tended to make cross-linked material and second, that the hydroxyl groups on catechol should be protected to avoid their involvement in CDI coupling. Therefore, a bis-O-protected catecholic monomer should first be activated by CDI then added to starch for conjugation to its hydroxyl groups. 3,4-dimethoxybenzoic acid seemed like a good choice for this strategy because its COOH group could be activated with CDI and its hydroxyl groups are methylated, eliminating the need to develop a protection scheme. Westwood et al. were successfully able to completely demethylate 3,4-dimethoxystyrene so it seemed conceivable that the same strategy could be used for starch-DMBA (Westwood et al., 2007).

4.3.2.1.1 Synthesis

Table 4.11 Results of Starch-DMBA Synthesis

	MW starch	[DMBA]/[CDI]:[AGU]	Activation time (hr)	Conjugation time (hr)	DS
1	Low	3	16	24	1.20
2	High	3	40	48	1.27
3	Med	3	20	20	1.00
4*	Med	3	20	24	1.12
5	Low	6	20	24	1.91
6	Low	1	2	16	0.30

As can be seen in Table 4.11, starch-DMBA conjugates with a range of DS could be achieved easily by varying DMBA/CDI:AGU. All of the starch-DMBA conjugates were soluble in DMSO, DMF and pyridine.

4.3.2.1.2 Characterization

A representative NMR spectra of starch-DMBA can be seen in Figure 4.10.

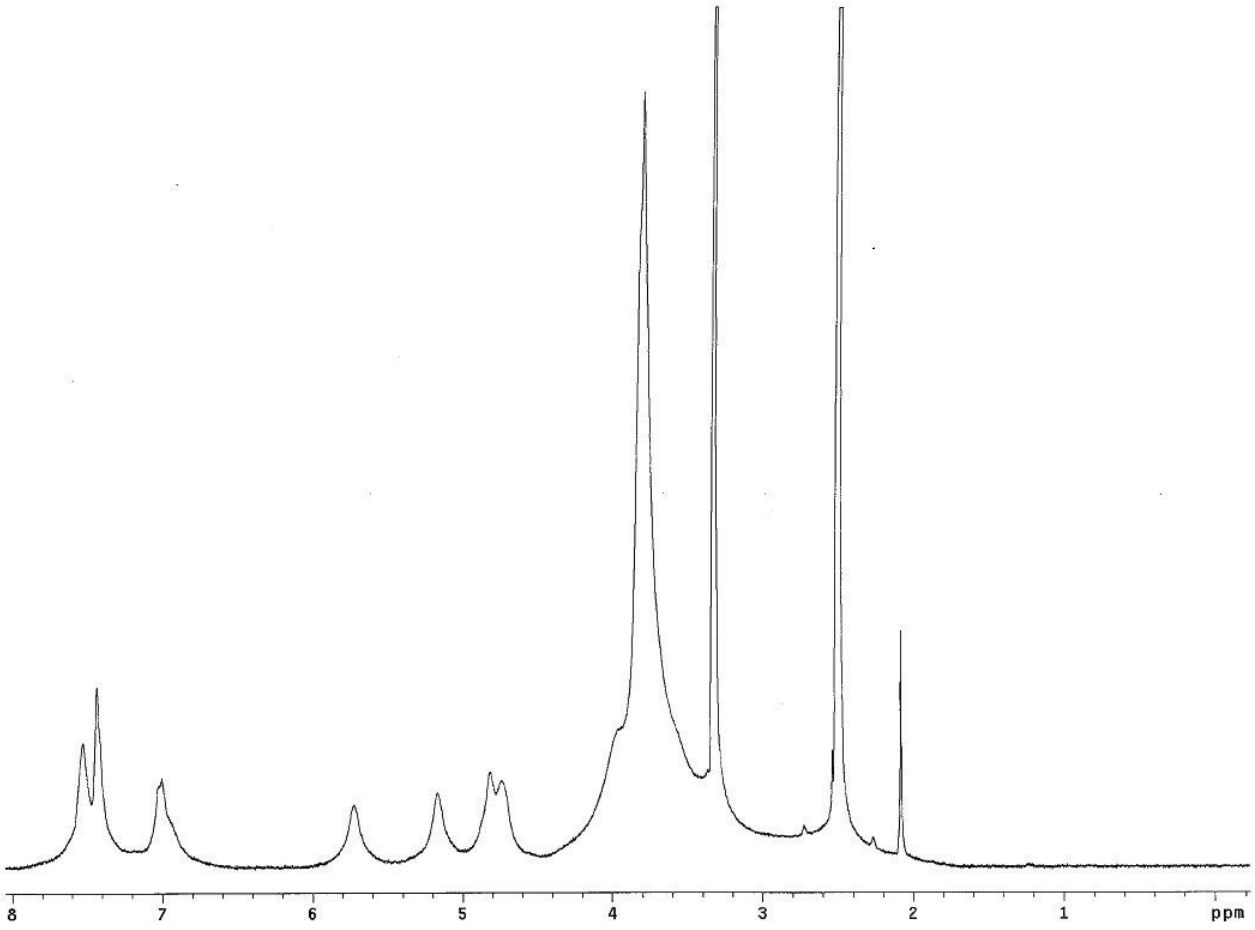

Figure 4.10 Representative H-NMR Spectrum of Starch-DMBA Conjugate

The triplet peaks at δ(ppm) = 6.9-7.7 and the decrease in starch OH peaks indicate successful conjugation of DMBA.

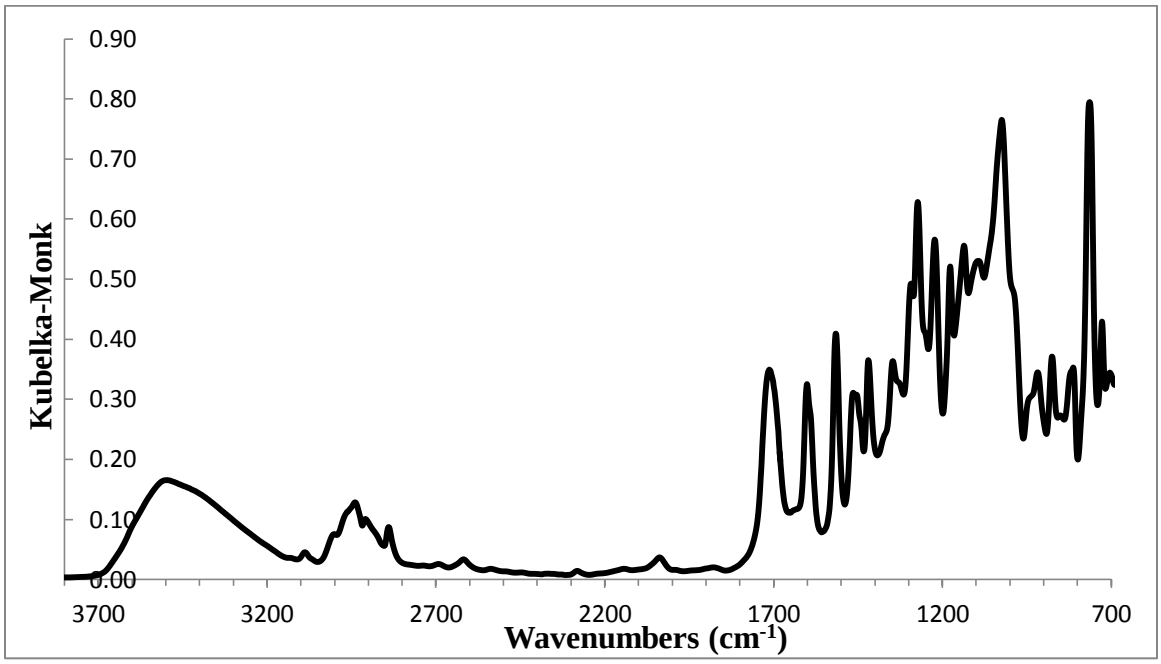

Figure 4.11 Representative FTIR spectrum of starch-DMBA conjugate (DS = 1.27)

The FTIR spectrum in Figure 4.10 verifies attachment of DMBA to starch. The band at 1712 cm^{-1} can be assigned to the carbonyl stretching vibration of the ester bond formed between starch and DMBA. The sharp peaks that arise between 1400 cm^{-1} and 1600 cm^{-1} can be assigned to C=C stretching of the aromatic ring. Peaks at 1222 cm^{-1} and 1272 cm^{-1} most likely arise from the aryl-O stretch of DMBA. Finally, the strong peak at 764 cm^{-1} is characteristic of ortho-disubstituted aromatic molecules.

4.3.2.1.3 Demethylation

4.3.2.1.3.1 By BBr_3

Demethylation of starch-DMBA in DMF by BBr_3 was unsuccessful as evident by H-NMR and by visual lack of color when the recovered polymer was subjected to oxidation by $NaIO_4$ or base. A summary of the parameters used in three different trials can be seen in Table 4.12.

The first attempt resulted in a solid mass. Oddly, the material was able to dissolve in fresh DMF or slowly dissolve into the original solution when left in open air.

The second attempt was made by using a lower polymer concentration and keeping the reaction on ice. These precautions prevented a solid mass from forming, but the recovered product was still not demethylated.

A third attempt at demethylation by BBr_3 was made using lower molecular weight starch-DMBA to see whether the lower molecular weight would result in greater reactivity while being less likely to fall out of solution. Additionally, the DS of the polymer was significantly higher than those previously used in order to increase the chance that BBr_3 would interact with the O-methyl groups of DMBA. Starch-DMBA of high DS was also made to see if it would lead to solubility of the polymer in lewis-base-devoid solvents such as chloroform or DCM, but this was not the case. Lastly, the solvent used was a 1:1

mixture of DMF/DCM in order to decrease possible interactions between DMF and BBr_3. This attempt resulted in a suspension of precipitated material and no demethylation.

Table 4.12 Summary of Conditions for BBr_3 Demethylation Attempts

	MW	DS	Concentration (mg/mL)	BBr3:DMBA	Temperature
1	High	1.24	30	3.5	0 - r.t.
2	High	1.24	10	1.5	0
3	Low	1.91	10	10	0 - r.t.

There are many factors that possibly complicated the reaction. First, BBr_3 is able to complex with the lone pair on the nitrogen atom of DMF, thus interfering with the desired reaction (Gore, Blears, & Danyluk, 1965). Second, there are many other sites on starch-DMBA that are susceptible to interactions with BBr_3 besides the O-methyl groups of DMBA. The oxygen atoms of the glycosidic linkages and hydroxyl groups on starch as well as the ester bond between starch and DMBA would also be capable of interacting with BBr_3 through their lone pairs. However, it does not appear that glycosidic linkages or ester bonds participated in the reaction because there was no evident depolymerization or decrease in DS of the recovered polymer.

It seems that reversible cross-linking between starch molecules was responsible for the solid material formed when the temperature was allowed to reach room temperature. Two possibilities seem most likely for this phenomenon. First, BBr_3 may have coordinated hydroxyl groups between different starch molecules, effectively cross-linking the starch. Second, boric acid is one of the degradation products of BBr_3 and its

ability to cross-link starch is well known; however, this option seems less likely because proper precautions were taken to exclude water from the reaction. In either case, above-freezing temperatures were apparently necessary for these interactions to take place.

4.3.2.1.3.2 By Sodium Ethanethiolate

Sodium ethanethiolate is a strong nucleophile that has been used to completely demethylate aryl methyl ethers when refluxed in DMF (Cutler, Majetich, Tian, & Spearing, 1997; Feutrill & Mirrington, 1970; Suzuki, Tanemura, Horaguchi, & Kaneko, 2006). Sodium ethanethiolate was attractive as a demethylating agent for starch-DMBA because of its effectiveness in DMF, a good solvent for starch-DMBA.

Attempts to demethylate starch by sodium ethanethiolate resulted in low yields of polymer with significantly reduced DS_{DMBA}. The low yield of polymer after demethylation can most likely be attributed to significant depolymerization by sodium ethanethiolate attacking the glycosidic bonds of starch. The reduced DS_{DMBA} of the product was evident by H-NMR; the ratio of the integral of the aromatic signal to H-1 of starch was significantly lower and the intensity of the starch OH peaks were significantly higher. The H-NMR spectra of starch-DMBA (high MW, DS = 1) and "demethylated" starch-DMBA are included in Appendix C for comparison. Additionally, there was no sign of bis-demethylation as there was no visible oxidation upon addition of $NaIO_4$ or base.

4.3.2.2 Starch-DHBA

While there were obvious benefits and relatively high efficiency of CDI coupling DMBA to starch, the main drawback was the difficulty in specifically demethylating the conjugated DMBA groups due to the other chemical groups on starch capable of interacting with the demethylating agents. Therefore, a new method of catechol protection was pursued. Previous work utilizing boric acid to protect dopamine in aqueous solution led to a search for methods to protect DHBA using borate chemistry.

4.3.2.2.1 Protection of 3,4-Dihydroxybenzoic Acid by Phenylboronic Acid

Researchers have successfully synthesized stable, protected catechols using boronic acids (Kaupp, Naimi-Jamal, & Stepanenko, 2003; Ketuly & Hadi, 2010). Most notably, Kaupp et al. protected various molecules, including catechol, with stoichiometric amounts of phenylboronic acid in solid-state. Complete conversion of catechol to its protected phenylboronic ester form was achieved by either ball-milling equimolar amounts of phenylboronic acid and catechol at 80°C for one hour or by co-grinding followed by heating to 115°C for one hour and drying under vacuum at 80°C (Kaupp et al., 2003).

By applying the method of Kaupp et al., DHBA could be protected near 100% with phenylboronic acid using similar conditions. Conversion was verified by gravimetric analysis and EI/CI mass spectrometry. Yields were >95%.

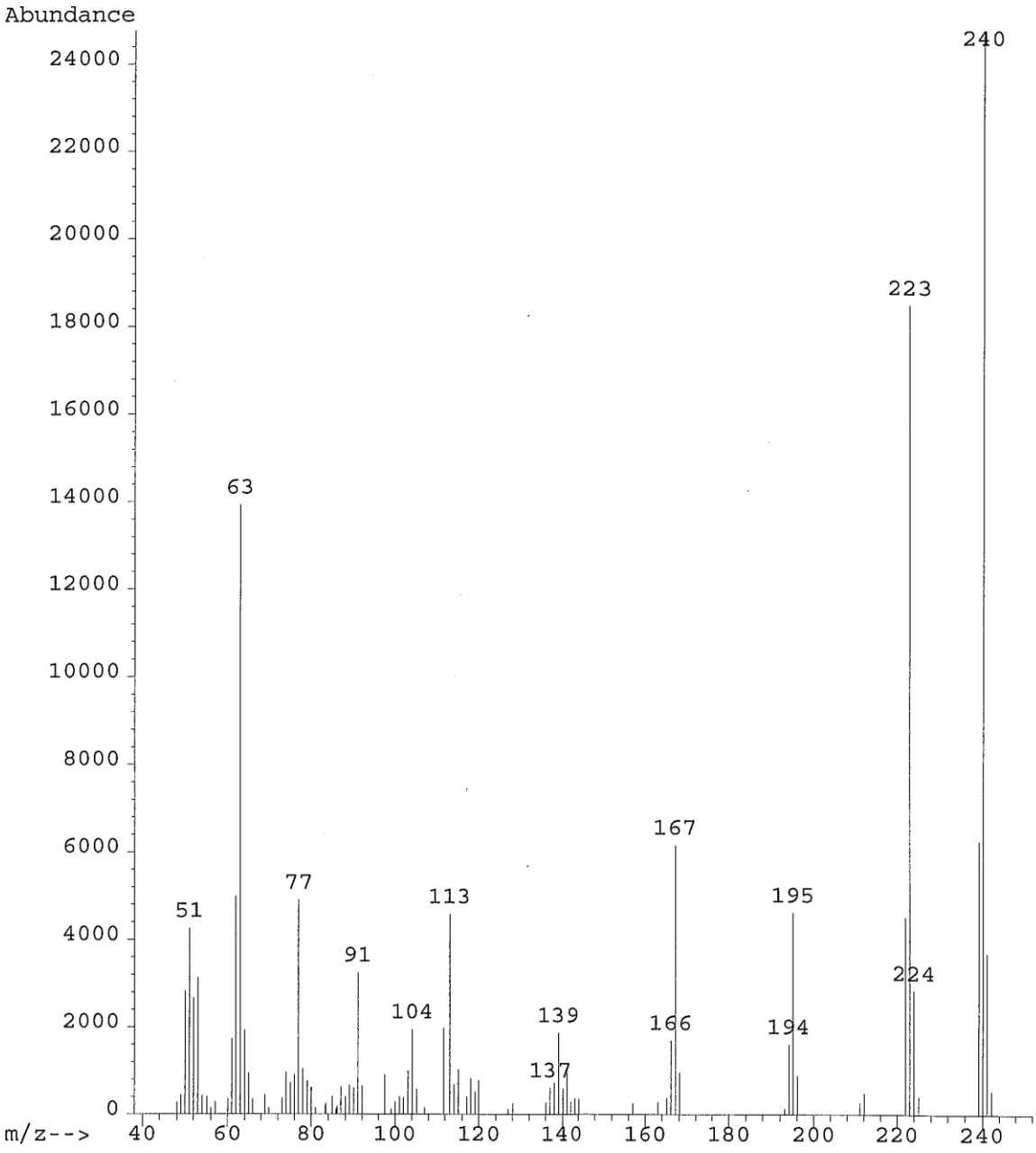

Figure 4.12 EI MS Spectrum of DHBA-PBA

The mass spectra can be seen in Figures 4.12 and 4.13 and verify formation of the boronate ester (m/z = 240). The peak at m/z = 223 represents the loss of a hydroxyl from the COOH group.

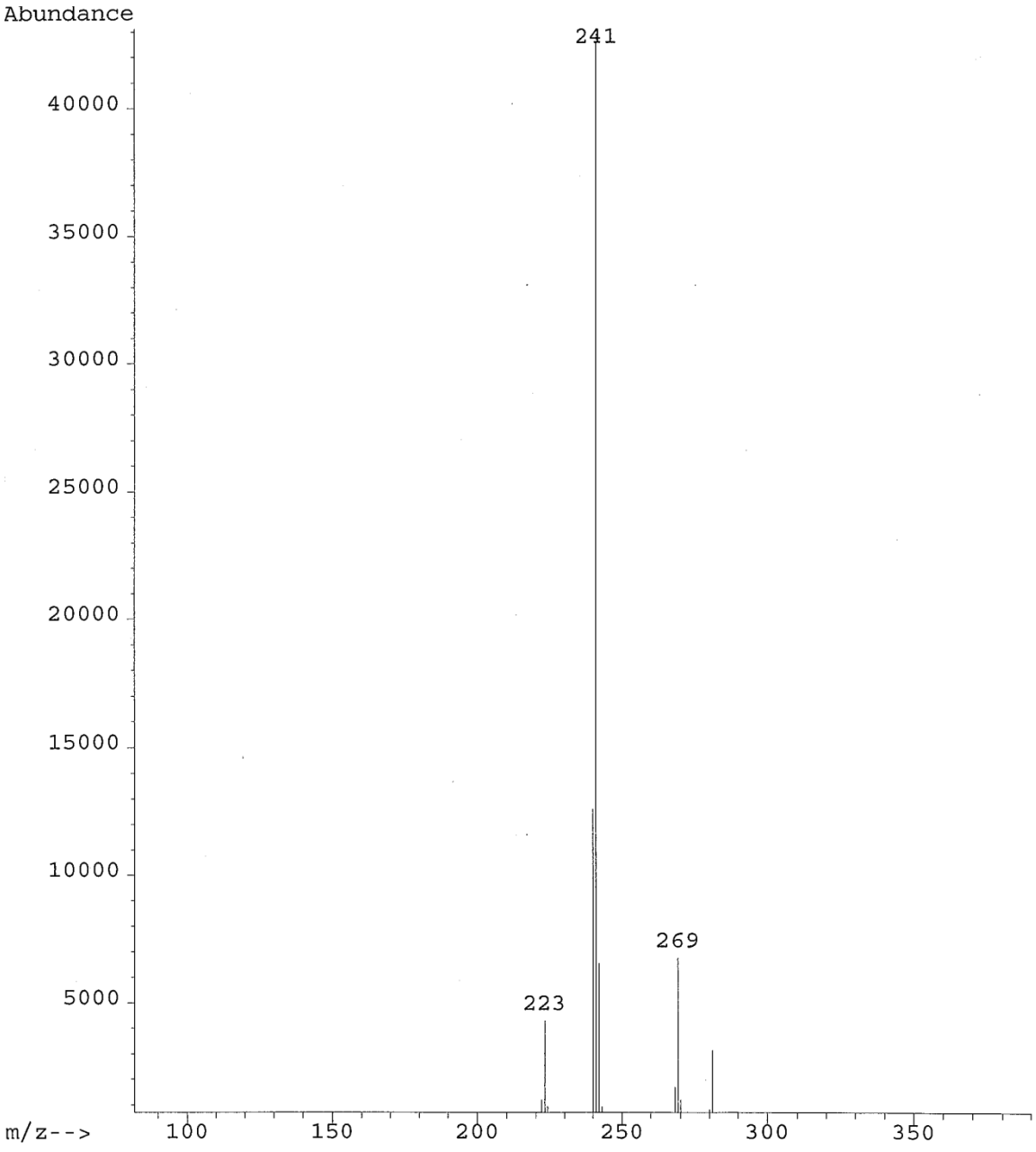

Figure 4.13 CI MS Spectrum of DHBA-PBA

The peak at 269 represents the methane adduct of DHBA-PBA.

4.3.2.2.2 Synthesis of Starch-DHBA-PBA by CDI

Upon addition of CDI to an equimolar amount of DHBA-PBA dissolved in DMSO, there was vigorous bubbling as expected. However, there was also a burst of vibrant yellow color in the solution which quickly faded to mostly colorless with a slightly green hue. There were no visible changes once the DHBA-PBA-CDI solution was added to a solution of starch in DMSO.

The reactions of CDI-activated DHBA-PBA with starch led to a water-soluble product with very low catechol content. The highest $DS_{catechol}$ achieved was 0.018 according to the colorimetric assay. H-NMR revealed the presence of many other peaks in the NMR spectrum, indicating the reaction was not specific for coupling of DHBA-PBA to starch. The only way a different product could have resulted was from disassociation of the DHBA-PBA boronate ester.

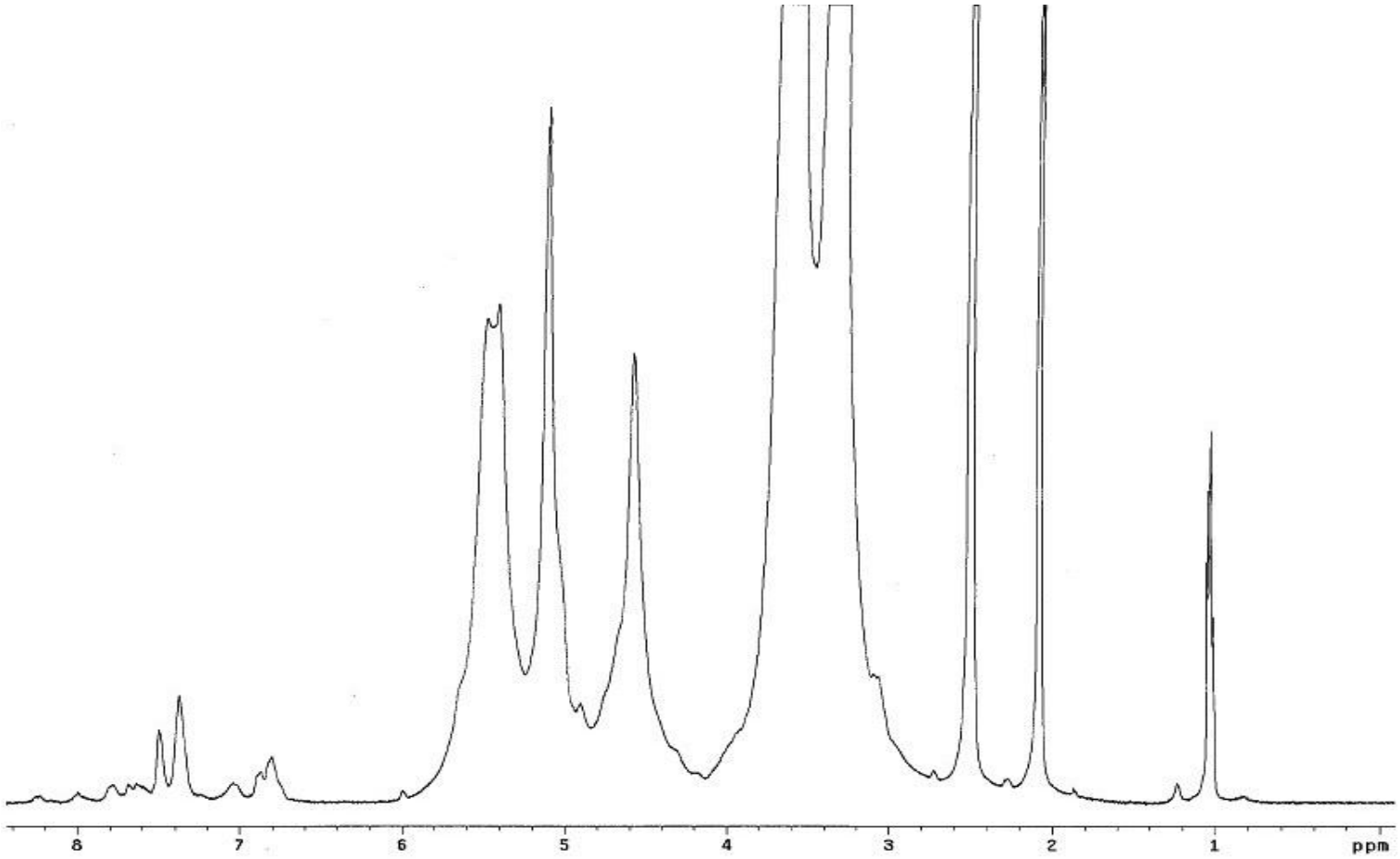

Figure 4.14 Representative H-NMR Spectrum of Starch-DHBA-PBA Conjugate

To investigate the source of the color change upon addition of CDI to DHBA-PBA, CDI was added to the both DHBA and PBA solutions in DMSO separately using concentrations similar to those used in the reaction. There was no visible color change when CDI was added to the individual components. This suggests that the color change was specific towards DHBA-PBA. The color change phenomenon also seemed to be specific to nitrogen-containing heterocyclic compounds like imidazole and pyridine. Addition of imidazole to a solution of DHBA-PBA produced a similar effect as CDI, but when DHBA-PBA was dissolved in pyridine the solution remained yellow instead of the color fading. Pyridine is known to coordinate with boron compounds that are sufficiently Lewis acidic. While phenylboronic acid is not a strong enough lewis acid to coordinate pyridine (Flores-Parra & Contreras, 2000), catechol ester derivatives of boronic acids exhibit greater lewis acidity due to conjugation between the aromatic ring of catechol and its oxygens (Hall, 2011). Therefore, the color produced by dissolution of DHBA-PBA in pyridine may have been the result of pyridine coordination by the boron atom in DHBA-PBA. It seemed odd then that solutions of imidazole or CDI with DHBA-PBA lose their initial yellow color. Assuming there is coordination between DHBA-PBA and imidazole, maybe there is a subsequent reaction or rearrangement that occurs, indicated by the loss of color.

4.3.2.2.3 Synthesis of Starch-DHBA-PBA by TosCl

TosCl has been successfully used to conjugate various carboxylic acids to polysaccharides with efficiency, including fatty acids to starch and cellulose, bioactive

molecules to dextran, and abietic acid to pullulan to name a few (Thomas Heinze et al., 2006). The mechanism is thought to proceed via activation of the carboxylic acid by TosCl to form a mixture of anhydrides and acid chlorides that are then reactive toward the hydroxyl groups of polysaccharides (Thomas Heinze et al., 2006). The general mechanism for activation of carboxylic acids and their conjugation to hydroxyl groups by TosCl can be seen in Figure 4.13.

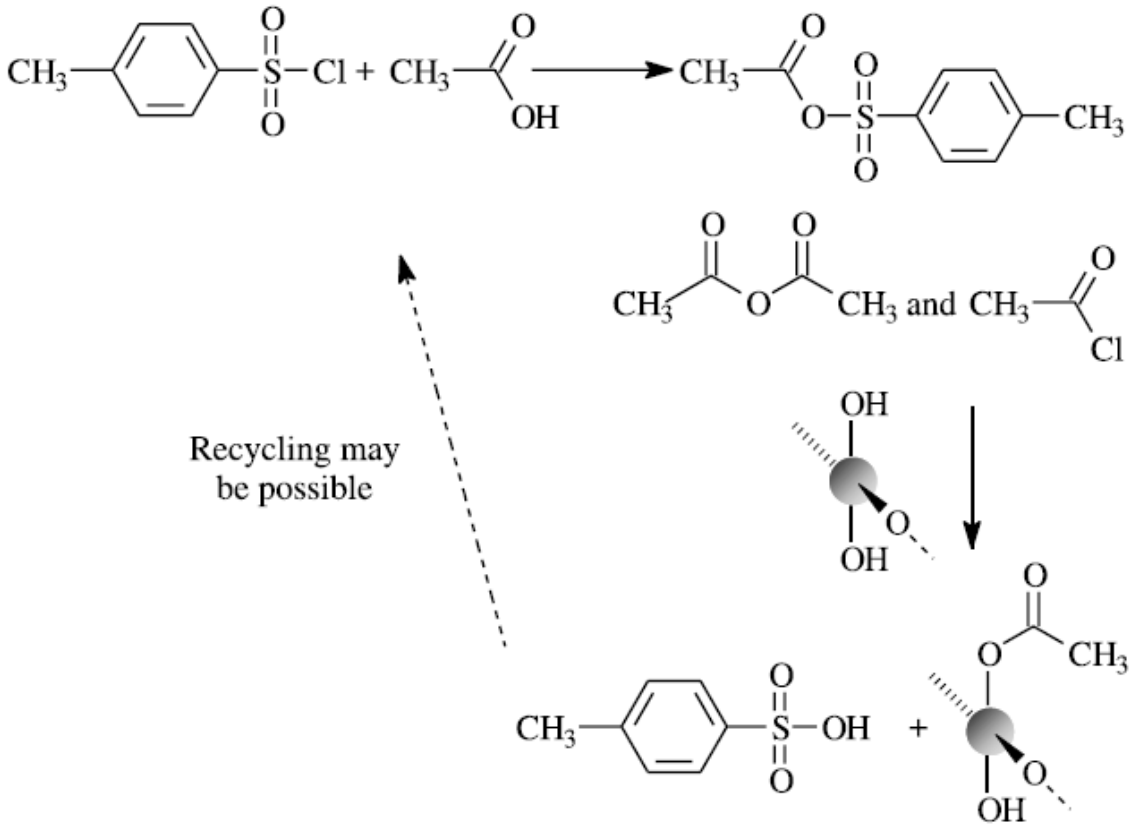

Figure 4.15 General mechanism for activation of carboxylic acids by TosCl and their conjugation to hydroxylic compounds (Thomas Heinze et al., 2006)

Because complication with coupling DHBA-PBA to starch was thought to be complicated by possible interactions between the imidazole rings of CDI and boron,

TosCl was investigated as a potential alternative because it lacks chemical groups that could potentially interact with boron.

Initial reactions did not include pyridine and resulted in complete hydrolysis of starch in as little time as a few hours. Pyridine, or some other moderately strong Lewis base, was therefore necessary as a hydrogen acceptor for the reaction to proceed for any length of time without significant depolymerization of starch. It should also be noted that there was no color change to the solutions upon addition of TosCl.

Reactions resulted in a water soluble product that tested positive for catechol; however, the $DS_{catechol}$ was very low and the H-NMR spectrum revealed many unexpected peaks, suggesting that other reactions were occurring. It is possible that tosylation of starch occurred under the reaction conditions used (Thomas Heinze et al., 2006). Additionally, if the boronate ester complex was dissociated, the catecholic hydroxyl groups may have become tosylated, leading to possible self-polymerization reactions, unwanted hydroxyl-hydroxyl coupling to starch, and/or combinations of both.

Based on the fact that attempted coupling of DHBA-PBA to starch by two different, but robust, coupling agents failed to result in starch-catechol conjugates of high DS and also caused unwanted and undefined starch conjugates, it seems that the boronate ester may be too labile of a protecting group for successful conjugation of DHBA to starch.

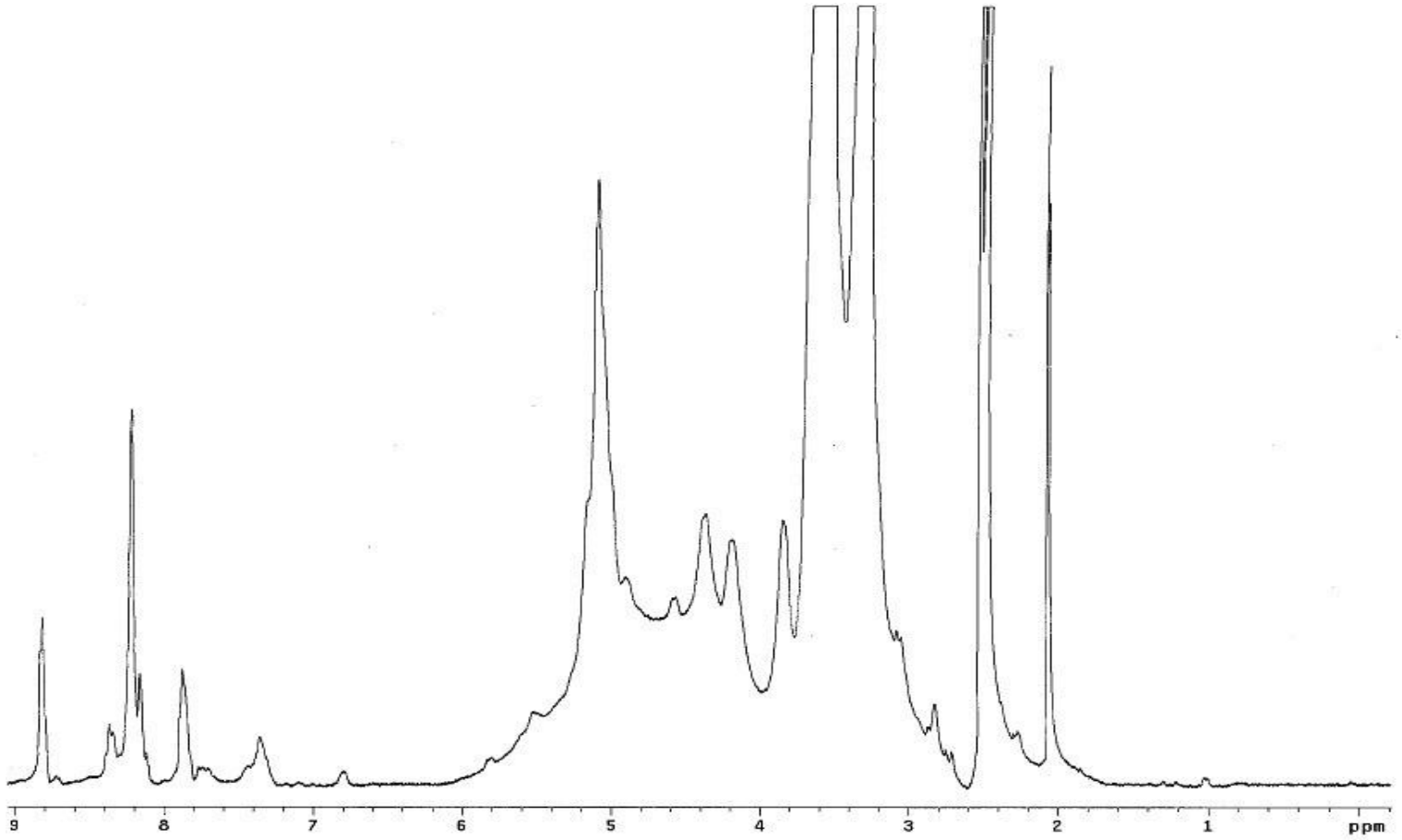

Figure 4.16 H-NMR Spectrum of Starch-DHBA-PBA by TosCl

4.3.2.2.4 Investigation of DHBA-PBA Stability

The low DS of DHBA-PBA to starch by CDI and TosCl and the unexpected peaks in their H-NMR spectra indicated instability of the boronate ester. Especially in the case of CDI, where for *O*-protected DHBA, the only possible reaction should have occurred between the carboxylic acid of DHBA and the hydroxyl groups of starch. Therefore, the DHBA-PBA complex must have been disassociating.

Mass spectrometry experiments were conducted to gain insight of whether the DHBA-PBA complex was inherently unstable in solution, or if CDI was directly disrupting the complex. The activated DHBA-PBA imidazolide has a mass of 290.

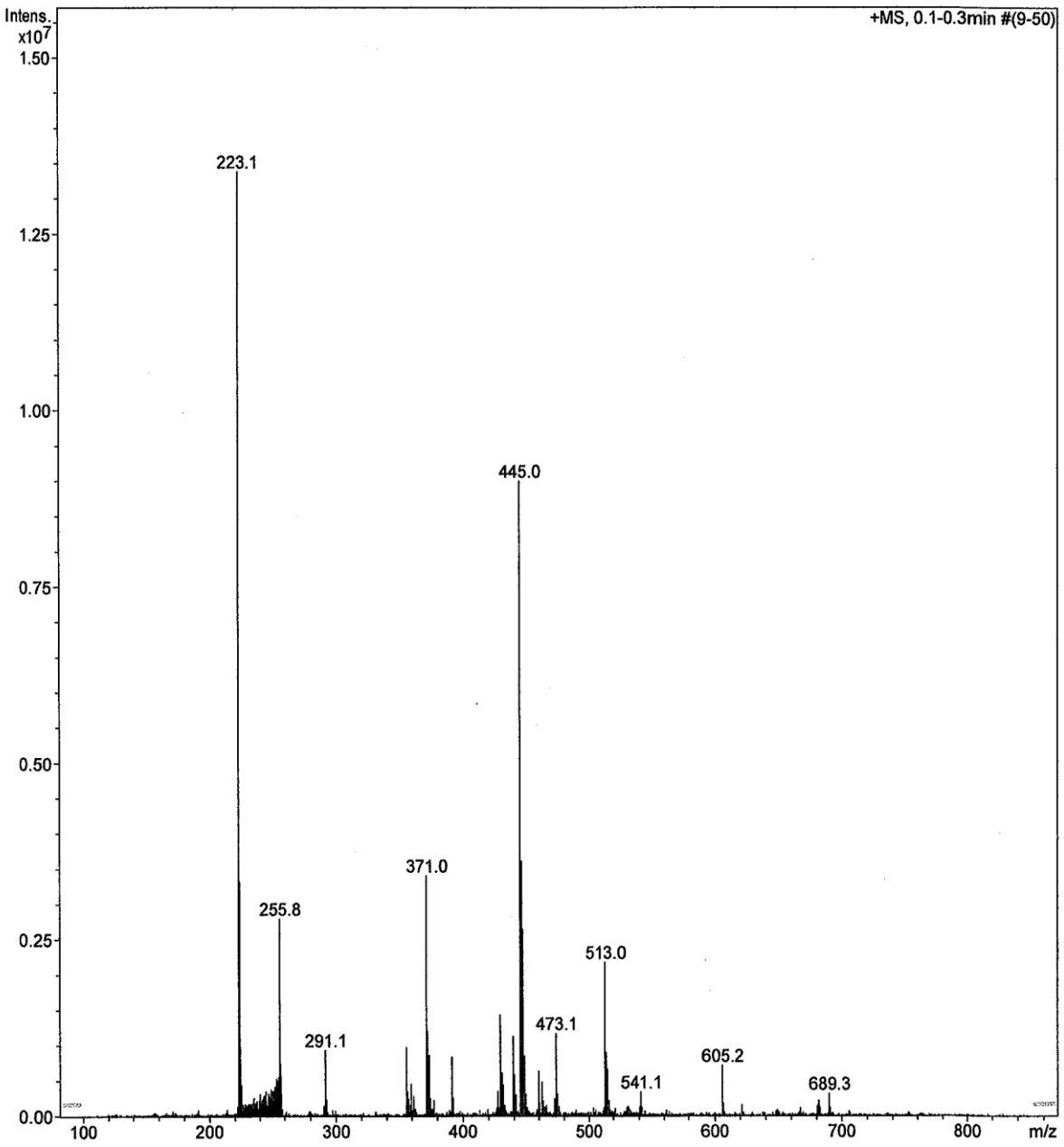

Figure 4.17 APCI MS Spectrum of DHBA-PBA and CDI in THF (positive ion mode)

For equal molar amounts of DHBA-PBA and CDI in THF, positive ion APCI revealed that there was some product formed, indicated by the small peak at m/z 291 $(290 + H)^+$, as well as starting material, indicated by the large peak at m/z 223 $(240 + H - H_2O)^+$.

Additionally, the peak at m/z 223 could result from 290 + H – imidazole, further implicating presence of the active DHBA-PBA imidazolide.

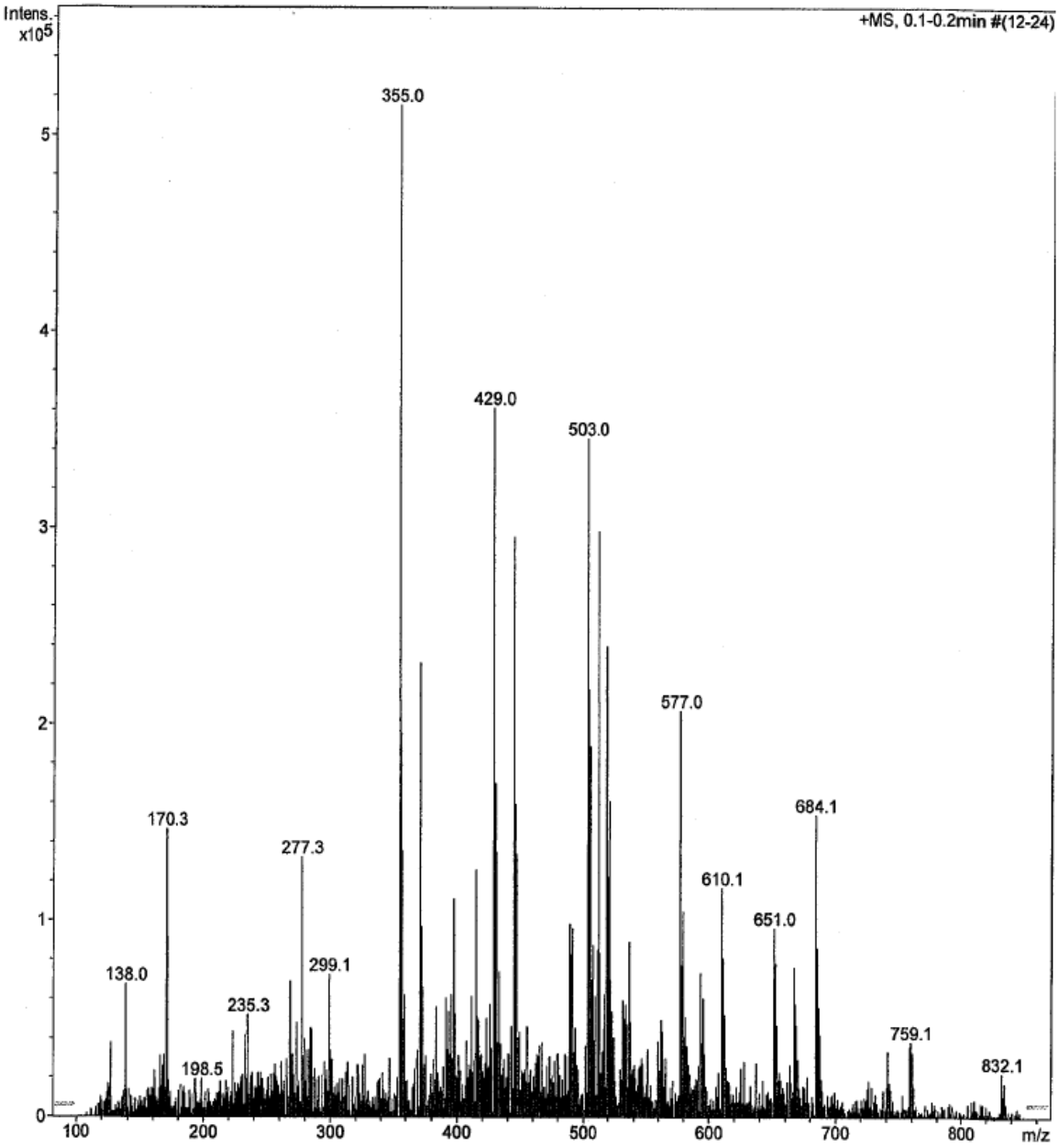

Figure 4.18 APCI MS Background Spectrum (positive ion mode)

Comparing the APCI spectrum of the product to the background spectrum, the peaks at m/z 291 and m/z 223 are clearly related to the sample.

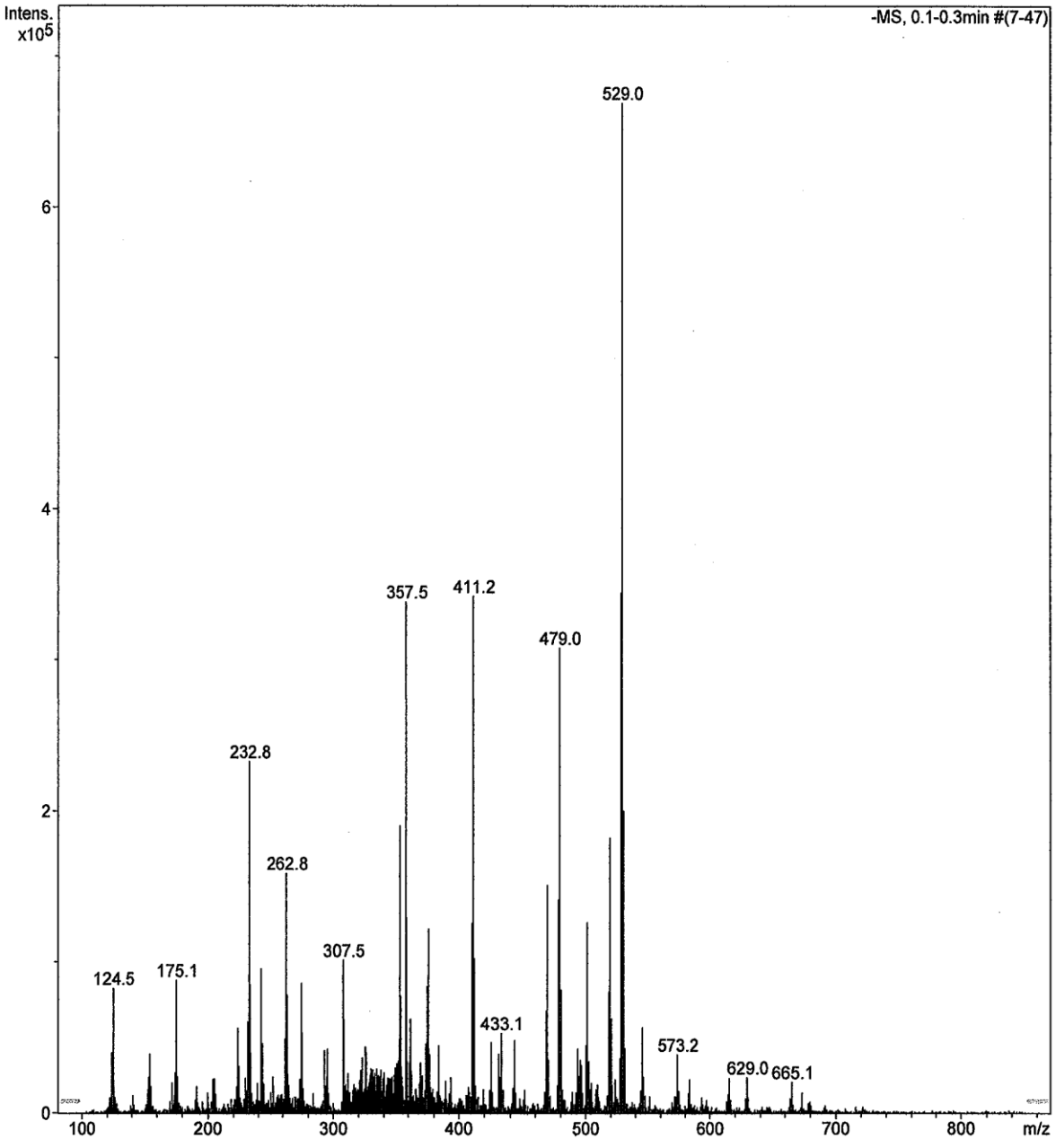

Figure 4.19 APCI Spectrum of DHBA-PBA and CDI in THF (negative ion mode)

Negative ion APCI showed large peaks for higher MW material; most notably at m/z 529, 411, and 357. Tandem MS spectra were obtained for these peaks showing evidence of ions related to the starting material, suggesting oligomerization.

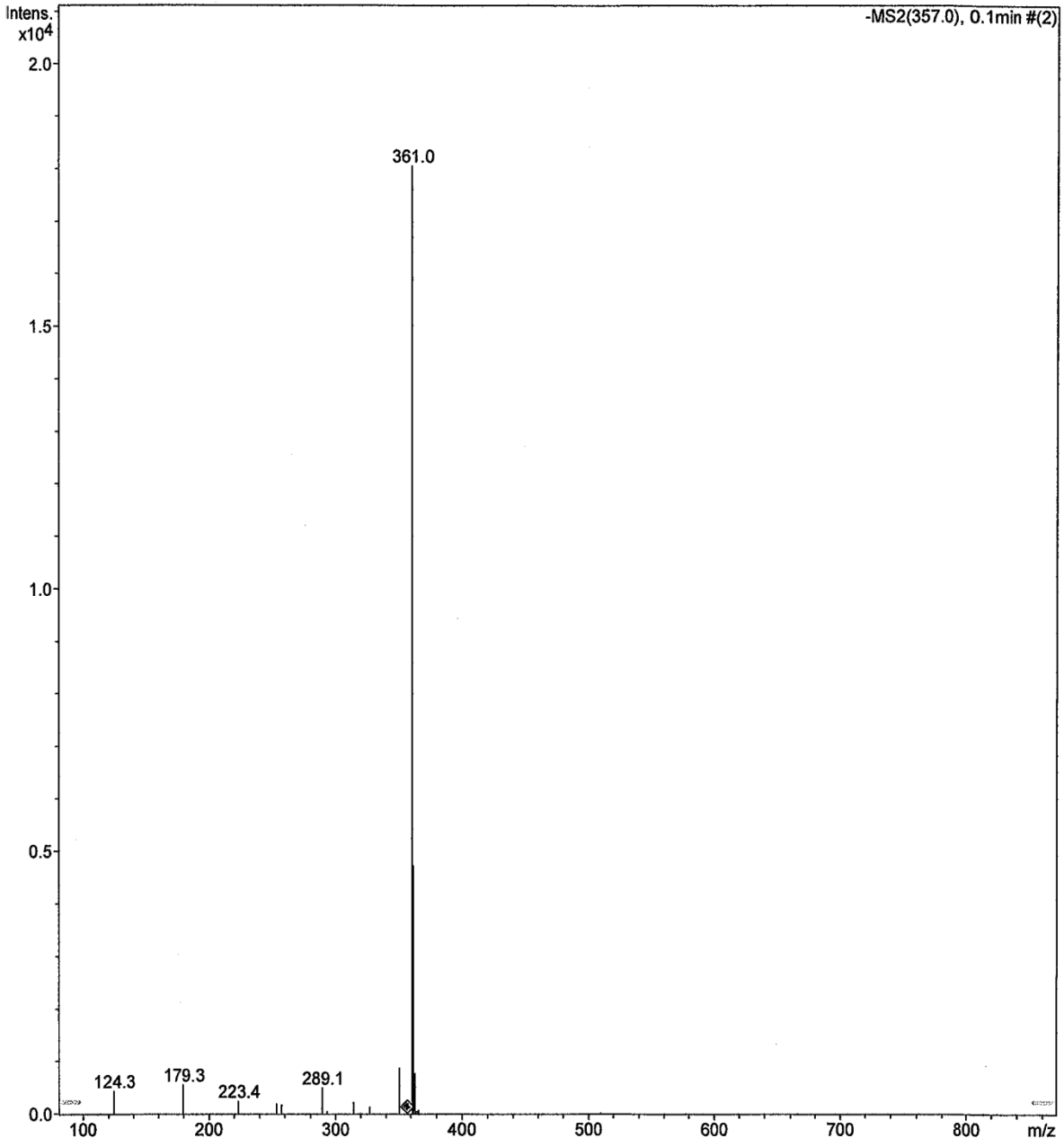

Figure 4.20 APCI MS/MS Spectrum of m/z 357 for DHBA-PBA and CDI in THF (negative ion mode)

MS/MS of the peak at m/z 357 showed some evidence of the components in the reaction.

The peak at m/z 289 represents a mass loss of 68, the mass of imidazole, or could also

represent the product (290 - H^+). The peak at m/z 223 may represent DHBA-PBA. It is baffling why the base MS/MS peak of m/z 357 is m/z 361.

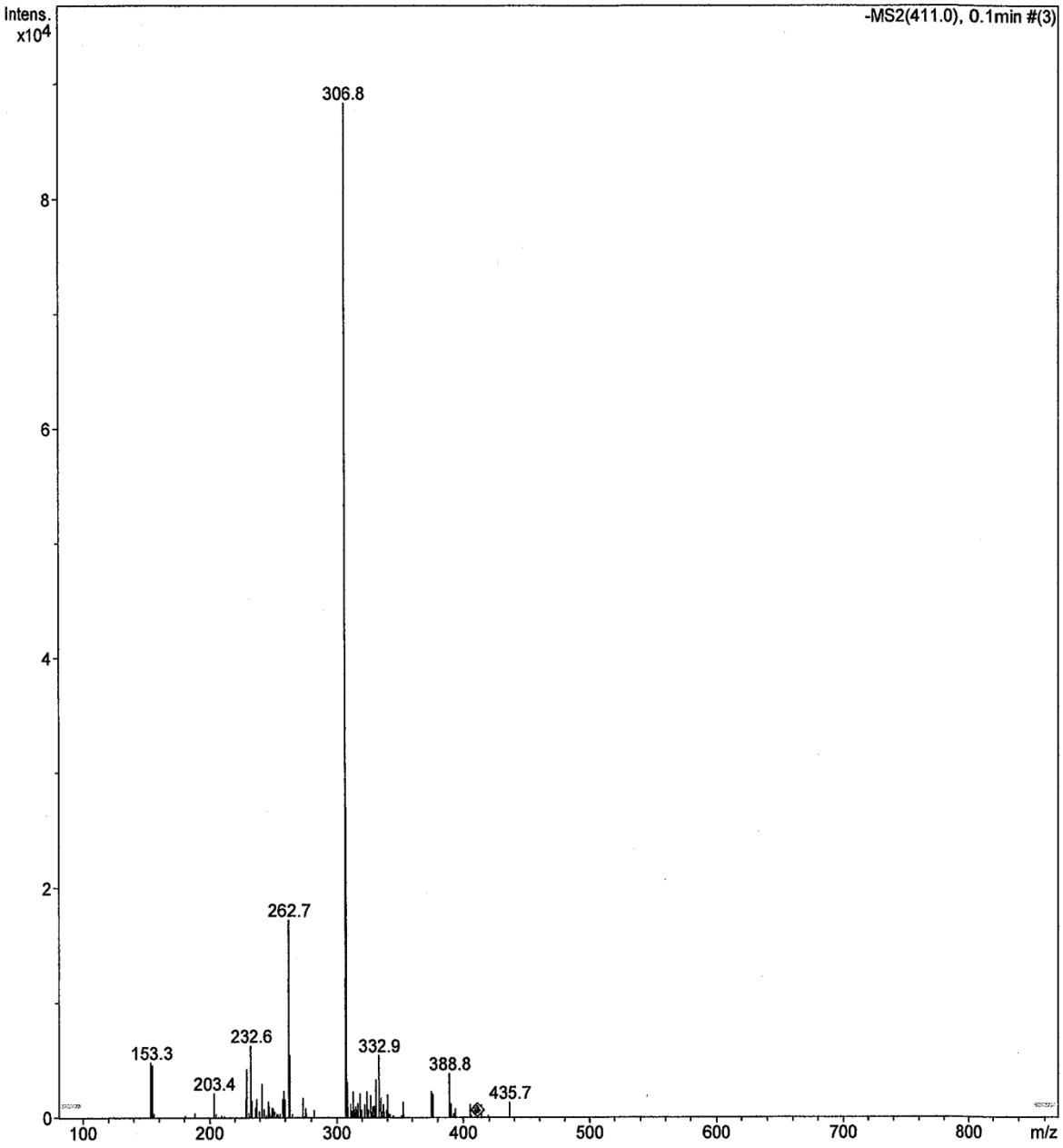

Figure 4.21 APCI MS/MS Spectrum of m/z 411 for DHBA-PBA and CDI in THF (negative ion mode)

The MS/MS spectrum of m/z 411 shows a peak at m/z 153 which could be related to DHBA (154 – H^+), but it is not clear how the other peaks may be related.

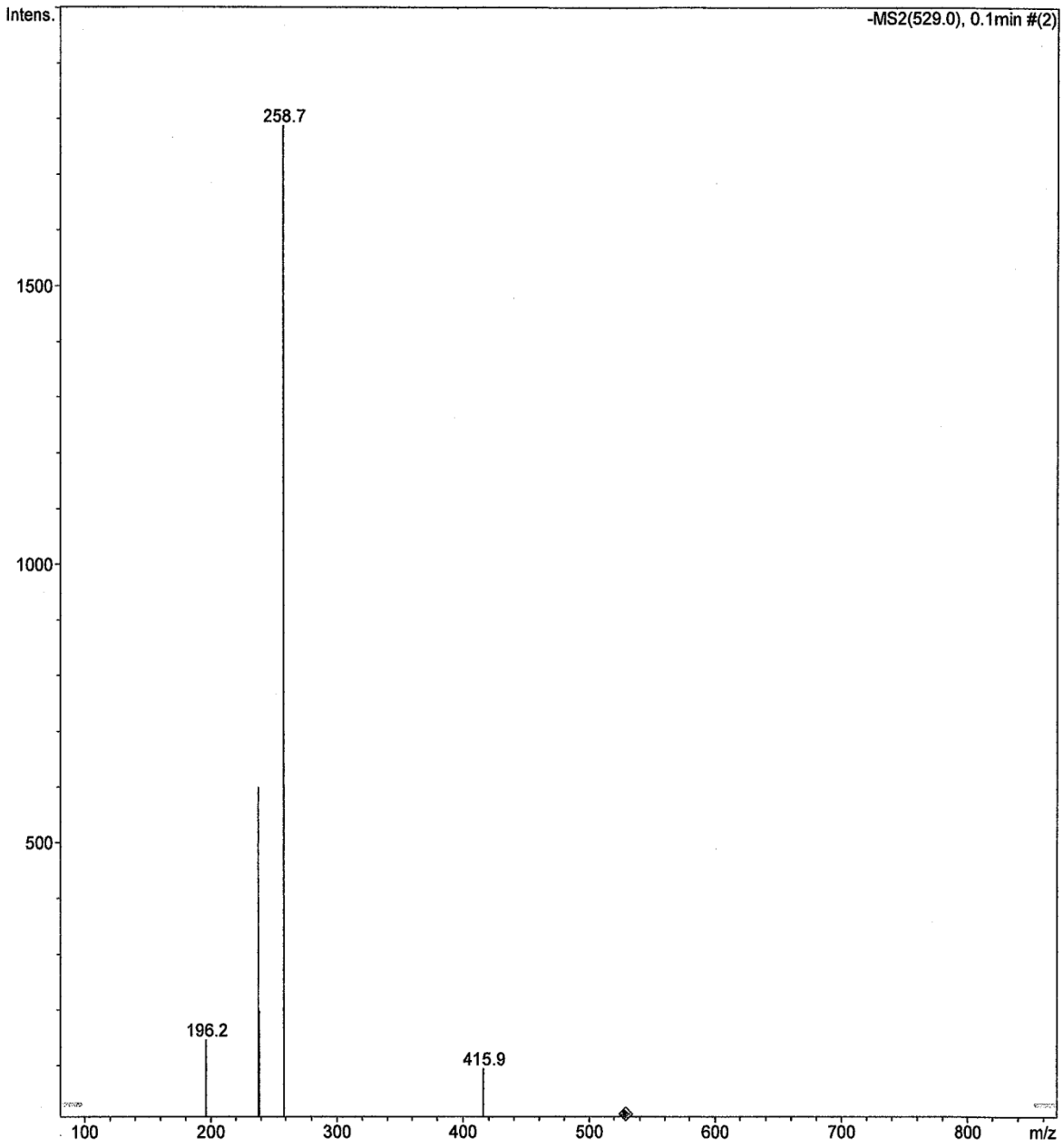

Figure 4.22 APCI MS/MS Spectrum of m/z 529 for DHBA-PBA and CDI in THF (negative ion mode)

Based on the ms/ms spectrum of peak m/z 529, there is no obvious relationship between the ions and the components of the reaction of DHBA-PBA with CDI.

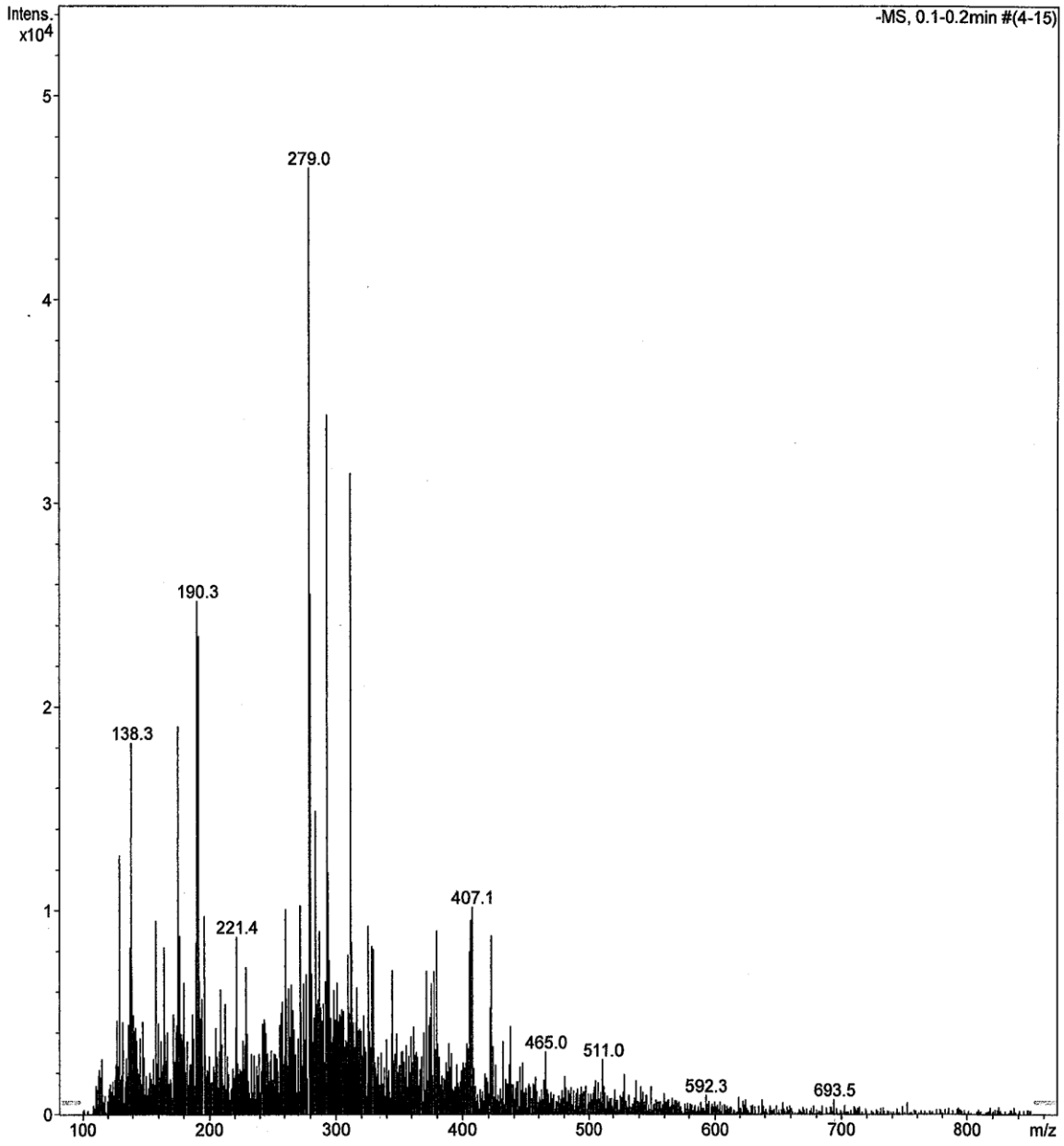

Figure 4.23 APCI Background Spectrum (negative ion mode)

While the ms/ms spectra of the peaks at m/z 529, 411, and 357 do not make an obvious connection with DHBA-PBA and CDI, the background spectrum strongly suggests that the peaks are related to the sample.

Based on the EI/CI MS data from the dry sample of DHBA-PBA it was clear that the dry compound was stable. ESI MS was used to gain insight on the stability of DHBA-PBA in solution.

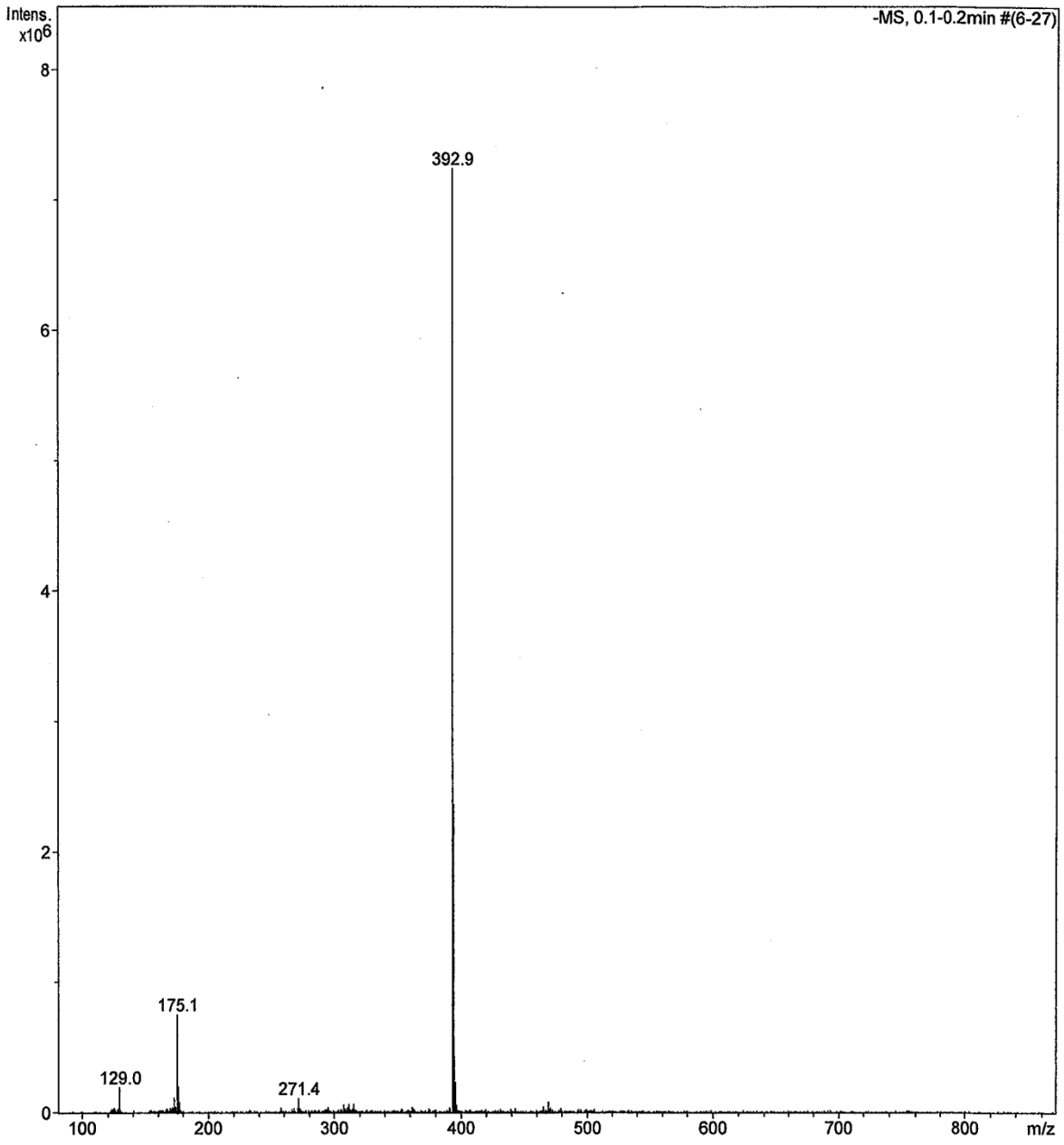

Figure 4.24 ESI Spectrum of DHBA-PBA (negative ion mode)

ESI in negative ion mode showed no trace of the expected m/z = 239 or 221 for DHBA-PBA. Instead, there was an intense ion peak at m/z 393. Figure 4.25 shows the MS/MS of the peak at m/z 393 resulted in an intense ion at m/z 153, indicating a loss of 240 mass units; the mass of DHBA-PBA. There was also a smaller peak at m/z 239, corresponding to a mass loss of 154; the mass of DHBA. The large peak at m/z 175 remains unclear. The ESI data indicates that DHBA-PBA is not stable in solution. Instead, it seems to form a larger complex. Therefore, phenylboronic acid is not an appropriate protecting group for DHBA for the purposes of activating its COOH group for subsequent conjugation.

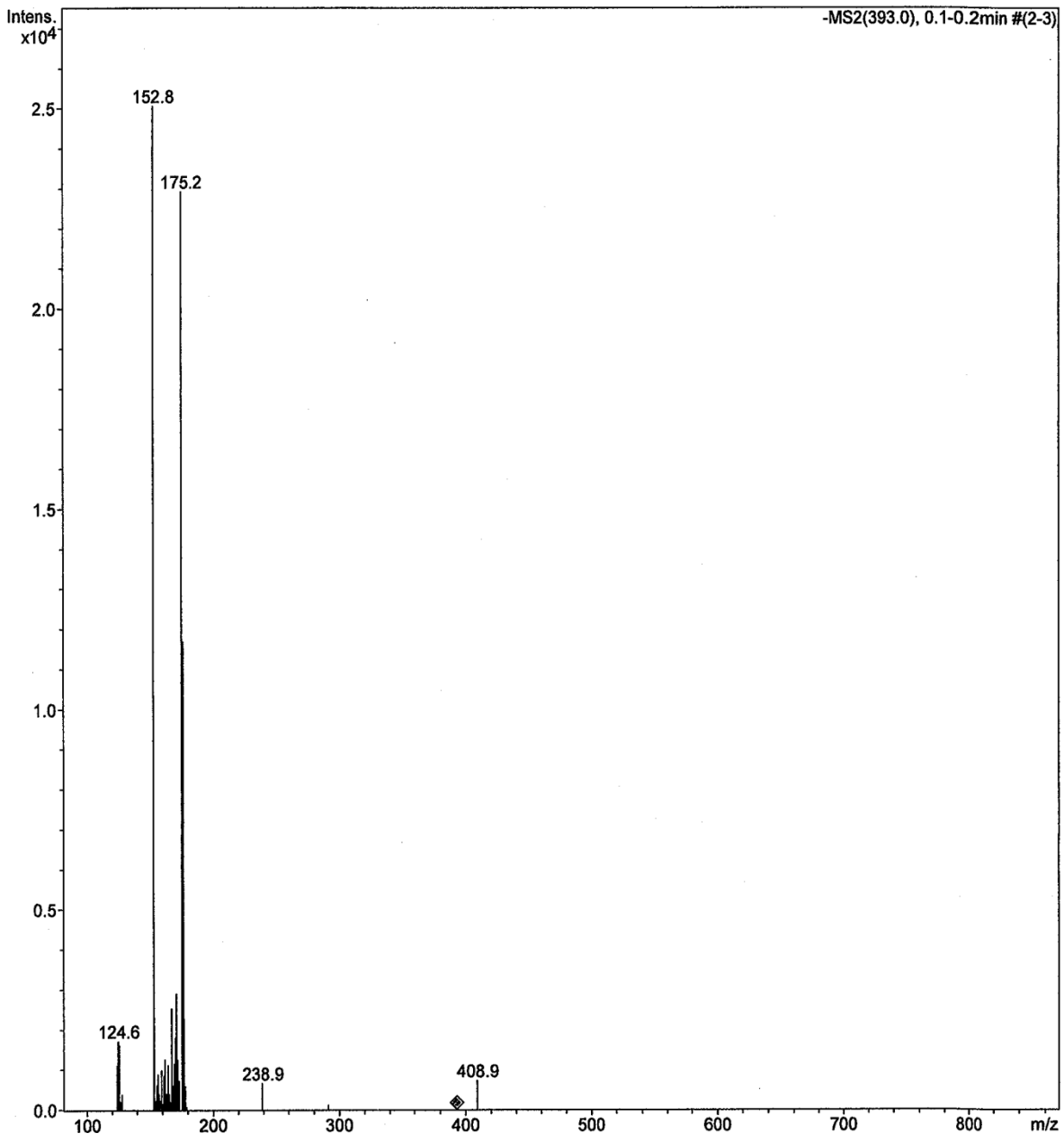

Figure 4.25 MS/MS Spectrum of m/z = 393 from ESI (negative ion mode) of DHBA-PBA

CHAPTER 5. CONCLUSIONS AND FUTURE CONSIDERATIONS

5.1 Molecular Weight Reduction of High-Amylose Starch

The molecular weight of high amylose starch was effectively and uniformly reduced through hydrolysis by fungal α-amylase in a mixture of DMSO and acetate buffer. This is a unique method for hydrolysis of high-amylose starch unable to undergo traditional hydrolysis through high temperature gelatinization and subsequent enzyme or acid treatment.

5.2 Synthesis of Carboxymethyl Starch

Heterogenous reaction of granular and non-granular starch was successfully carried out to produce CMS with DS as high as 1.7. There are little to no reports of carboxymethylation of non-granular starch in literature. The results reported in this thesis show that non-granular starch can undergo heterogenous reaction conditions similar to those used for non-granular starch to produce CMS with relatively high DS. However, non-granular CMS may be more prone to gelatinization during synthesis so special care should be taken with respect to water content and temperature to avoid unwanted gelatinization. To achieve greater DS for granular high-amylose starch, tighter optimization of parameters in a multiple-step reaction strategy should be investigated. Because high-amylose starch granules are most likely more resistant to penetration by

water due to the nature of amylose vs. amylopectin, temperature, reaction time and/or water content should be adjusted so that the product of the reaction has a DS similar to that obtained for other varieties of starch while avoiding gelatinization. Each parameter should be evaluated separately with respect to DS in order to determine what factors have the greatest impact on DS and whether some relationship can be drawn between those parameters and properties of the starch granule such as amylose/amylopectin ratio. Based on the results from the different multi-step carboxymethylation procedures, time, water content, and SMCA/NaOH:AGU all greatly affect both the DS of the product and its tendency to gelatinize.

5.3 Synthesis of CMS-Dopamine

After struggling with solubility issues, CMS-dopamine conjugates with very low $DS_{catechol}$ (≤ 0.02) were synthesized using EDC. Experiments showed that precipitation of the reaction product occurred when excess EDC was used. Precipitation did not appear to be caused by cross-linking induced by auto-oxidation of conjugated dopamine, as evident from occurrence of precipitation despite anaerobic, low pH conditions. Addition of ascorbic acid as an antioxidant allowed high concentrations of EDC to be used without precipitation of the product, but did not result in significantly higher DS of dopamine. Moreover, it was evident by UV-vis that ascorbic acid was actually acting as a nucleophile and conjugating to CMS. Addition of NHS to the reaction did not greatly increase the $DS_{catechol}$, but did allow higher concentrations of EDC to be used. When sodium borate was added, very high concentrations of all reactants could be used at

elevated pH, but ultimately did not increase the $DS_{catechol}$. Therefore, EDC was not an effective coupling agent for CMS and dopamine.

Based on the observations made from numerous reactions of CMS, dopamine, and EDC under various conditions, the combination of EDC and dopamine is responsible for precipitation of the polymer. One way in which cross-linking could have been mediated by excess EDC is if activated COOH groups on neighboring CMS molecules were bridged by dopamine molecules through nucleophilic attack by both its amine and a hydroxyl group. High concentration of EDC would increase the availability of activated COOH groups and potential cross-linking sites. This would explain why both EDC and dopamine had to be present for precipitation to occur and also why precipitation occurred under non-oxidizing conditions, but was prevented when borate was employed to protect the hydroxyl groups of dopamine.

There are a couple of explanations possible for the low $DS_{catechol}$ of CMS-dopamine conjugates. First, EDC may have been interacting with dopamine in addition to carboxylic acid groups of CMS as indicated by increased pH upon addition of EDC to a dopamine solution. This would lower the likelihood of successful coupling of dopamine to carboxylic acid groups. Second, EDC-activated carboxylic acid groups are able to rearrange to form a stable, covalently attached N-acylurea group resistant to displacement by nucleophilic attack. Obviously, this would reduce the potential $DS_{catechol}$ of CMS-dopamine because there would be a lower number of potentially reactive carboxylic acid

groups. N-acylurea has been reported as the major product in the coupling of tyramine to hyaluronan (Mojarradi, 2011).

Future studies for this reaction should include clearly identifying the reason behind precipitation of polymer in the presence of excess EDC; specifically looking for signs of dopamine's ability to bridge two activated COOH groups . This could be investigated by replacing CMS with glucuronic acid and looking for either glucuronic acid oligomers, or glucuronic acid-dopamine conjugates connected through ester bonds, indicating the ability of the hydroxyl groups of dopamine to participate in nucleophilic attack of EDC-activated COOH groups.

It would also be useful to further investigate the reasons for low $DS_{catechol}$, especially potential interaction between dopamine and EDC. If an interaction between EDC and dopamine existed similar to that documented for EDC and tyramine, then the expected product would be dopamine-O-EDC or dopamine-O,O'-EDC, where the hydroxyl groups of dopamine are activated in the same manner as carboxylic acids. Along this line of reasoning, then it would also be conceivable that dopamine oligomers would be present due to substation of dopamine on dopamine-O-EDC.

Finally, it would be helpful to understand whether the efficiency of the coupling reaction is dictated by the ability of EDC/NHS to activate COOH groups or their subsequent substitution with dopamine. NHS esters are relatively stable and detectable by UV-vis at 260 nm, therefore NHS content of activated CMS could be determined through

separation of the polymer from excess reactants followed by detection via HPLC. Then, by comparing the initial NHS ester content to the final dopamine content, the limiting reaction could be identified.

If it can be shown that EDC-dopamine interactions do exist and conversion of COOH to its activated NHS ester is highly efficient, without significant conversion to N-acylurea, a two-step reaction should be adopted where CMS is first converted to its active NHS-ester form by reaction with EDC and NHS in low pH. Excess NHS and EDC should then be quickly removed from the activated CMS by preparative chromatography before being combined with borate-protected dopamine in high pH. Only then, could an increase in the coupling efficiency of dopamine to CMS by EDC possibly be realized.

5.4 Synthesis of Catechol-Starch Conjugates in Non-Aqueous Reactions

Because of the presence of hydroxyl groups on both starch and catecholic monomers, O-protection of the catechol group is necessary because coupling of molecules to unmodified starch must occur between its hydroxyl groups and a reactive site on the catecholic molecule. The specificity and high efficiency of CDI-mediated coupling of carboxylic acid-containing molecules with starch was obvious from the high $DS_{catechol}$ achieved with starch-DMBA conjugates. Additionally, this pathway removes the need for prior modification of starch as it can be conveniently carried out in DMSO or other solvents such as DMA/LiCl and DMF/LiCl capable of dissolving polysaccharides.

However, while high $DS_{catechol}$ is easily achieved with CDI, O-demethylation of starch-catechol polymers is inherently tricky because of the susceptibility of glycosidic linkages and esters to common O-demethylation techniques. Additionally, the relative insolubility of starch limits the choice of solvent for deprotection which, in the case of BBr_3 demethylation, may have determined the success of the procedure.

If demethylation of starch-DMBA by BBr_3 was pursued further, two main issues should be addressed. First, in order to rule out solvent effects, it would be ideal to create a starch polymer soluble in water-immiscible solvents traditionally used in BBr_3 demethylations such as DCM or chloroform. Second, complete functionalization of starch should be attained in order to eliminate the possibility that the hydroxyl groups interact with BBr_3 and lead to cross-linking. It would be best to first check whether starch-DMBA of low MW with DS near 3 would be capable of dissolving in chloroform or DCM because that would address both issues. Otherwise, starch could be first functionalized with a chemical group capable of imparting enhanced solubility in the solvents mentioned, followed by conjugation of DMBA. Even then, demethylation by BBr_3 is most likely not a viable route due to potential interactions with glycosidic or ester oxygen molecules, unless the favorable position of the catechol oxygens to complex trigonal boron compounds favors selective bis-O-demethylation of the DMBA groups.

Instead of O-methylated catechol molecules, less stable protecting groups are preferable due to ease of removal. Boronate esters of DHBA were easily synthesized, but apparently not stable enough to be compatible with CDI or TosCl chemistry. Results

from mass spectrometry experiments suggest that there was a small amount of the desired product, but a higher MW complex of DHBA-PBA may exist when in solution. While adding to general knowledge of boronate chemistry, greater insight into the stability of DHBA-PBA boronate esters and possible dimerization would be beneficial if a more stable boronate ester could be achieved for application purposes. Future studies could include seeing whether the carboxylic acid of DHBA plays a role in DHBA-PBA instability. This could be done by evaluating the stability of non-carboxylic catechol boronate esters using the methods described in this thesis. Additionally, the stability of DHBA-boronate esters derived from boronic acids besides phenylboronic acid could be evaluated to see whether the boronic acid side group has an influence. It would be interesting to determine the coordination state of the boron atom when in solution as a boronate ester. This information could be useful in understanding whether the boronate ester is somehow destabilized by interactions of boron with solvent or other molecules in solution, favoring rearrangement and formation of a higher MW complex.

Future studies could investigate other protection/deprotection techniques for DHBA that are specific enough to deprotect the catechol while leaving starch and its esters intact. Acetonide and ketal groups are commonly used for protecting catechol and are easily removed, but have proved inefficient when applied to DOPA (Sever & Wilker, 2001). While it is possible that these protective groups may be more effective when used with DHBA instead of DOPA, there are other protecting groups that should first be investigated.

TBDMS has been successfully used to protect DOPA for synthesis of DOPA-containing polypeptides (Nakonieczna, Przychodzen, & Chimiak, 1994; Sever & Wilker, 2001). Deprotection methods for TBDMS ethers are somewhat easier and the reactants are less harsh than those for demethylations. For instance, TBDMS can be removed by combination of concentrated HCl and heat or in the presence of TBAF at room temperature (Matos-Perez & Wilker, 2012). Clearly, hot concentrated HCl could potentially hydrolyze starch and/or the ester bond between starch and DHBA, but perhaps proper tweaking of the reaction conditions could minimize the undesired reactions. While TBAF would not cause substantial depolymerization, it has been shown to significantly reduce the DS of cellulose acetate by disruption of the ester bond (Xu & Edgar, 2012). However, according to the proposed reaction mechanism of TBAF and acetyl esters by the researchers just mentioned, benzoate esters would be more stable to cleavage by TBAF. Therefore, synthesis of starch-DHBA with TBDMS protection followed by deprotection with TBAF may be a viable pathway towards synthesis of a highly substituted starch-catechol conjugate.

Somewhat more convincing is the work by Gu et al. in which chloroacetyl esters of small carbohydrate molecules were selectively cleaved by TBAF, even in the presence of other esters, including benzoate ester (Gu, Fang, & Du, 2011). Assuming complete protection of DHBA by chloroacetic anhydride is possible, its conjugation to starch followed by cleavage with TBAF may be a promising route towards catechol-functionalized starch of high DS. In any case, tailoring TBAF deprotection to be selective towards the protected

catechol and not the starch ester will require attention to various parameters including reaction time, molar excess of TBAF, reaction temperature, and solvent choice.

Finally, an alternative method could be to completely modify starch with carboxylic acid groups so that it could be activated by CDI, followed by conjugation to dopamine - assuming the nucleophilicity of the amine group is sufficiently more reactive than the hydroxyl groups so that protection is not necessary and the major product formed is the carbamate bond. This approach was used by Bruneel et al. to couple 1-aminopropan-2-ol to pullulan (Bruneel & Schacht, 1994).

5.5 Closing Remarks

The reactions investigated in this thesis require further insight and optimization for synthesizing starch-catechol conjugates for adhesive use. EDC coupling between dopamine and CMS in aqueous media is not a viable route towards catechol-functionalized starch due to very low substitution. Reactions of starch and protected DHBA with CDI in organic media yield high substitution, but selective deprotection of the protected DHBA is difficult due to other ester and ether bonds present in the polymer. While other potential routes exist and it may be scientifically feasible to create catechol-functionalized starch, these strategies are necessarily more complex and require more material and expense. From an applications stand-point, an adhesive requiring more processing, materials, and expense can greatly impact the economic viability and environmental benefits of such an adhesive.

LIST OF REFERENCES

LIST OF REFERENCES

Anderson, T., Yu, J., Estrada, A., Hammer, M., Waite, J., & Israelachvili, J. (2010). The Contribution of DOPA to Substrate-Peptide Adhesion and Internal Cohesion of Mussel-Inspired Synthetic Peptide Films. *Advanced Functional Materials, 20*(23), 4196-4205. doi: 10.1002/adfm.201000932

Arnow, L. (1937). Colorimetric determination of the components of 3,4-dihydroxyphenylalanine tyrosine mixtures. *Journal of Biological Chemistry, 118*(2), 531-537.

BeMiller, J. N., & Whistler, R. L. (2009). *Starch - chemistry and technology Food science and technology* (pp. xx, 879 p.).

Bendahou, K., Dufresne, A., Magnin, A., Mortha, G., & Kaddami, H. (2014). Control of size and viscoelastic properties of nanofibrillated cellulose from palm tree by varying the TEMPO-mediated oxidation time (Vol. 99, pp. 74-83): Carbohydrate Polymers.

Bosik, D. (2012). Adhesives and Sealants: Global Markets, 3rd Edition. Rockville, Maryland: SBI.

Brooksby, P., Schiel, D., & Abell, A. (2008). Electrochemistry of catechol terminated monolayers with Cu(II), Ni(II) and, Fe(III) cations: A model for the marine adhesive interface. *Langmuir, 24*(16), 9074-9081. doi: 10.1021/la8007816

Brubaker, C., Kissler, H., Wang, L., Kaufman, D., & Messersmith, P. (2010). Biological performance of mussel-inspired adhesive in extrahepatic islet transplantation. *Biomaterials, 31*(3), 420-427. doi: 10.1016/j.biomaterials.2009.09.062

Bruce P. Lee, J. L. D., Phillip B. Messersmith. (2006). Biomimetic Adhesive Polymers Based on Mussel Adhesive Proteins. In J. A. C. A.M. Smith (Ed.), *Biological Adhesives* (pp. 257-273): Springer.

Bruneel, D., & Schacht, E. (1994). Chemical modification of pullulan .3. Succinoylation. *Polymer, 35*(12), 2656-2658. doi: 10.1016/0032-3861(94)90395-6

Burke, S., Ritter-Jones, M., Lee, B., & Messersmith, P. (2007). Thermal gelation and tissue adhesion of biomimetic hydrogels. *Biomedical Materials, 2*(4), 203-210. doi: 10.1088/1748-6041/2/4/001

Chen, M., & Bergman, C. (2007). Method for determining the amylose content, molecular weights, and weight- and molar-based distributions of degree of polymerization of amylose and fine-structure of amylopectin. *Carbohydrate Polymers, 69*(3), 562-578. doi: 10.1016/j.carbpol.2007.01.018

Chi, H., Xu, K., Wu, X., Chen, Q., Xue, D., Song, C., . . . Wang, P. (2008). Effect of acetylation on the properties of corn starch. *Food Chemistry, 106*(3), 923-928. doi: 10.1016/j.foodchem.2007.07.002

Crisp, D., Walker, G., Young, G., & Yule, A. (1985). Adhesion and substrate choice in mussels and barnacles. *Journal of Colloid and Interface Science, 104*(1), 40-50. doi: 10.1016/0021-9797(85)90007-4

Cutler, H., Majetich, G., Tian, X., & Spearing, P. (1997). Syntheses of 3,7-dimethyl-8-hydroxy-6-methoxyisochroman the 3,7-dimethyl-6-hydroxy-8-methoxy isomer, and their ester and ether derivatives: Plant growth regulatory activity. *Journal of Agricultural and Food Chemistry, 45*(4), 1422-1429. doi: 10.1021/jf960618l

Danishefsky, I., & Siskovic, E. (1971). Conversion of carboxyl groups of mucopolysaccharides into amides of amino acid esters. *Carbohydrate Research, 16*(1), 199-&. doi: 10.1016/S0008-6215(00)86114-5

Deming, T. (1999). Mussel byssus and biomolecular materials. *Current Opinion in Chemical Biology, 3*(1), 100-105. doi: 10.1016/S1367-5931(99)80018-0

Deschamps, N. (2010). Biorenewable Chemicals World Market. Rockville, Maryland: SBI.

El-Sheikh, M. (2010). Carboxymethylation of maize starch at mild conditions. *Carbohydrate Polymers, 79*(4), 875-881. doi: 10.1016/j.carbpol.2009.10.013

Eyler, R., Klug, E., & Diephuis, F. (1947). Determination of degree of substitution of sodium carboxymethylcellulose. *Analytical Chemistry, 19*(1), 24-27. doi: 10.1021/ac60001a007

Feutrill, G., & Mirrington, R. (1970). Demethylation of aryl methyl ethers with thioethoxide ion in dimethyl formamide. *Tetrahedron Letters*(16), 1327-&.

Flores-Parra, A., & Contreras, R. (2000). Boron coordination compounds derived from organic molecules of biological interest. *Coordination Chemistry Reviews, 196*, 85-124. doi: 10.1016/S0010-8545(99)00053-3

Frank, B., & Belfort, G. (2001). Atomic force microscopy for low-adhesion surfaces: Thermodynamic criteria, critical surface,tension, and intermolecular forces. *Langmuir, 17*(6), 1905-1912. doi: 10.1021/la0011533

Gore, E., Blears, D., & Danyluk, S. (1965). Hindered internal rotation in boron halide complexes of n,n-dimethylformamide. *Canadian Journal of Chemistry, 43*(8), 2135-&. doi: 10.1139/v65-288

Gozzo, A., Glittenberg, D., & Hofer, R. (2009). Starch: A Versatile Product from Renewable Resources for Industrial Applications. *Sustainable Solutions For Modern Economies,* 238-263. doi: 10.1039/9781847552686-00238

Gu, G., Fang, M., & Du, Y. (2011). Efficient and selective removal of chloroacetyl group promoted with tetra-n-butylammonium fluoride (TBAF). *Carbohydrate Research, 346*(17), 2801-2804. doi: 10.1016/j.carres.2011.09.033

Guvendiren, M., Messersmith, P., & Shull, K. (2008). Self-assembly and adhesion of DOPA-modified methacrylic triblock hydrogels. *Biomacromolecules, 9*(1), 122-128. doi: 10.1021/bm700886b

Haemers, S., Koper, G., & Frens, G. (2003). Effect of oxidation rate on cross-linking of mussel adhesive proteins. *Biomacromolecules, 4*(3), 632-640. doi: 10.1021/bm025707n

Hall, D. (2011). *Boronic acids preparation and applications in organic synthesis, medicine and materials* (pp. 1 online resource (1 v.)).

Hattori, M., Yang, W., & Takahashi, K. (1995). Functional-changes of carboxymethyl potato starch by conjugation with whey proteins. *Journal of Agricultural and Food Chemistry, 43*(8), 2007-2011. doi: 10.1021/jf00056a009

Heinze, T., & Koschella, A. (2005). Carboxymethyl ethers of cellulose and starch - A review. *Macromolecular Symposia, 223,* 13-39. doi: 10.1002/masy.200550502

Heinze, T., Liebert, T., Heinze, U., & Schwikal, K. (2004). Starch derivatives of high degree of functionalization 9: carboxymethyl starches. *Cellulose, 11*(2), 239-245. doi: 10.1023/B:CELL.0000025386.68486.a4

Heinze, T., Liebert, T., & Koschella, A. (2006). *Esterification of polysaccharides Springer laboratory* (pp. xv, 232 p.).

Hermanson, G. T. (2008). *Bioconjugate techniques* (pp. 1 v.).

Hoare, D., & Koshland, D. (1967). A method for quantitative modification and estimation of carboxylic acid groups in proteins. *Journal of Biological Chemistry, 242*(10), 2447-&.

Hoffmann, B., Volkmer, E., Kokott, A., Augat, P., Ohnmacht, M., Sedlmayr, N., . . . Ziegler, G. (2009). Characterisation of a new bioadhesive system based on polysaccharides with the potential to be used as bone glue. *Journal of Materials Science-Materials in Medicine, 20*(10), 2001-2009. doi: 10.1007/s10856-009-3782-5

Huang, K., Lee, B., Ingram, D., & Messersmith, P. (2002). Synthesis and characterization of self-assembling block copolymers containing bioadhesive end groups. *Biomacromolecules, 3*(2), 397-406. doi: 10.1021/bm015650p

Humphreys, R., & Solarek, D. (2001). Adhesives from renewable raw materials: Design of adhesives based on starch technology. *Wood Adhesives 2000*, 3-9.

Kaneko, D., Wang, S., Matsumoto, K., Kinugawa, S., Yasaki, K., Chi, D., & Kaneko, T. (2011). Mussel-mimetic strong adhesive resin from bio-base polycoumarates. *Polymer Journal, 43*(10), 855-858. doi: 10.1038/pj.2011.77

Karabulut, E., Pettersson, T., Ankerfors, M., & Wagberg, L. (2012). Adhesive Layer-by-Layer Films of Carboxymethylated Cellulose Nanofibril Dopamine Covalent Bioconjugates Inspired by Marine Mussel Threads. *Acs Nano, 6*(6), 4731-4739. doi: 10.1021/nn204620j

Kaupp, G., Naimi-Jamal, M., & Stepanenko, V. (2003). Waste-free and facile solid-state protection of diamines, anthranilic acid, diols, and polyols with phenylboronic acid. *Chemistry-a European Journal, 9*(17), 4156-4160. doi: 10.1002/chem.200304793

Kesinger, N., & Stevens, J. (2009). Covalent interaction of ascorbic acid with natural products. *Phytochemistry, 70*(17-18), 1930-1939. doi: 10.1016/j.phytochem.2009.09.028

Ketuly, K., & Hadi, A. (2010). Boronate Derivatives of Functionally Diverse Catechols: Stability Studies. *Molecules, 15*(4), 2347-2356. doi: 10.3390/molecules15042347

Kobayashi, M., Yanagihara, S., & Ichishima, E. (1989). Preparation and characterization of taka-amylase-a attached to carboxymethyl dextran by water-soluble carbodiimide. *Agricultural and Biological Chemistry, 53*(12), 3133-3138.

Kwon, K., Auh, J., Kim, J., Park, K., Park, C., & Ko, C. (1997). Physicochemical properties and functionality of highly carboxymethylated starch. *Starch-Starke, 49*(12), 499-505. doi: 10.1002/star.19970491207

Lawal, O., Lechner, M., & Kulicke, W. (2008). Single and multi-step carboxymethylation of water yam (Dioscorea alata) starch: Synthesis and characterization. *International Journal of Biological Macromolecules, 42*(5), 429-435. doi: 10.1016/j.ijbiomac.2008.02.006

Lee, B., Chao, C., Nunalee, F., Motan, E., Shull, K., & Messersmith, P. (2006). Rapid gel formation and adhesion in photocurable and biodegradable block copolymers with high DOPA content. *Macromolecules, 39*(5), 1740-1748. doi: 10.1021/ma0518959

Lee, B., Dalsin, J., & Messersmith, P. (2002). Synthesis and gelation of DOPA-Modified poly(ethylene glycol) hydrogels. *Biomacromolecules, 3*(5), 1038-1047. doi: 10.1021/bm025546n

Lee, B., Dalsin, J., & Messersmith, P. (2006). Biomimetic Adhesive Polymers Based on Mussel Adhesive Proteins. In J. A. C. A.M. Smith (Ed.), *Biological Adhesives* (pp. 257-273): Springer.

Lee, B., Huang, K., Nunalee, F., Shull, K., & Messersmith, P. (2004). Synthesis of 3,4-dihydroxyphenylalanine (DOPA) containing monomers and their co-polymerization with PEG-diacrylate to form hydrogels. *Journal of Biomaterials Science-Polymer Edition, 15*(4), 449-464. doi: 10.1163/156856204323005307

Lee, H., Lee, B., & Messersmith, P. (2007). A reversible wet/dry adhesive inspired by mussels and geckos. *Nature, 448*(7151), 338-U334. doi: 10.1038/nature05968

Lee, H., Scherer, N., & Messersmith, P. (2006). Single-molecule mechanics of mussel adhesion. *Proceedings of the National Academy of Sciences of the United States of America, 103*(35), 12999-13003. doi: 10.1073/pnas.0605552103

Li, W., Kong, X., Ruan, M., Ma, F., Jiang, Y., Liu, M., . . . Zuo, X. (2012). Green waxes, adhesives and lubricants (Retraction of vol 368, pg 4869, 2010). *Philosophical Transactions of the Royal Society a-Mathematical Physical and Engineering Sciences, 370*(1970), 3269-3269. doi: 10.1098/rsta.2012.0141

Lin, Q., Gourdon, D., Sun, C., Holten-Andersen, N., Anderson, T., Waite, J., & Israelachvili, J. (2007). Adhesion mechanisms of the mussel foot proteins mfp-1 and mfp-3. *Proceedings of the National Academy of Sciences of the United States of America, 104*(10), 3782-3786. doi: 10.1073/pnas.0607852104

Liu, Y., & Li, K. (2002). Chemical modification of soy protein for wood adhesives. *Macromolecular Rapid Communications, 23*(13), 739-742. doi: 10.1002/1521-3927(20020901)23:13<739::AID-MARC739>3.0.CO;2-0

Markarian, S., & Sargsyan, H. (2011). Electronic absorption spectra of ascorbic acid in water and water-dialkylsulfoxide mixtures. *Journal of Applied Spectroscopy, 78*(1), 6-10.

Matos-Perez, C., & Wilker, J. (2012). Ambivalent Adhesives: Combining Biomimetic Cross-Linking with Antiadhesive Oligo(ethylene glycol). *Macromolecules, 45*(16), 6634-6639. doi: 10.1021/ma300962d

Measuring the dynamic viscosity of starch adhesives in the paper and packaging industry. (2011): Anton Paar.

Mehdizadeh, M., Weng, H., Gyawali, D., Tang, L., & Yang, J. (2012). Injectable citrate-based mussel-inspired tissue bioadhesives with high wet strength for sutureless wound closure. *Biomaterials, 33*(32), 7972-7983. doi: 10.1016/j.biomaterials.2012.07.055

Mojarradi, H. (2011). *Coupling of Substances Containing a Primary Amine to Hyaluronan via Carbodiimide-Mediated Amidation.* Uppsala University.

Monahan, J., & Wilker, J. (2004). Cross-linking the protein precursor of marine mussel adhesives: Bulk measurements and reagents for curing\. *Langmuir, 20*(9), 3724-3729. doi: 10.1021/la0362728

Murphy, J., Vollenweider, L., Xu, F., & Lee, B. (2010). Adhesive Performance of Biomimetic Adhesive-Coated Biologic Scaffolds. *Biomacromolecules, 11*(11), 2976-2984. doi: 10.1021/bm1007794

Nakajima, N., & Ikada, Y. (1995). Mechanism of amide formation by carbodiimide for bioconjugation in aqueous-media. *Bioconjugate Chemistry, 6*(1), 123-130. doi: 10.1021/bc00031a015

Nakonieczna, L., Przychodzen, W., & Chimiak, A. (1994). A new convenient route for the synthesis of dopa peptides. *Liebigs Annalen Der Chemie*(10), 1055-1058. NHS and Sulfo-NHS. In T. Scientific (Ed.).

Ni, K., Zhou, X., Zhao, L., Wang, H., Ren, Y., & Wei, D. (2012). Magnetic Catechol-Chitosan with Bioinspired Adhesive Surface: Preparation and Immobilization of omega-Transaminase. *Plos One, 7*(7). doi: 10.1371/journal.pone.0041101

Ogushi, Y., Sakai, S., & Kawakami, K. (2007). Synthesis of enzymatically-gellable carboxymethylcellulose for biomedical applications. *Journal of Bioscience and Bioengineering, 104*(1), 30-33. doi: 10.1263/jbb.104.30

Onusseit, H., VonByern, J., & Grunwald, I. (2010). Renewable (Biological) Compounds in Adhesives for Industrial Applications. *Biological Adhesive Systems: From Nature To Technical and Medical Application*, 189-199. doi: 10.1007/978-3-7091-0286-2_12

Onusseit, H., VonByern, J., & I, G. (2010). Renewable (Biological) Compounds in Adhesives for Industrial Applications. *Biological Adhesive Systems: From Nature To Technical and Medical Application*, 189-199. doi: 10.1007/978-3-7091-0286-2_12

Packham, D. E. (2005). *Handbook of adhesion* (2nd ed.). Hoboken, N.J.: John Wiley.

Peng, Q., & Perlin, A. (1987). Observations on NMR-spectra of starches in dimethylsulfoxide, iodine-complexing, and solvation in water dimethylsulfoxide. *Carbohydrate Research, 160*, 57-72. doi: 10.1016/0008-6215(87)80303-8

Pizzi, A., & Mittal, K. L. (2003). *Handbook of adhesive technology* (pp. xii, 1024 p.).

Pocius, A. V. (2002). *Adhesion and adhesives technology : an introduction* (2nd ed.). Munich Cincinnati: Hanser ; Distributed in the USA by Hanser/Gardner Publications.

Richardson, S., & Gorton, L. (2003). Characterisation of the substituent distribution in starch and cellulose derivatives. *Analytica Chimica Acta, 497*(1-2), 27-65. doi: 10.1016/j.aca.2003.08.005

Rischka, K., Richter, K., Hartwig, A., Kozielec, M., Slenzka, K., Sader, R., . . . I, G. (2010). Bio-inspired Polyphenolic Adhesives for Medical and Technical Applications. *Biological Adhesive Systems: From Nature To Technical and Medical Application*, 201-211. doi: 10.1007/978-3-7091-0286-2_13

Ruffing, T., Smith, P., & Brown, N. (2010). Resin Suppliers' Perspectives on the "Greening" of the North American Interior Wood Composite Panel Market. *Forest Products Journal, 60*(2), 119-125.

Sagert, J., Sun, C., & Waite, H. (2006). Chemical Subtleties of Mussel and Polychaete Holdfasts. In J. A. C. A.M. Smith (Ed.), *Biological Adhesives* (pp. 125-140): Springer.

Schnurrer, J., & Lehr, C. (1996). Mucoadhesive properties of the mussel adhesive protein. *International Journal of Pharmaceutics, 141*(1-2), 251-256. doi: 10.1016/0378-5173(96)04625-X

Scott, P. J. H. (2009). *Linker strategies in solid-phase organic synthesis* (pp. 1 online resource (xxviii, 677 p.)).

Sever, M., Weisser, J., Monahan, J., Srinivasan, S., & Wilker, J. (2004). Metal-mediated cross-linking in the generation of a marine-mussel adhesive. *Angewandte Chemie-International Edition, 43*(4), 448-450. doi: 10.1002/anie.200352759

Sever, M., & Wilker, J. (2001). Synthesis of peptides containing DOPA (3,4-dihydroxyphenylalanine). *Tetrahedron, 57*(29), 6139-6146. doi: 10.1016/S0040-4020(01)00601-9

Shazly, T., Baker, A., Naber, J., Bon, A., Van Vliet, K., & Edelman, E. (2010). Augmentation of postswelling surgical sealant potential of adhesive hydrogels. *Journal of Biomedical Materials Research Part a, 95A*(4), 1159-1169. doi: 10.1002/jbm.a.32942

Shuttleworth, P., Clark, J., Mantle, R., & Stansfield, N. (2010). Switchable adhesives for carpet tiles: a major breakthrough in sustainable flooring. *Green Chemistry, 12*(5), 798-803. doi: 10.1039/b922735k

Stewart, R., Ransom, T., & Hlady, V. (2011). Natural Underwater Adhesives. *Journal of Polymer Science Part B-Polymer Physics, 49*(11), 757-771. doi: 10.1002/polb.22256

Stojanovic, Z., Jeremic, K., Jovanovic, S., & Lechner, M. (2005). A comparison of some methods for the determination of the degree of substitution of carboxymethyl starch. *Starch-Starke, 57*(2), 79-83. doi: 10.1002/star.200400342

Suzuki, T., Tanemura, K., Horaguchi, T., & Kaneko, K. (2006). Synthesis and structure of 8-hydroxy-6-methoxy-3,7-dimethylisochromane and its analogues. *Tetrahedron, 62*(15), 3739-3751. doi: 10.1016/j.tet.2006.01.079

Takahashi, K., Ogata, A., Yang, W., & Hattori, M. (2002). Increased hydrophobicity of carboxymethyl starch film by conjugation with zein. *Bioscience Biotechnology and Biochemistry, 66*(6), 1276-1280.

Thompson, D. (2000). On the non-random nature of amylopectin branching. *Carbohydrate Polymers, 43*(3), 223-239. doi: 10.1016/S0144-8617(00)00150-8

Tijsen, C., Kolk, H., Stamhuis, E., & Beenackers, A. (2001). An experimental study on the carboxymethylation of granular potato starch in non-aqueous media. *Carbohydrate Polymers, 45*(3), 219-226. doi: 10.1016/S0144-8617(00)00243-5

Volkert, B., Loth, F., Lazik, W., & Engelhardt, J. (2004). Highly substituted carboxymethyl starch. *Starch-Starke, 56*(7), 307-314. doi: 10.1002/star.200300266

Waite, J. (2002). Adhesion a la Moule. *Integrative and Comparative Biology, 42*(6), 1172-1180. doi: 10.1093/icb/42.6.1172

Waite, J., Andersen, N., Jewhurst, S., & Sun, C. (2005). Mussel adhesion: Finding the tricks worth mimicking. *Journal of Adhesion, 81*(3-4), 297-317. doi: 10.1080/00218460590944602

Waite, J., & Benedict, C. (1984). Assay of dihydroxyphenylalanine (DOPA) in invertebrate structural proteins. *Methods in Enzymology, 107*, 397-413.

Wang, X., Jiang, Z., Shi, J., Liang, Y., Zhang, C., & Wu, H. (2012). Metal-Organic Coordination-Enabled Layer-by-Layer Self-Assembly to Prepare Hybrid Microcapsules for Efficient Enzyme Immobilization. *Acs Applied Materials & Interfaces, 4*(7), 3476-3483. doi: 10.1021/am300559j

Wesslen, K., & Wesslen, B. (2002). Synthesis of amphiphilic amylose and starch derivatives. *Carbohydrate Polymers, 47*(4), 303-311. doi: 10.1016/S0144-8617(01)00196-5

Westwood, G., Horton, T., & Wilker, J. (2007). Simplified polymer mimics of cross-linking adhesive proteins. *Macromolecules, 40*(11), 3960-3964. doi: 10.1021/ma0703002

Wiegemann, M. (2005). Adhesion in blue mussels (Mytilus edulis) and barnacles (genus Balanus): Mechanisms and technical applications. *Aquatic Sciences, 67*(2), 166-176. doi: 10.1007/s00027-005-0758-5

Wilker, J. (2011). Biomaterials: Redox and adhesion on the rocks. *Nature Chemical Biology, 7*(9), 579-580.

Wu, J., Zhang, L., Wang, Y., Long, Y., Gao, H., Zhang, X., . . . Xu, J. (2011). Mussel-Inspired Chemistry for Robust and Surface-Modifiable Multilayer Films. *Langmuir, 27*(22), 13684-13691. doi: 10.1021/la2027237

Xu, D., & Edgar, K. (2012). TBAF and Cellulose Esters: Unexpected Deacylation with Unexpected Regioselectivity. *Biomacromolecules, 13*(2), 299-303. doi: 10.1021/bm201724s

Yaacob, B., Amin, M., Hashim, K., & Abu Bakar, B. (2011). Optimization of Reaction Conditions for Carboxymethylated Sago Starch. *Iranian Polymer Journal, 20*(3), 195-204.

Yamada, K., Aoki, T., Ikeda, N., Hirata, M., Hata, Y., Higashida, K., & Nakamura, Y. (2008). Application of chitosan solutions gelled by melB tyrosinase to water-resistant adhesives. *Journal of Applied Polymer Science, 107*(4), 2723-2731. doi: 10.1002/app.27339

Yamada, K., Chen, T., Kumar, G., Vesnovsky, O., Topoleski, L., & Payne, G. (2000). Chitosan based water-resistant adhesive. Analogy to mussel glue. *Biomacromolecules, 1*(2), 252-258. doi: 10.1021/bm0003009

Yu, J., Wei, W., Danner, E., Ashley, R., Israelachvili, J., & Waite, J. (2011). Mussel protein adhesion depends on interprotein thiol-mediated redox modulation. *Nature Chemical Biology, 7*(9), 588-590. doi: 10.1038/NCHEMBIO.630

Yu, J., Wei, W., Danner, E., Israelachvili, J., & Waite, J. (2011). Effects of Interfacial Redox in Mussel Adhesive Protein Films on Mica. *Advanced Materials, 23*(20), 2362-+. doi: 10.1002/adma.201003580

Yu, M., & Deming, T. (1998). Synthetic polypeptide mimics of marine adhesives. *Macromolecules, 31*(15), 4739-4745. doi: 10.1021/ma980268z

Yu, M., Hwang, J., & Deming, T. (1999). Role of L-3,4-dihydroxyphenylalanine in mussel adhesive proteins. *Journal of the American Chemical Society, 121*(24), 5825-5826. doi: 10.1021/ja990469y

Yu, X., Bichtelen, A., Wang, X., Yan, Y., Lin, F., Xiong, Z., . . . Lu, Q. (2005). Collagen/chitosan/heparin complex with improved biocompatibility for hepatic tissue engineering. *Journal of Bioactive and Compatible Polymers, 20*(1), 15-28. doi: 10.1177/0883911505049653

Zeng, H., Hwang, D., Israelachvili, J., & Waite, J. (2010). Strong reversible Fe3+-mediated bridging between dopa-containing protein films in water. *Proceedings of the National Academy of Sciences of the United States of America, 107*(29), 12850-12853. doi: 10.1073/pnas.1007416107

Zhang, J., & Wu, D. (1992). Characteristics of the aqueous-solution of carboxymethyl starch ether. *Journal of Applied Polymer Science, 46*(2), 369-374. doi: 10.1002/app.1992.070460218

APPENDICES

Appendix A Results for Improperly Washed CMS-Dopamine Conjugates

Table A.1 Results for One-Step CMS-Dopamine Reaction

	MW	DS	[CMS] (mg/mL)	EDC:COOH	NHS:COOH	dopa:COOH	pH	DS_{dopa}	Precipitation?
1	Low	0.5	10	1	-	2	< 4.5	0.05	N
2	Low	0.5	10	1	-	20	< 4.5	0.09	N

Table A.2 Results for Two-Step CMS-Dopamine Reaction

	MW	DS	[CMS] (mg/mL)	EDC:COOH	NHS:COOH	dopa:COOH	pH	DS_{dopa}	Precipitation?
1	Low	0.5	10	2	2	10	< 4.5	0.16	N
2	High	0.84	10	1	1	2	< 4.5	0.09	N
3	High	0.84	10	2	2	4	< 4.5	0.14	N

Table A.3 Results for Two-step CMS-Dopamine Reaction – Washed Intermediate

	MW	DS	[CMS] (mg/mL)	EDC:COOH	NHS:COOH	dopa:COOH	pH 1	pH 2	DS_{dopa}	Precipitation?
1	High	0.84	10	5	5	10	4.5	-	0.16	N
2	Low	0.52	10	2	2	10	4.75	6.9	0.19	N
3	High	1.7	10	2	2	5	4.75	6.6	0.35	N
4	High	1.7	10	2	2	5	4.9	7	0.4	N

Appendix B FTIR Spectra

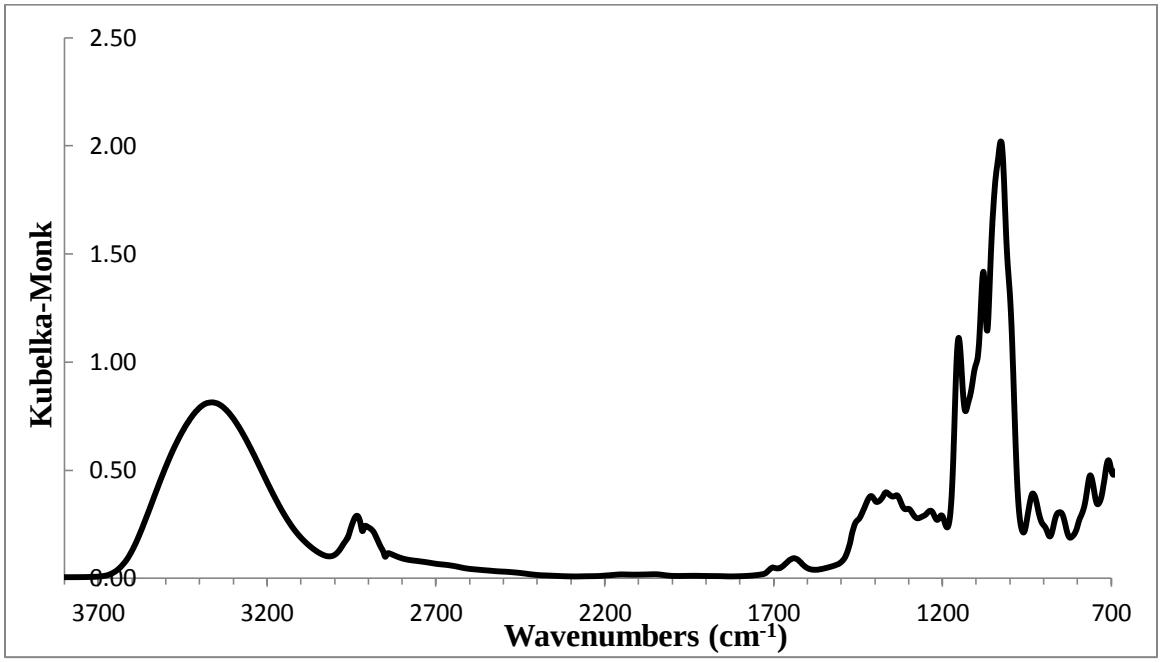

Figure B.1 FTIR Spectrum of Unhydrolyzed Non-Granular Starch

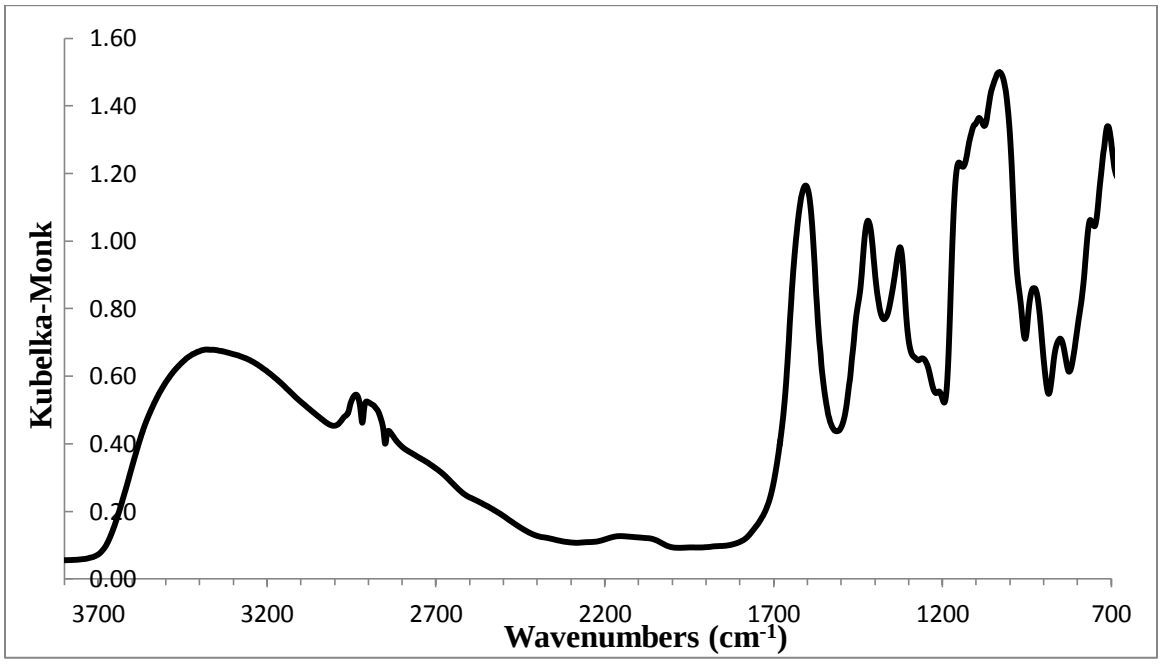

Figure B.2 FTIR Spectrum of High MW CMS (DS = 1.12)

Figures A.3-A.7 show the FTIR spectra of a one-step reaction with 10 mg/mL low MW CMS (DS = 0.7), 2:1 EDC:COOH, and 2:1 dopamine:COOH, ultimately resulting in precipitation. Samples were taken at various times and the reaction stopped by addition of excess mercaptoethanol to quench EDC, followed by precipitation in 4 volumes of ethanol and extensive washing of the solid product with 80% ethanol before a final wash with acetone and dried at 50°C.

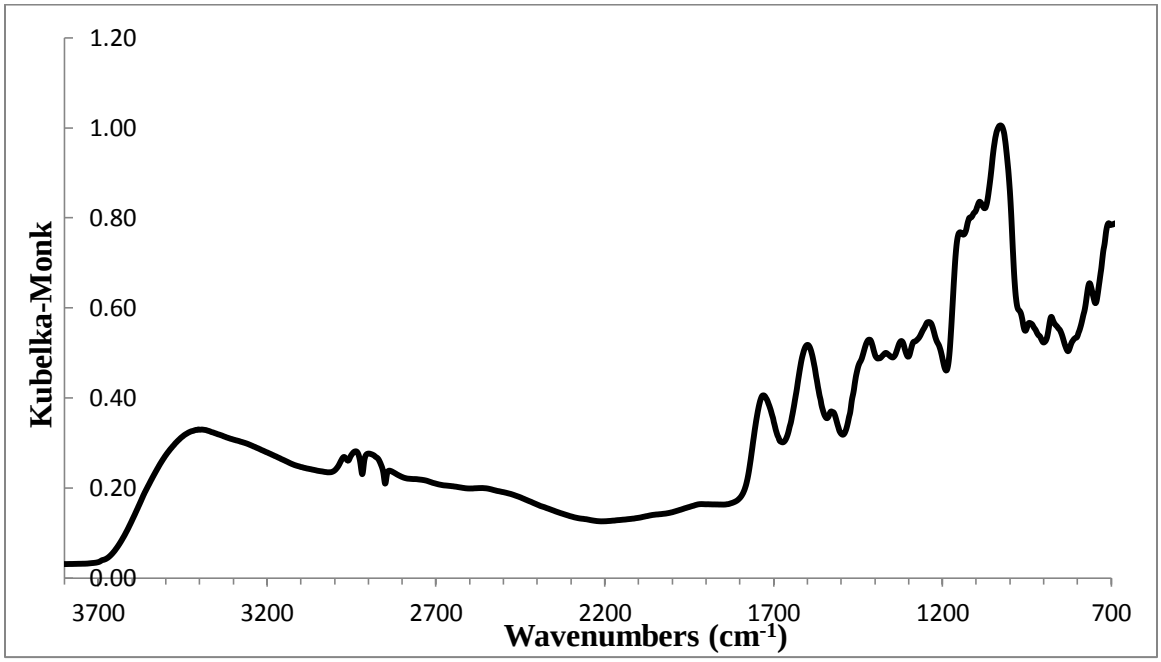

Figure B.3 FTIR Spectrum of One-Step Reaction CMS-Dopamine, time = 0, no EDC added.

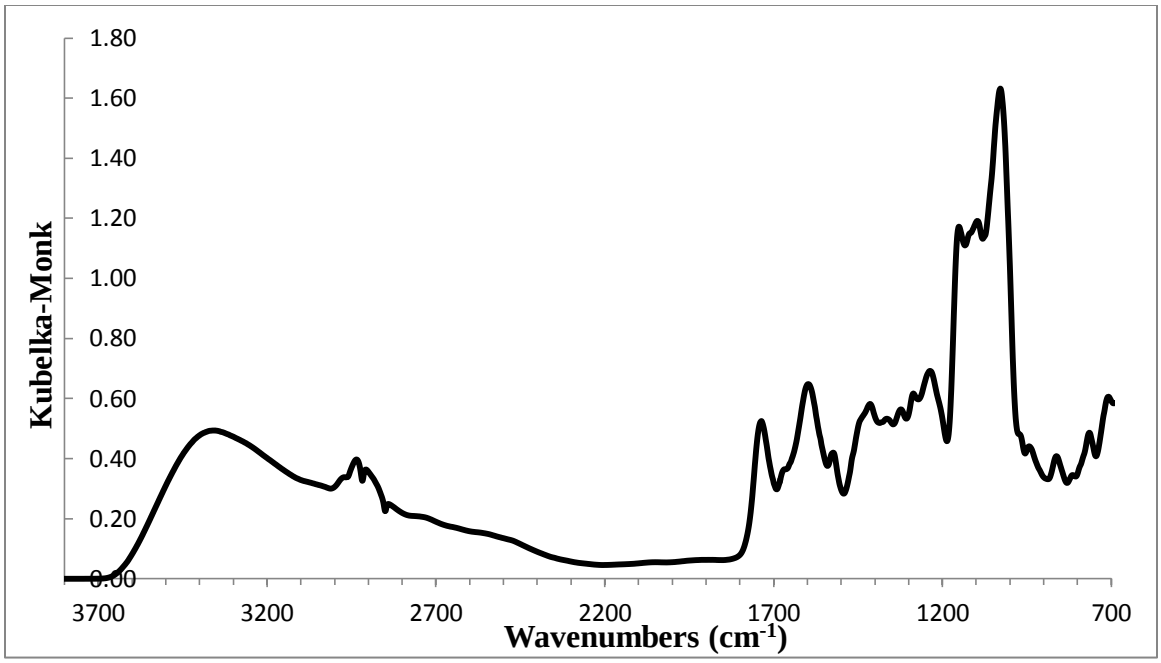

Figure B.4 FTIR Spectrum of One-Step Reaction CMS-Dopamine, time = 1 min after addition of EDC

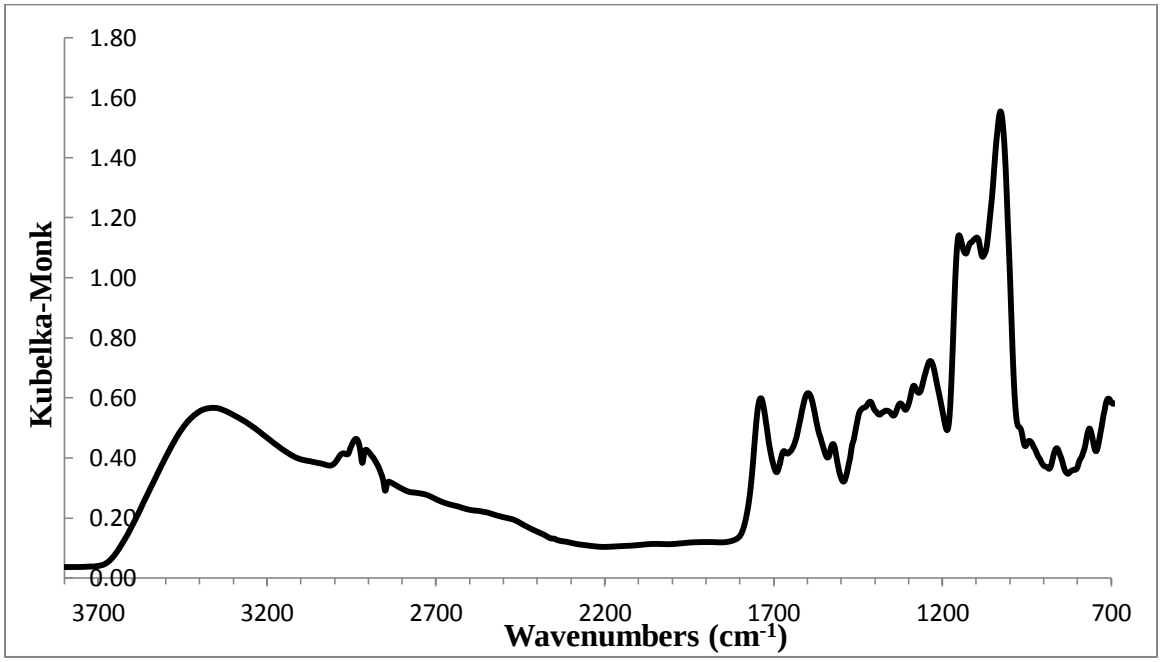

Figure B.5 FTIR Spectrum of One-Step Reaction CMS-Dopamine, time = 3 min after addition of EDC

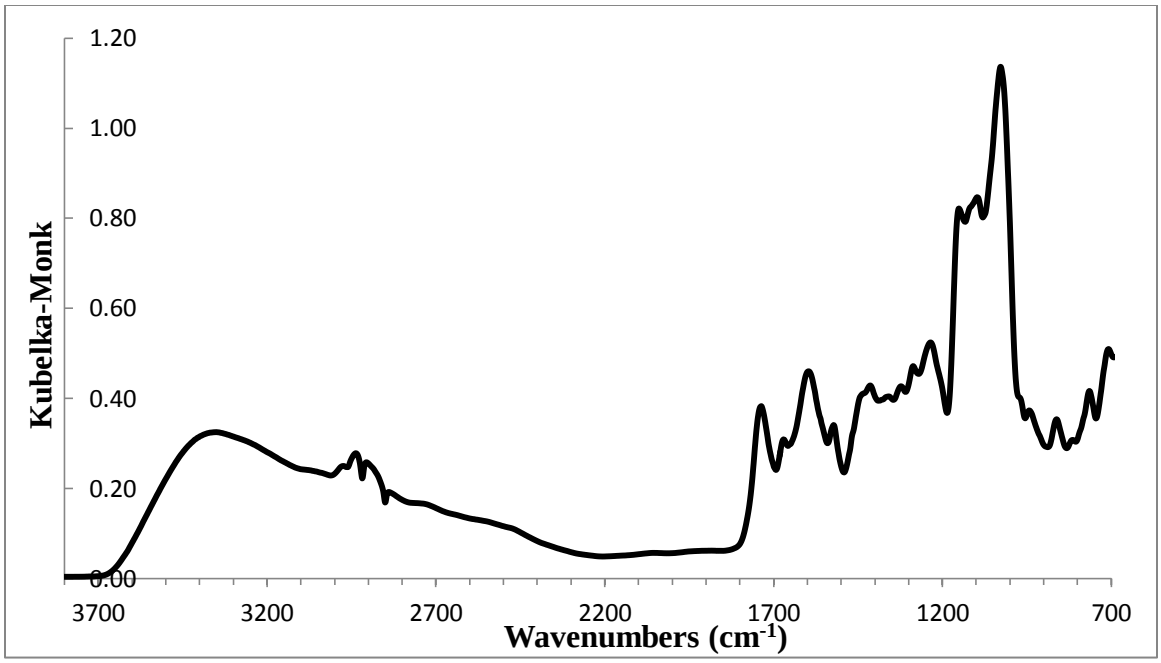

Figure B.6 FTIR Spectrum of One-Step Reaction CMS-Dopamine, time = 5 min after addition of EDC

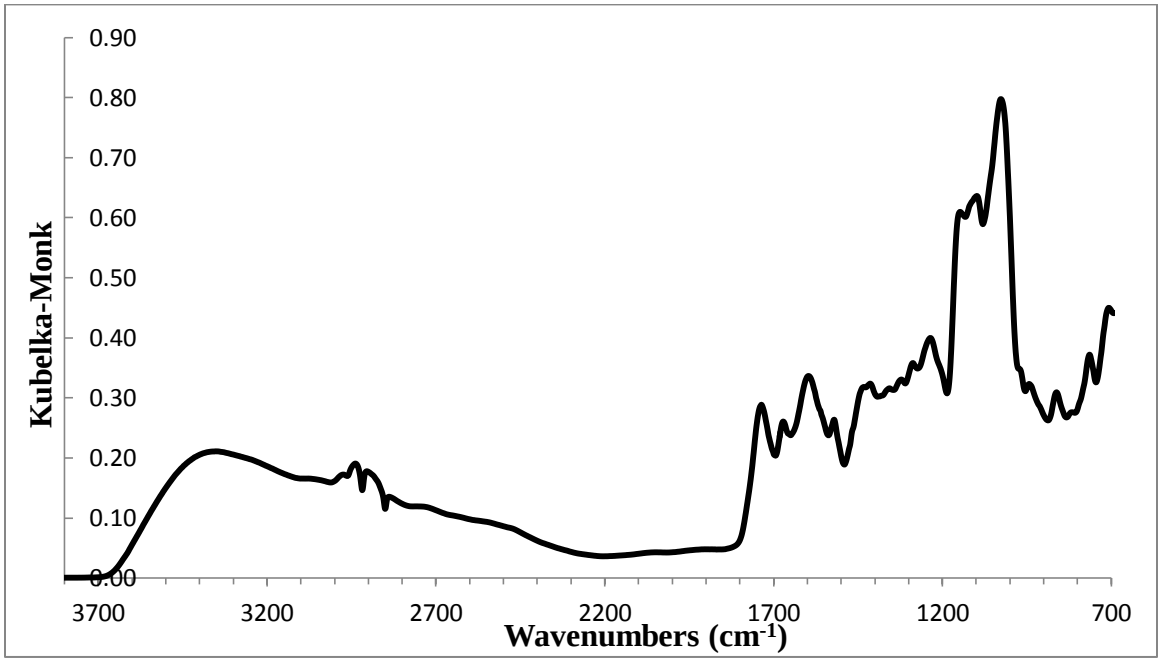

Figure B.7 FTIR Spectrum of One-Step Reaction CMS-Dopamine, time = 15 min after addition of EDC

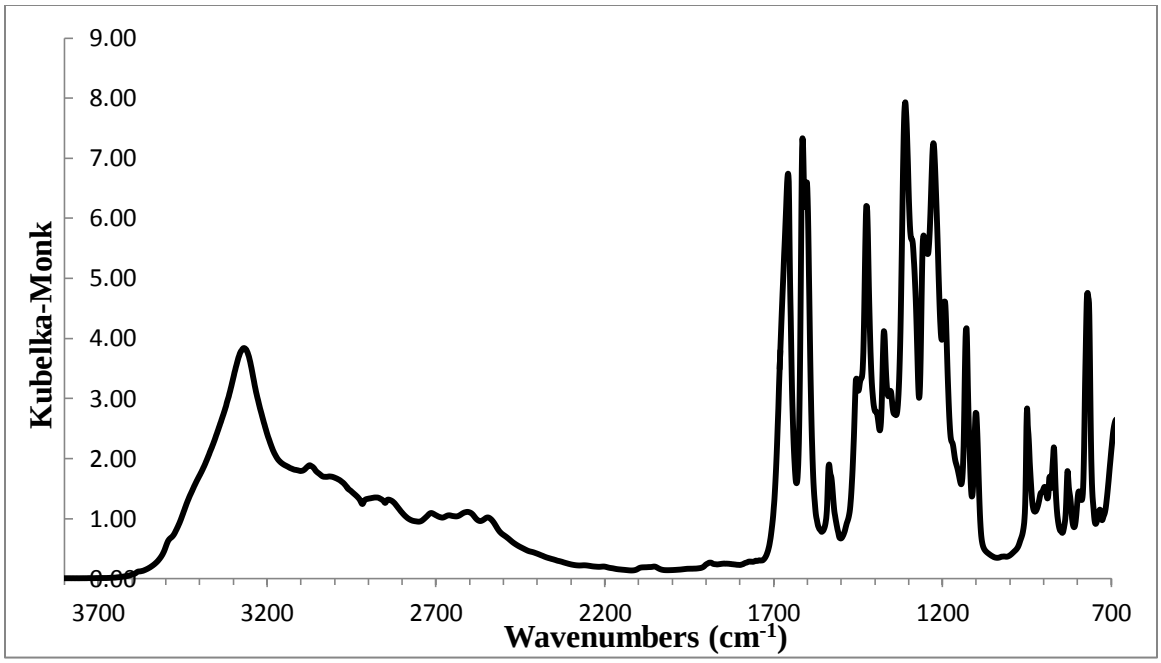

Figure B.8 FTIR Spectrum of DHBA

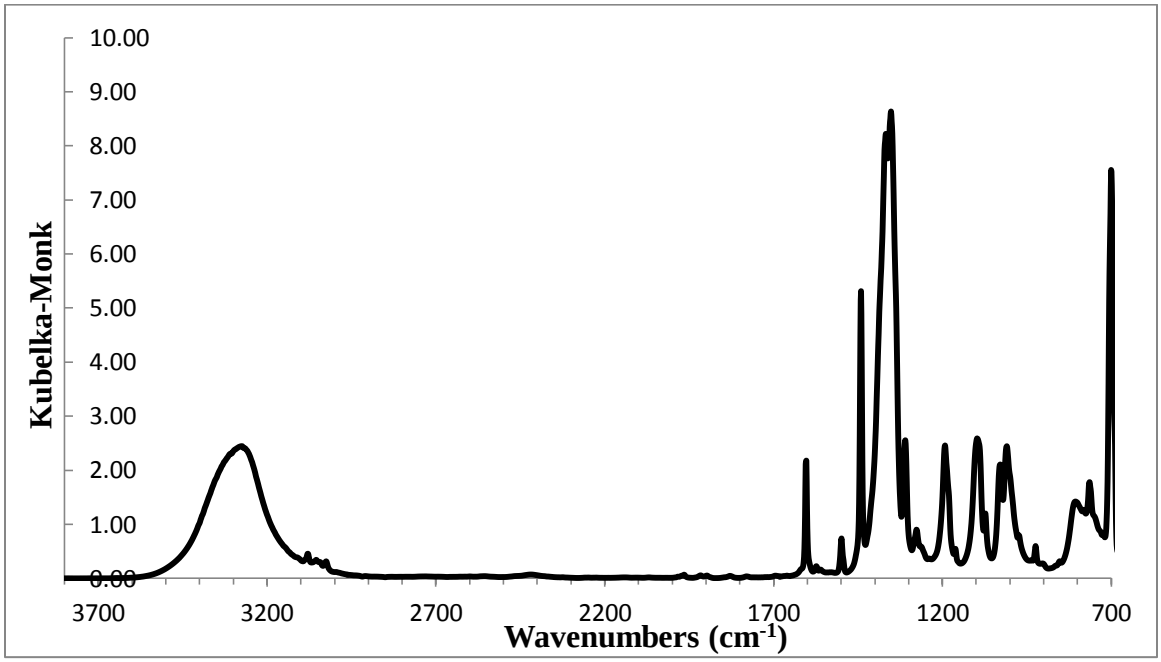

Figure B.9 FTIR Spectrum of PBA

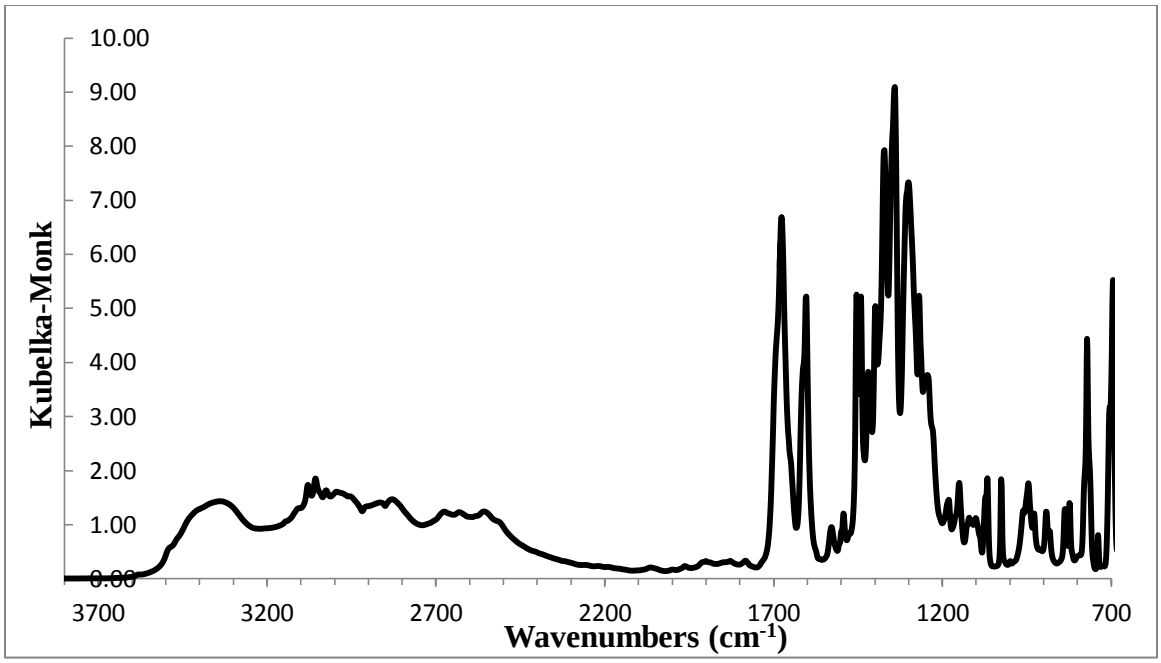

Figure B.10 FTIR Spectrum of DHBA-PBA

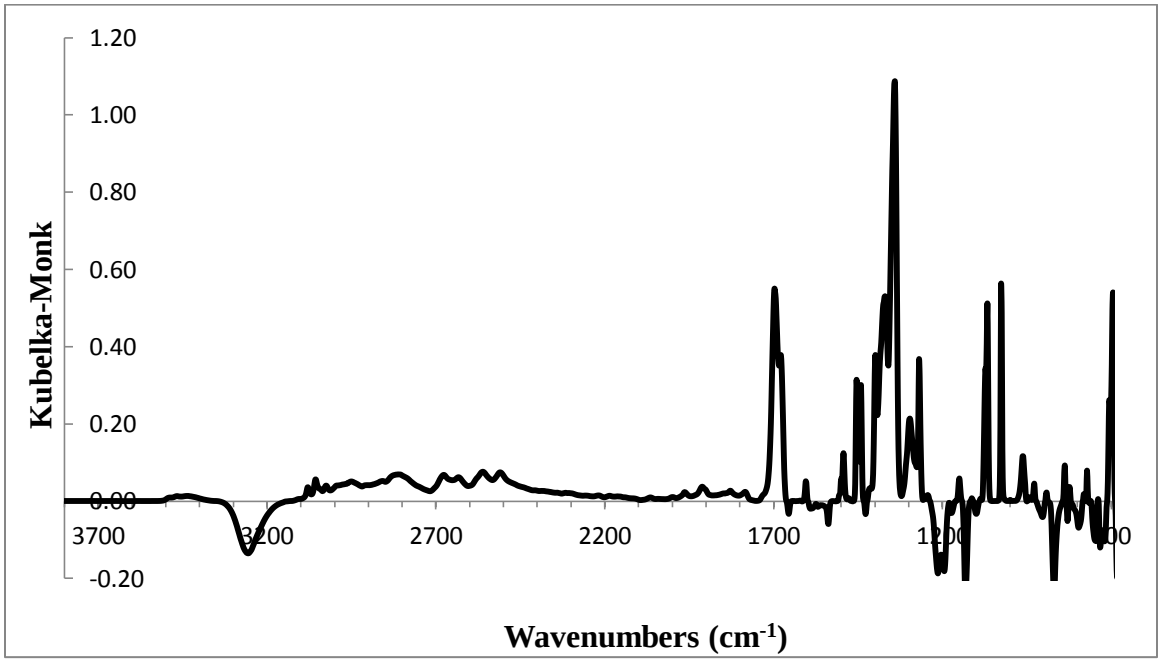

Figure B.11 Subtraction Spectrum of DHBA-PBA minus DHBA and PBA

Appendix C H-NMR Spectra

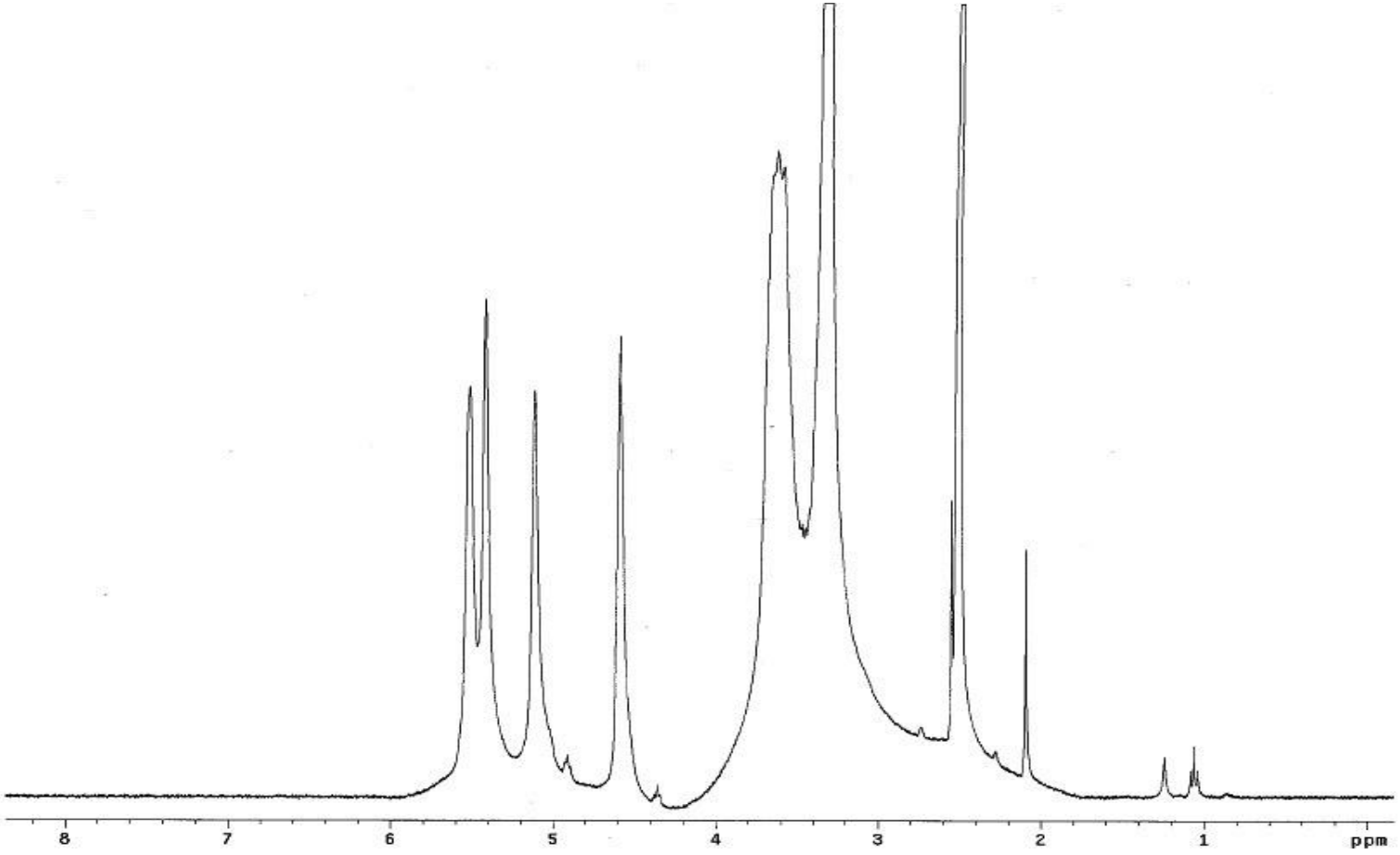

Figure C.1 H-NMR Spectrum of Low MW Starch in DMSO-d6

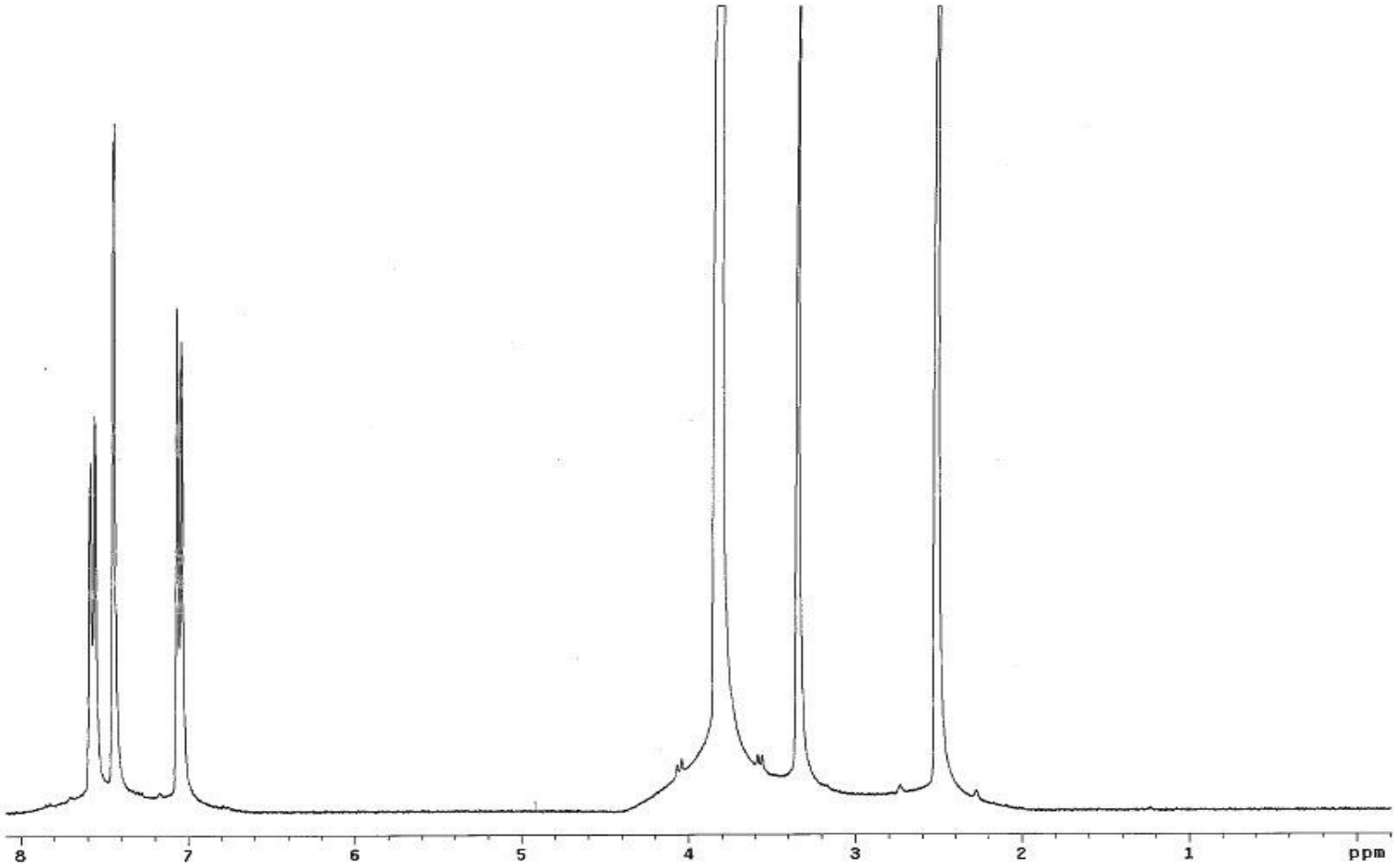

Figure C.2 H-NMR Spectrum of DMBA in DMSO-d6

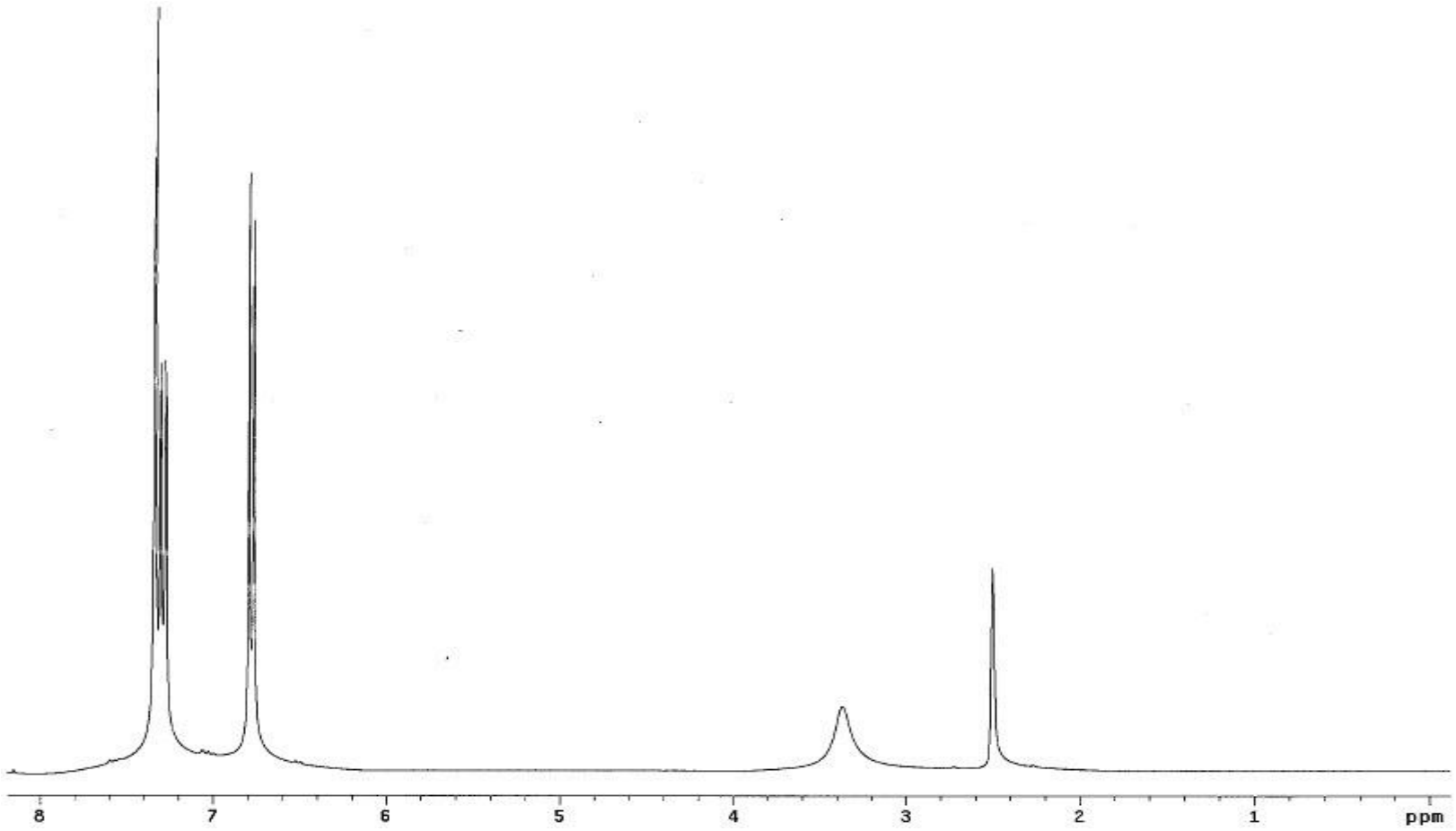

Figure C.3 H-NMR Spectrum of DHBA in DMSO-d6

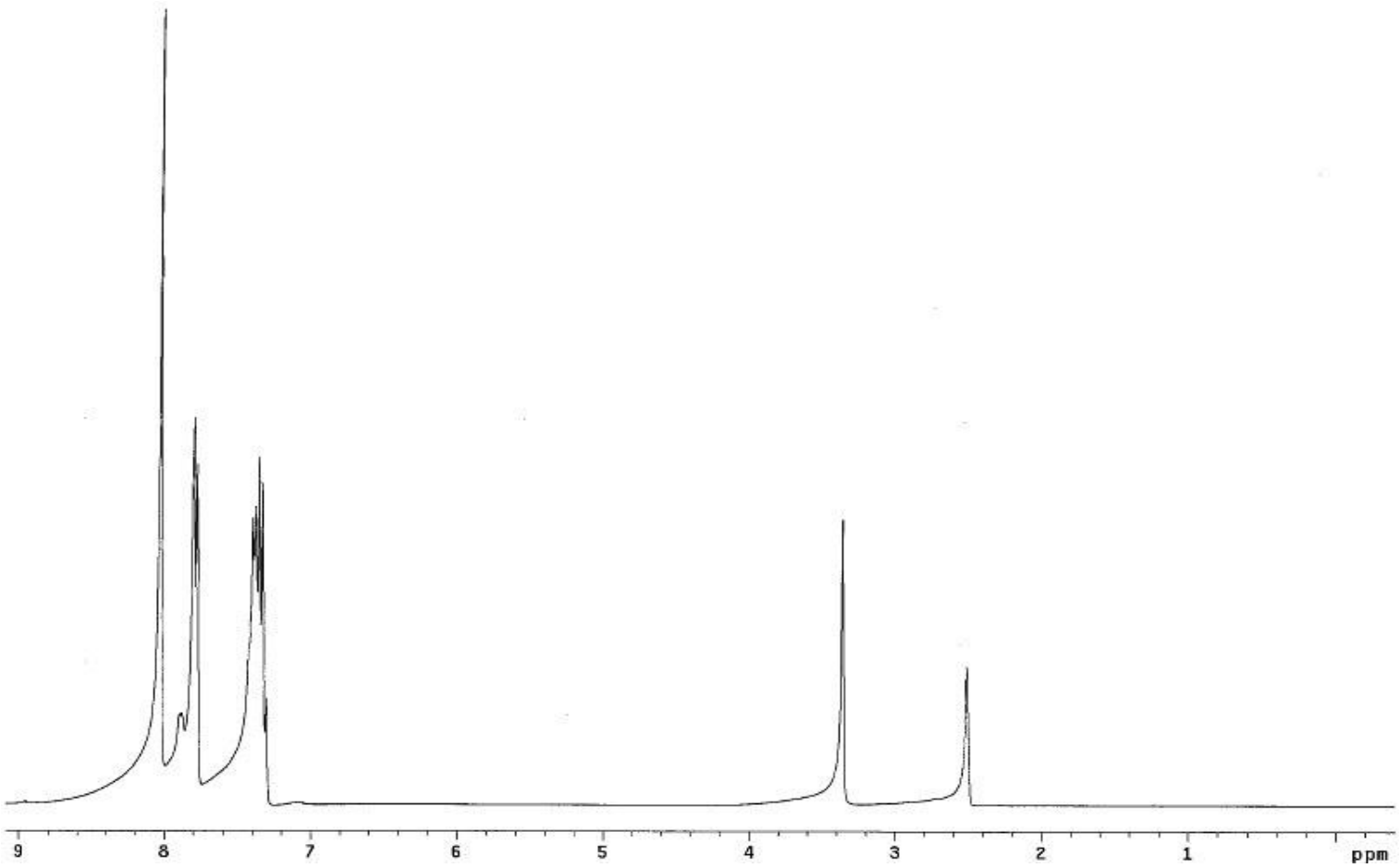

Figure C.4 H-NMR Spectrum of PBA in DMSO-d6

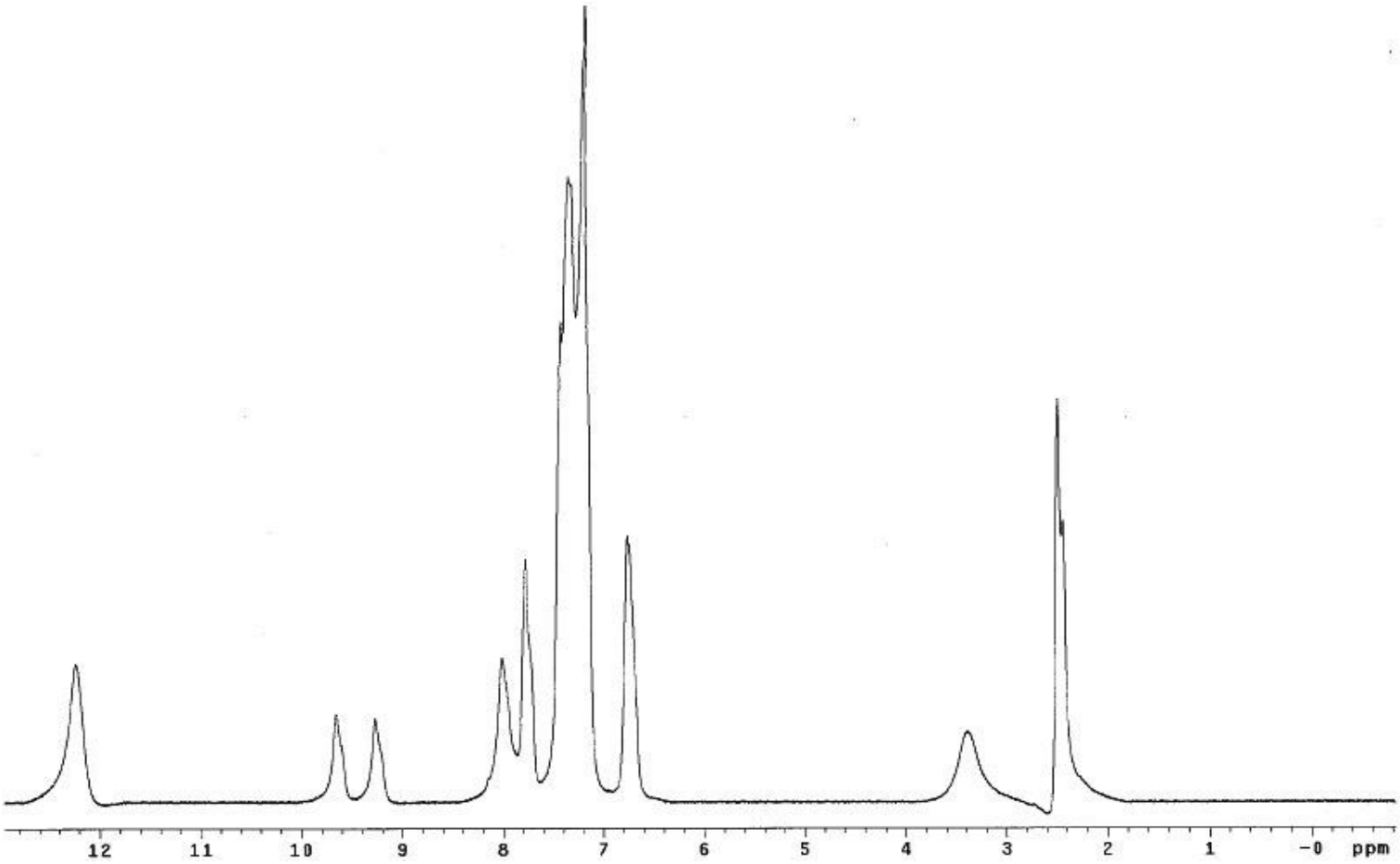

Figure C.5 H-NMR Spectrum of DHBA-PBA in DMSO-d6

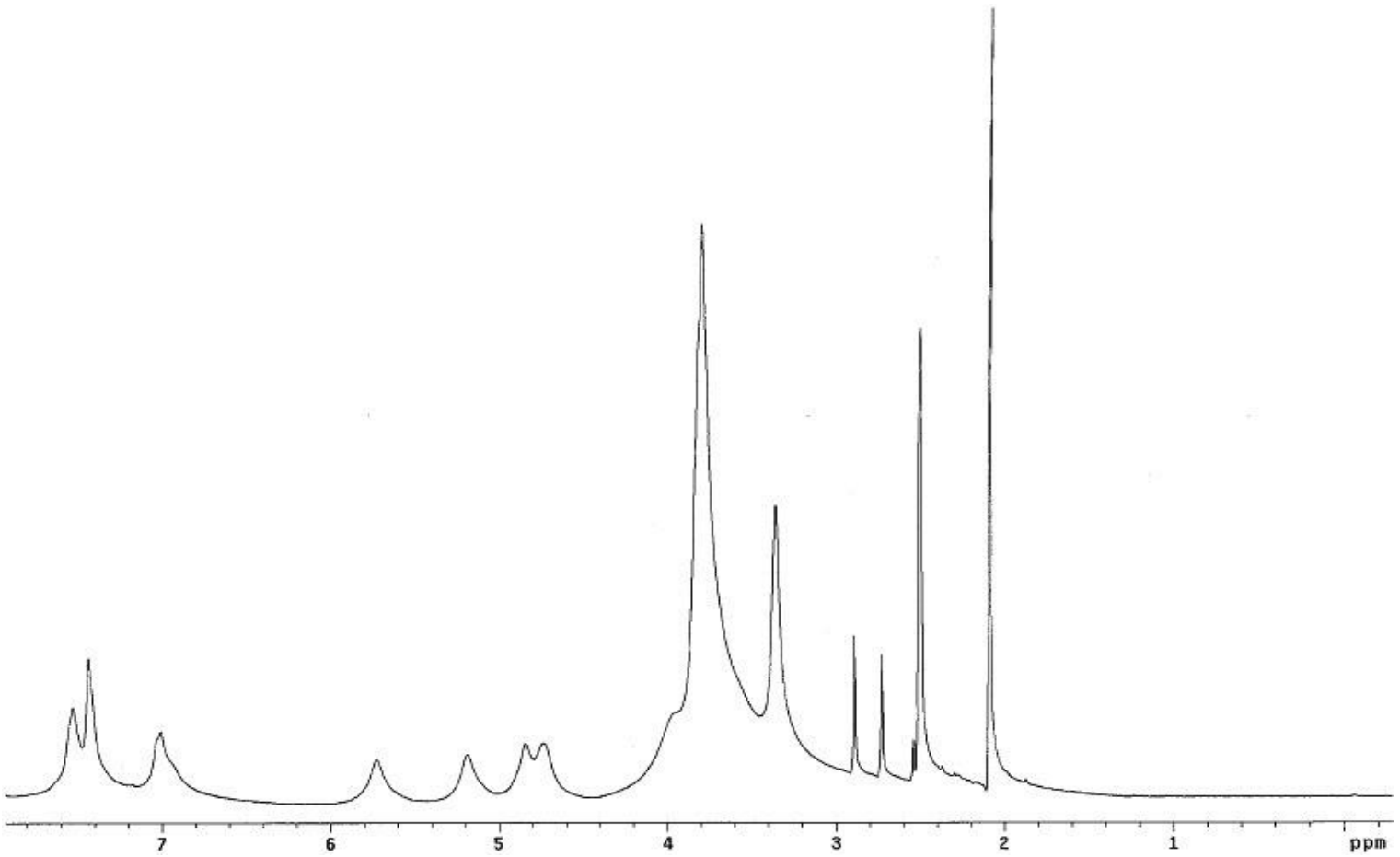

Figure C.6 Starch-DMBA (DS = 1.24) after BBr_3 Demethylation Attempt #2 in DMSO-d6

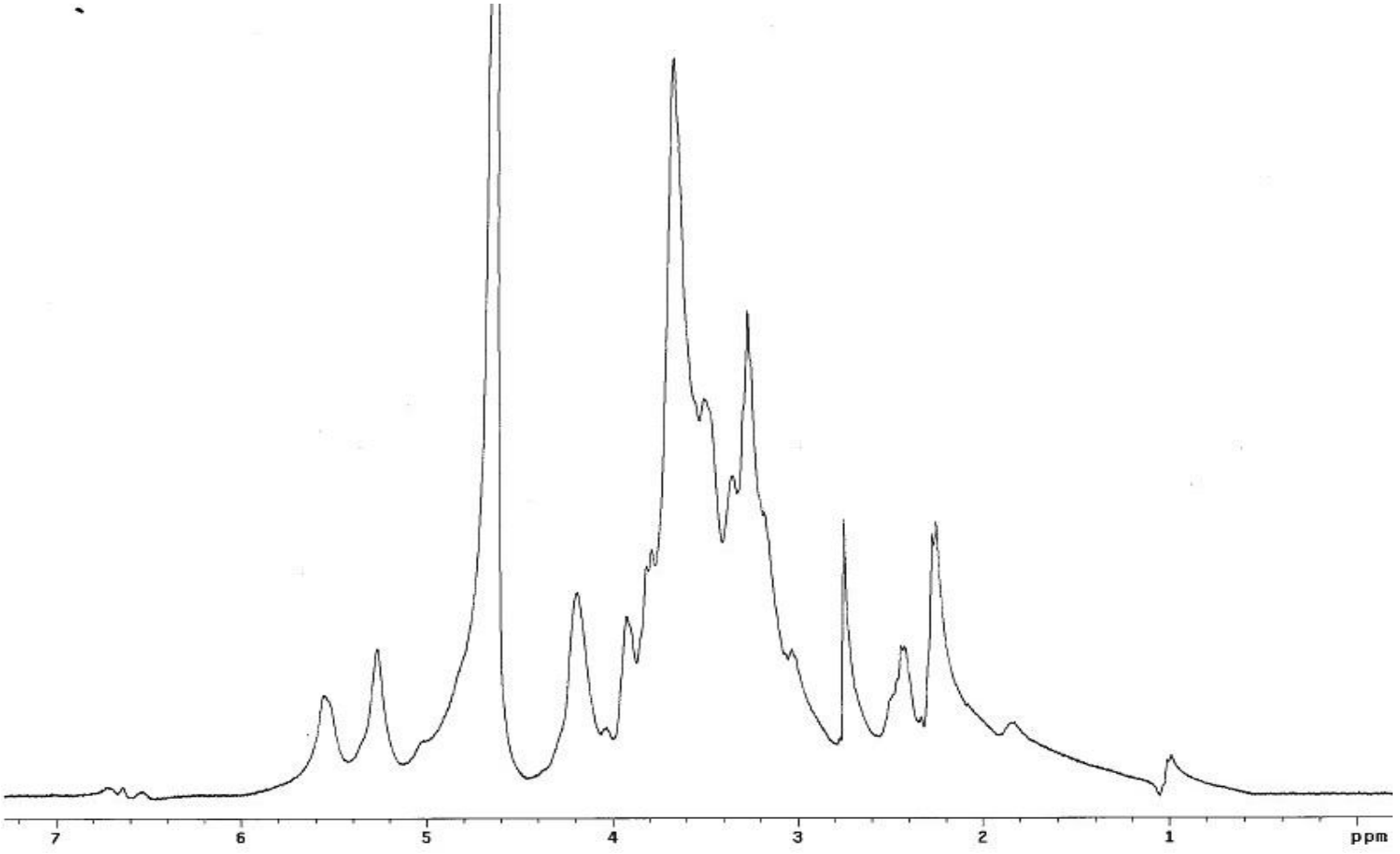

Figure C.7 CMS-Dopamine (two-step reaction with sodium borate, low MW, $DS_{catechol}$ = 0.015) in D_2O

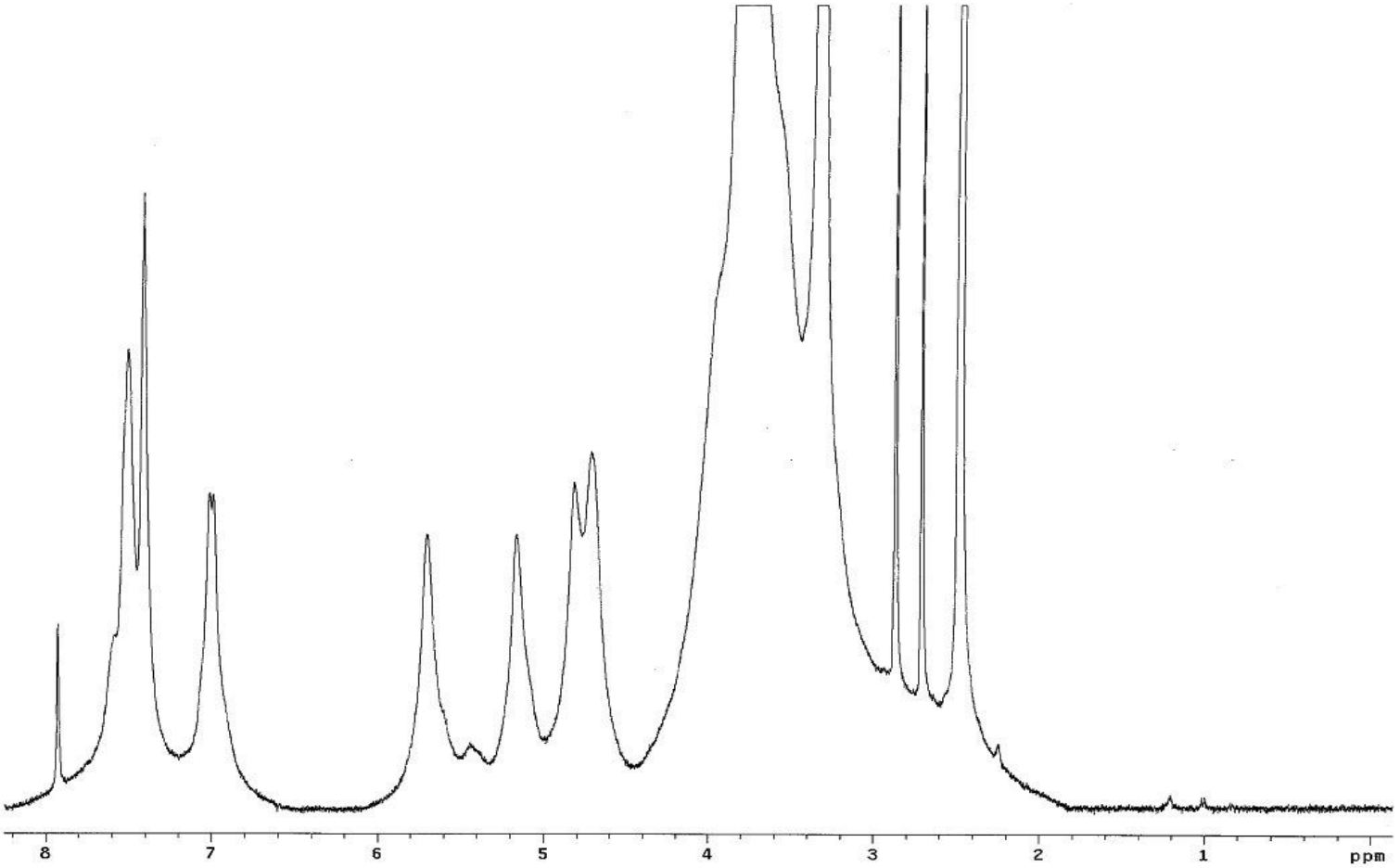

Figure C.8 H-NMR Spectrum of Starch-DMBA (High MW, DS = 1.00) in DMSO-d6

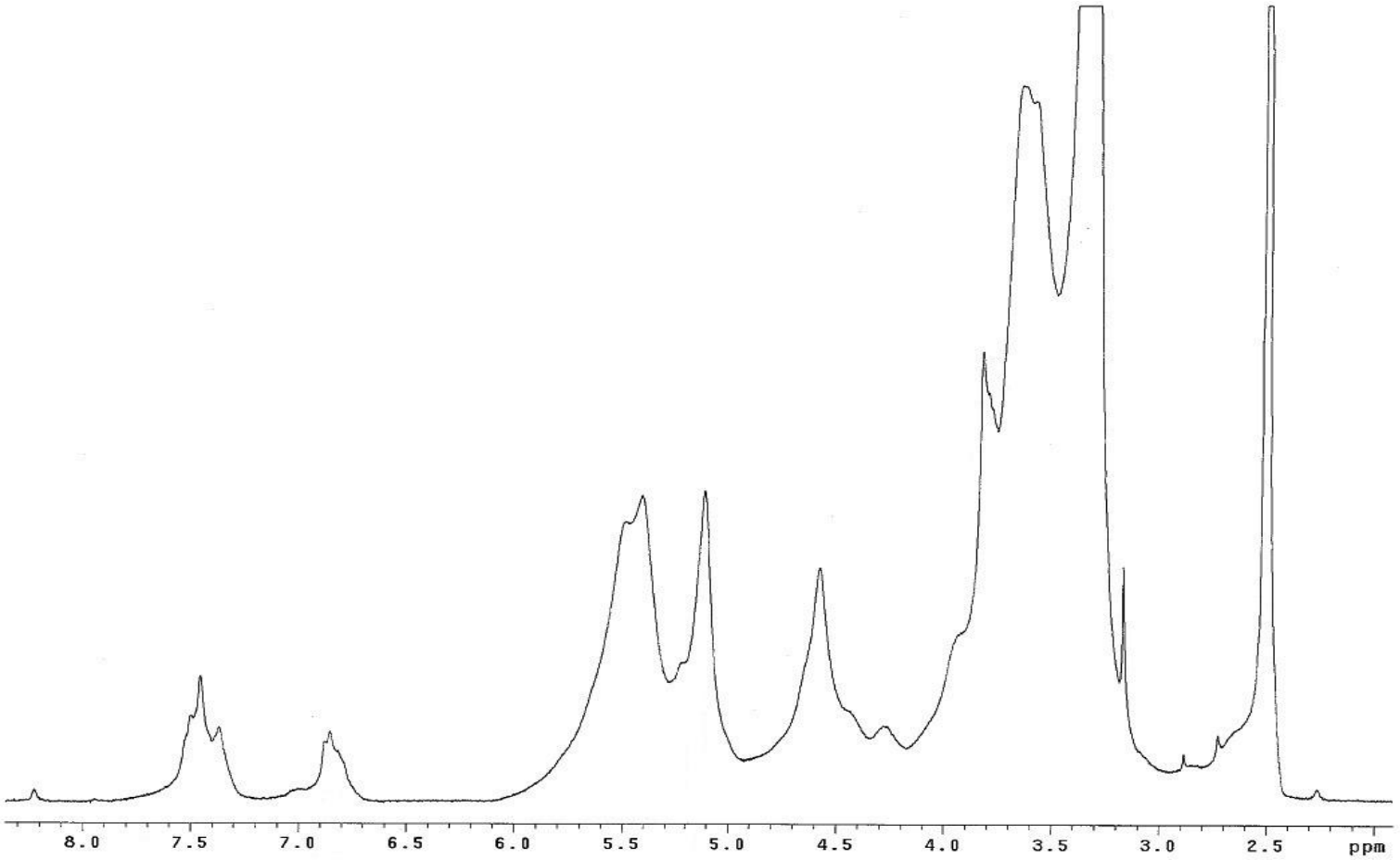

Figure C.9 H-NMR Spectrum of Starch-DMBA (Originally High MW, DS = 1.00; New DS = 0.25) After Reaction with Sodium Ethanethiolate

VITA

VITA

Jeffrey Kazimir de Kozlowski grew up in Columbia, South Carolina. He obtained his Bachelor of Science degree in Biosystems Engineering from Clemson University where he graduated Magna Cum Laude in 2010. After an internship at Savannah River National Laboratory, travelling in Europe, and working as a research assistant at the Medical University of South Carolina, he began his Master's program at Purdue University beginning in August 2011. His future plans are to enter the biotechnology industry working as a Fermentation Research Associate for DuPont Industrial Biosciences.